Improving Pavement Management and Assessment through Connected Vehicle Technology and Highway Safety Analysis

A Dissertation

Presented to

the faculty of the School of Engineering and Applied Science

University of Virginia

in partial fulfillment

of the requirements for the degree

Doctor of Philosophy

by

Huanghui Zeng

December

2014

APPROVAL SHEET

The dissertation

is submitted in partial fulfillment of the requirements

for the degree of

Doctor of Philosophy

AUTHOR

The dissertation has been read and approved by the examining committee:

Brian L. Smith

Advisor

Byungkyu Park

Michael D. Fontaine

William T. Scherer

Hyungjun Park

Accepted for the School of Engineering and Applied Science:

Dean, School of Engineering and Applied Science

December

2014

ABSTRACT

Transportation agencies devote significant resources towards the collection of highly detailed and accurate pavement condition data using instrumented vans to support pavement maintenance decisions. However, they often cannot afford to measure pavement condition annually for the whole roadway network. In addition, pavement maintenance is traditionally based only on asset management condition targets but do not explicitly account for the role of pavement condition in roadway safety. This dissertation introduced a connected vehicle-enabled approach to improve the pavement assessment method in terms of data collection cost and frequency, and applied highway safety analysis to demonstrate a new way to use pavement condition data beyond current practice.

Three related studies were conducted. The first study developed an improved acceleration-based metric, an index normalized by vehicle operating speed, for a connected vehicle-enabled pavement network screening application. The application can be used on a regular basis to "prescreen" pavement segments that are likely to deficient, and then a profile van can be sent to measure the accurate roughness condition. It was found that the proposed acceleration-based metric is able to correctly identify between 80 and 93 percent of all deficient pavement sections on three different functional classes of highways.

Considering that connected vehicle data will come from a good variety of vehicle dynamic systems, a follow-up study investigated the impact of vehicle dynamic systems on the acceleration-based roughness metric. Sensitivity analysis based on the quarter-car model found that vehicle vibration response is most sensitive to the spring stiffness of the sprung mass and least sensitive to the loading of the vehicle. Furthermore, the relationship analysis shows that the resulting acceleration-based metrics are linearly correlated between different vehicle systems. Assuming that transportation agencies will use agency-owned vehicles to build a pavement condition network screening system, a vehicle calibration procedure was developed to help them calibrate vehicles in the fleet.

The third study focused on filling the gap between traditional pavement management and highway safety management. It quantitatively evaluated the safety effectiveness of good pavement conditions versus deficient pavement conditions on rural two-lane undivided highways in Virginia. Using the Empirical Bayes method, it was found that good pavements are able to reduce fatal and injury (FI) crashes by 26 percent over deficient pavements, but do not have a statistically significant impact on the overall crash frequency. As a result, improving pavement condition from deficient to good can offer a significant safety benefit in terms of reducing crash severity.

In conclusion, the results from the first two studies point to the feasibility of using a cost-effective acceleration-based application for the purpose of network screening. The network screening process will reduce the total mileage of pavement sections that need to be measured by the instrumented van and meanwhile still identify locations where maintenance work is necessary. The third study enhances transportation agencies' ability to account for safety in their pavement maintenance decision making process, which helps to better set priorities for maintenance.

ACKNOWLEGEMENTS

I would like to acknowledge key individuals who helped me with understanding the complexity of the problem and with the execution of this research. First and foremost, I would like to give my best appreciation to my advisor, Dr. Brian Smith for his patience and consistent mentorship. He has given me the opportunity to work on an interesting and challenging problem and help me learn to think as a research scientist. This dissertation cannot be completed without his time, efforts, and resources. Next, I would like to acknowledge Dr. Michael Fontaine, Dr. Hyungjun Park and Mr. Kevin McGhee for their assistance and guidance in research design and organization, data collection and manuscript review. My appreciation also goes to my dissertation committee for its guidance and valuable inputs when I needed it. I would also like to thank staffs and students in the Center for Transportation Studies for giving useful feedbacks/comments in the group meeting. This research was funded by the Connected Vehicle/Infrastructure University Transportation Center and the Virginia Center for Transportation Innovation and Research. I would like to acknowledge their commitments to connected vehicle and infrastructure research.

Finally, I would like to dedicate this dissertation to my fiancé, my parents and sisters, who always believe in me in my every decision, enjoy the happiness with me for my every accomplishment, and encourage me whenever I am down. Thank you and I love you all.

TABLE OF CONTENTS

LIST OF TABLES

LIST OF FIGURES

CHAPTER 1 INTRODUCTION

1.1 Problem Statement

With more than 100 years of investment in infrastructure, the current highway network supports the economic activities and the mobility of people and goods throughout the whole country. Transportation agencies devote significant resources toward highway maintenance to protect and enhance the transportation infrastructure and the safety of the traveling public. For example, the Virginia Department of Transportation (VDOT), which maintains the third-largest state network of roadways (more than 125,000 lane miles) in the United States, spent about one third ($1.56 billion) of its 2014 budget ($4.66 billion) on the highway system maintenance program (*1*). Highway pavement management is a core area of the program. This includes development of strategies and systems for periodically assessing pavement condition and maintenance plans to maximize pavement life within limited budgets. It also requires making tactical decisions regarding treatment during adverse weather conditions to keep roadways functional. A fundamental requirement in these management activities is to collect data to assess the condition of the pavement, which allows the pavement maintenance decisions to be made using a systematic, performance-based and data-driven approach. Like many other transportation agencies, the Virginia Department of Transportation (VDOT) began automated pavement condition data collection using digital images and an automated crack detection methodology in 2007, which led to significant improvements in the consistency and efficiency of pavement condition data assessments. Since then, pavement condition information has been updated annually for the entire interstate and primary highway systems and every five years in the secondary system (*2*).

Although the automated data collection is making good progress in data-driven pavement management, there is still room for improvement. The progress of the connected vehicle program offers an opportunity to improve the pavement assessment method. In addition, highway safety analysis could demonstrate a new way to use pavement condition data beyond current practice.

1.1.1 Connected Vehicle Opportunity

Given the need for specialized equipment and skilled personnel, it is very difficult to collect data at more locations in a timely and cost effective manner. Even though VDOT spends approximately $1.8 million per year in automated pavement condition data collection (*3*), for a large portion of the roadway system (i.e., secondary roadways and local systems), the pavement condition data is usually measured infrequently, only once every 5 years.

Highway transportation is undergoing significant technological transformations to a connected vehicle environment as wireless communication increasingly enables vehicles to communicate with each other and with the infrastructure (*4*). The US Department of Transportation (USDOT)'s ITS initiative is intended to introduce intelligent vehicles, infrastructure, and communications systems to the United States' transportation system. The core of the ITS program is the connected vehicle research program, which aims to connect vehicles, infrastructure, and mobile devices for safety, efficiency, and environmental improvements through wirelessly shared information (*5*). This connected, data-rich environment will allow for innovative connected vehicle applications for transportation infrastructure maintenance. The use of simple sensors such as accelerometers, already installed either in vehicles or mobile devices, enable us to directly measure the vehicle vibration responses, which is believed to highly correlate with pavement roughness. In other words, the entire vehicle fleet

– if equipped with appropriate communication devices – can be transformed into probes, measuring pavement roughness at more locations, more frequently with minimal additional costs. As designed, the Basic Safety Message (BSM), which includes vehicle body accelerations, location, speed and other information, will be sent from each connected vehicle every 0.1 second (*6*). Under a connected vehicle environment, these data can be collected through people's daily travel, does not need specifically equipped vehicles, and thus may be used to assess pavement roughness in a more timely manner with minimal additional data collection cost.

1.1.2 Incorporating Highway Safety in Pavement Management

When transportation agencies develop paving schedules for their roadways, they often make decisions based on asset management condition targets but do not explicitly account for the role of pavement condition in roadway safety. However, pavement condition can have an important effect on highway safety. For instance, skidding crashes, a major concern in highway safety, are usually related to pavement rutting, polishing, bleeding, and dirty pavements (*7*). Previous research regarding the safety effect of pavement condition usually focused on either maintenance activities such as resurfacing or a certain type of pavement distress and was not based on consistent and accurate pavement condition data (*8*, *9*). If the safety effect information were available, it could be used for a variety of applications, including prioritizing sites for the agency's annual paving program or quantifying the benefits of preventative maintenance treatments.

The automated pavement data collection provides an excellent opportunity to investigate the safety effectiveness of pavement condition. Thanks to the significant improvements in the consistency and efficiency of pavement condition data, assessments, engineers are able to track historic pavement condition information now. This progress facilitates safety research regarding the effect of pavement conditions on crash frequency and severity. It will provide DOTs with information that will allow them to include safety in the pavement management decision making process.

1.2 Research Motivations

With shrinking budgets after the economic crisis, transportation agencies have strong incentives to maximize the returns on their investments in highway systems. The work of this dissertation can help to enhance DOTs' investments in pavement maintenance and connected vehicle programs, either through exploring a low-cost pavement condition measurement application under a connected vehicle environment or extending the capability of current pavement condition data to account for safety.

The connected vehicle-enabled pavement condition assessment approach offers opportunities to improve the current pavement assessment practice. First, it allows more frequent updates of roughness data and wider network coverage. Currently, it takes most transportation agencies at least a year to update the network roughness information due to budget constraint (*10*). As a result, the pavement maintenance decision making is based on information that are months or even years old, which may be very different than the current condition. Under a connected vehicle environment, it is likely that DOTs can obtain near-real-time pavement roughness information, which can result in faster and more efficient pavement repair and maintenance.

In addition, the data collection can be completed with minimal cost as it is a byproduct of people's daily trips. The required data collection devices are low-cost and already installed in many vehicles and most smartphones. In addition, the BSM, which is essential for connected vehicle safety and mobility applications, contains all necessary data elements for accessing pavement roughness. No additional data collection efforts are needed if the connected vehicle program is implemented in the future.

Studying the safety effect of the general pavement condition will fill the gap between traditional pavement management activities and highway safety research. Originally, the pavement condition indexes calculated from the automated collected data are intended to help transportation agencies make decisions based on assets management targets. However, it can also be linked to crash history and other roadway features and thus evaluate safety effects of pavement conditions. Given the information, transportation agencies will be able to incorporate safety objective into pavement maintenance applications, such as prioritizing sites for the agency's annual paving program or quantifying the benefits of preventative maintenance treatments.

1.3 Objectives and Scope

The overall goal of this dissertation is to improve pavement assessment and management activities. To accomplish this goal, exploratory analyses were conducted to address three specific objectives, with the first two objectives focusing on connected vehicle as an opportunity to improve current pavement assessment practice and the third objective demonstrating a new way to use data beyond current pavement management practice.

Several past efforts investigated the feasibility of assessing pavement roughness based on probe vehicle data (i.e., acceleration and GPS data) collected under controlled environments (*11*, *12*, *13*). They found that the vehicle vibration responses, or the acceleration data, correlate very well with the International Roughness Index (IRI), the most commonly used pavement roughness index. One critical issue about the acceleration-only index is that its value depends on a combined effect of vehicle operating speeds, vehicle dynamic features, and pavement characteristics (i.e., wavelength). The expected data source of the connected vehicle-based pavement condition measurement is the numerous general vehicles naturalistically running on the road. In the real world, vehicles will encounter different surface types, changing speeds, divergent travel paths and other factors which may cause variations in terms of vehicle-body vibration responses and result in very different acceleration datasets. It is therefore necessary to extend previous studies to a real world situation to investigate the feasibility of identifying deficient pavements using the connected vehicle-enabled application. The first two objectives focus specifically on the two most significant impact factors of vehicle vibration responses: vehicle speeds and vehicle dynamic systems. It is important to note that the goal of this study is not to propose a new method to replace the current IRI practice, but to improve current practice by introducing a supplemental method for pavement roughness assessment.

The intent of the third objective is to quantify the safety effect of the general pavement conditions and thus provide DOTs with information that will allow them to include safety in the pavement management decision making process. It is not intended to be used as a justification to repave a road section that has a demonstrated pavement friction problem. The effect of pavement condition on both overall crash frequency and crash severity was examined. The targeted facility type is segments on rural two-lane primary highways in the Commonwealth of Virginia. The

Empirical Bayes (EB) approach was applied using data from VDOT databases, including roadway inventory information, crash history, and pavement condition between 2007 and 2011.

In summary, the three related objectives are listed below and they were addressed in three related papers, as presented in Chapters 3, 4, and 5.

- Paper 1: Present and evaluate a data processing method that is able to estimate pavement roughness based on acceleration data collected under naturalistic driving situations (with changing speed),
- Paper 2: Investigate the impacts of vehicle dynamic systems and develop a procedure to calibrate individual vehicles to reduce the variety of data from different vehicles, and
- Paper 3: Quantify the safety effectiveness of good pavement conditions versus deficient pavement conditions.

1.4 Dissertation Layout

The three-paper format was applied in this dissertation. This dissertation consists of six chapters, including the general introduction presented in this chapter, which introduces the research problem, motivations, and objectives. Chapter 2 contains a comprehensive literature review that gives a view of current pavement management and assessment activities, the connected vehicle program, as well as several theoretical foundations such as the EB method and the calculation of the IRI.

The first objective was addressed by Paper 1 presented in Chapter 3. This chapter introduces and evaluates an improved acceleration-based metric to identify deficient pavement sections. The effect of vehicle speeds was investigated and incorporated into the proposed metric.

Chapter 4 covers Paper 2 that addressed the second objective. This chapter presents the analysis results regarding the impact of vehicle dynamic systems and proposes a procedure for transportation agencies to calibrate its fleet vehicles if necessary.

Chapter 5 presents Paper 3 to address the last objective of this dissertation. It applied the EB method to quantify the safety effects of good pavement conditions versus deficient pavement conditions on rural two-lane undivided highways in Virginia. The chapter covers the details from research design and data collection to conclusions and recommendations.

The last chapter summarizes this dissertation. It discusses the findings and limitations of the three studies, delivers recommendations, and provides suggestions for future research.

1.5 Attribution

Dr. Brian Smith, professor of civil engineering at the University of Virginia and dissertation advisor, aided in the organization, conceptual design, and execution of the research discussed in Chapters 3, 4, and 5; therefore, is listed as a co-author in all three Chapters. Dr. Mike Fontaine, associate principal research scientist at the Virginia Center for Transportation Innovation and Research, is listed as a co-author in Chapters 3 and 5 for his assistance in research design, data collection and manuscript review. Dr. Hyungjun Park, senior scientist at the University of Virginia Center for Transportation Studies, is listed as a co-author of both studies presented in Chapters 3 and 4 for his contributions to the organization, conceptual design and manuscript review. Mr. Kevin McGhee, associate principal scientist at the Virginia Center for Transportation Innovation and Research, is listed as a co-author for Chapter 3 for providing insights in pavement management systems and resources for pavement condition data collection, and reviewing manuscript.

CHAPTER 2 LITERATURE REVIEW

This Chapter presents the results from a literature review to show the background and theoretical foundation for this dissertation. The following sections focus on reviewing current pavement roughness assessment practice, the calculation of IRI, relationship between IRI and vibration-based measurement, probe-based pavement roughness measurement, the connected vehicle program, the EB approach, and pavement-related safety studies.

2.1 Current Pavement Management and Assessment Practice

Pavement condition assessment is generally known as the assessment of pavements for the purposes of maintaining level of service and choosing the appropriate maintenance practices associated with a pavement section (*14*). Thanks to decades of development in pavement assessment method, the main method has been changed from windshield survey to automated data collection. Compared with windshield survey, the automated methods significantly improve pavement data consistency by limiting subjective visual scans.

Currently, pavement condition data in Virginia are collected using automated methods conducted by a contractor (*2*, *15*). The system relies on advanced computing technology and a multitude of sensors and equipments (including high-speed lasers, cameras and accelerometers) to collect rutting, cracking, roughness, texture, and surface distress information for translation into pavement performance indices (*3*). To assess the network roughness condition, Fugro Roadware (VDOT's current contractor) uses its instrumented vans to measure roadway profiles and take images of the surface every year for the interstate and primary highway systems and every five years for the secondary systems. The two most important pavement performance indexes are the Critical Condition Index (CCI) and the IRI, which indicate the general pavement condition and the pavement roughness, respectively.

FIGURE 2.1 Fugro data collection van and interior environment (*16*).

CCI was first derived in 1998 by the US Army Corps of Engineers (*15*). CCI is represented on a scale of 0 to 100, with 100 representing a pavement with no visible distress. For asphalt pavements, the CCI is calculated based on alligator cracking, longitudinal cracking, transverse cracking, patching, potholes, delaminations, bleeding, and rutting (*2*). The details of the CCI calculation methodology are provided in a VDOT report published in 2002 (*17*). VDOT does not collect friction data on a systematic basis at this time, although that capability is under investigation. Friction may or may not be correlated with the CCI. If cracking is driving CCI at a site, then friction factor and the CCI may be correlated. If rutting is driving CCI, then friction may not be correlated with the CCI.

IRI is defined by the American Association of State Highway and Transportation Officials (AASHTO) and the American Society of Testing and Materials (ASTM). By definition, IRI is the accumulated suspension stroke in a mathematical car model divided by the distance traveled by the model during a simulated ride on a pavement section whose profile is measured (*18*). It is recorded in inches per mile (in/mile), or meters per kilometer (m/km). IRI was chosen as the standard reference roughness index of the Highway Performance Monitoring System (HPMS), a national database of roadway information kept by the Federal Highway Administration (FHWA). According to HPMS Field Manual, the primary advantages of the IRI include (*19*):

- it is a time-stable, reproducible mathematical processing of the known profile;
- it is broadly representative of the effects of roughness on vehicle response and user's perception over the range of wavelengths of interest, and is thus relevant to the definition of roughness;
- it is a zero-origin scale consistent with the roughness definition;
- it is compatible with profile measuring equipment available in the U.S. market;
- it is independent of section length and amenable to simple averaging; and
- it is consistent with established international standards and able to be related to other roughness measures.

For the purpose of pavement maintenance, VDOT uses CCI and IRI for overall awareness of road condition in terms of pavement condition and ride quality/roughness and awarding contractor payments according to final project roughness readings (*15*). Table 2.1 below shows the qualitative pavement condition and ride quality terms and corresponding quantitative CCI and IRI. Note that the IRI rating depends on the functional class of the roadway.

TABLE 2.1 Ride Quality Category Based on IRI Rating (*15*)

Pavement Condition/ Ride Quality	CCI Scale	IRI Rating (inch/mile)	
		Interstate & Primary	Secondary Roads
Excellent	≥ 90	< 60	< 95
Good	70 - 89	60 - 99	95 - 169
Fair	60 - 69	100 - 139	170 - 219
Poor	50 - 59	140 - 199	220 - 279
Very Poor	< 50	≥ 200	≥ 280

A pavement with a CCI value lower than 60 is considered as deficient in terms of pavement condition. Interstate and Primary pavement sections with an average IRI of 140 or more or a Secondary pavement section with an average of IRI of 220 or more are considered 'deficient' in terms of ride quality (*15*). Every year VDOT makes its maintenance activity decisions for the pavement system based on both CCI and IRI information. The maintenance activities include Do Nothing, Preventive Maintenance, Correlative Maintenance, Restorative Maintenance, and Rehabilitation/Reconstruction. CCI is applied as the primary reference index for a selection of maintenance activity and IRI is used to enhance the selection (*20*). Table 2.2 shows the recommended maintenance activities based on CCI and IRI ranges for asphalt-based surfaces.

TABLE 2.2 Recommended Maintenance Activities based on CCI and IRI Ranges (*20*)

Maintenance Activity Category	Index Ranges	
	CCI	IRI
Do Nothing (DN)	> 85	--
Preventive Maintenance (PM)	70 - 85	< 140
Corrective Maintenance (CM)	50 - 70	140 - 200
Restorative Maintenance (RM**)**	30 - 50	200 - 250
Rehabilitation/Reconstruction (RM**)**	≤ 30	≥ 250

Besides supporting pavement maintenance decision-making, VDOT also awards contractor payments according to final project IRI readings (*21*). As an example, the current pay adjustment chart on Secondary road projects based on IRI can be found in Table 2.3 below.

TABLE 2.3 IRI to Pay Adjustment Chart on Secondary Road Projects *(21)*

IRI After Completion	Pay Adjustment (% Unit
55.0 and Under	115
55.1-65.0	110
65.1-80.0	100
80.1-90.0	90
90.1-100.0	80
100.1-110.0	70
110.1-130.0	60 or Subject To Corrective
130.1-150.0	40 or Subject to Corrective
150.1-170.0	20 or Subject to Corrective
Over 170.1	0 or Subject to Corrective

2.2 Calculation of International Roughness Index

Since the IRI was used as the reference index to evaluate the performance of the proposed methods in Chapters 3 and 4, it is necessary to understand how it is created. This section gives a brief introduction about the calculation of IRI.

The quarter-car simulation model mandated by the ASTM for calculation of IRI uses physical movement and resistance relationships to evaluate the movement of a wheel, tire, and suspension system. The essential physics of the quarter-car model involve two masses (vehicle and wheel/tire/axle) and two springs (tire and the suspension), as shown in Figure 2.2. This model is the basis for calibration of response-type roughness measuring equipment and provides "a means for evaluating traveled surface-roughness characteristics directly from a measured profile (*22*)." The quarter car parameters for masses, damping and stiffness are set to represent a reference passenger car, "the Golden Car". The parameters (normalized to $m_s = 1$) for the Golden Car are (*18*):

$c_s = 6.$ [1/s], $k_t = 653$ [1/s2],

$k_s = 63.3$ [1/s2], $m_u/m_s = 0.15$

The simulated speed v is set to 80 km/h, or 50 mph. The calculation of IRI is expressed mathematically as (*18, 23*):

$$\text{IRI} = \frac{1}{L}\int_{0}^{L/v} |\dot{z_s} - \dot{z_u}|dt$$

Where:
v = simulated speed, set to 80 km/h;
L = Length of the profile (i.e. 0.1 mile);
$\dot{z_s}$= Vertical velocity of the quarter-car sprung mass (m/s), its value is determined by measured profile and the Golden Car parameters;
$\dot{z_u}$= Vertical velocity of the quarter-car unsprung mass (m/s), determined by measured profile and the Golden Car parameters;
dt = Small increment of time (s), as defined by the definite integral.

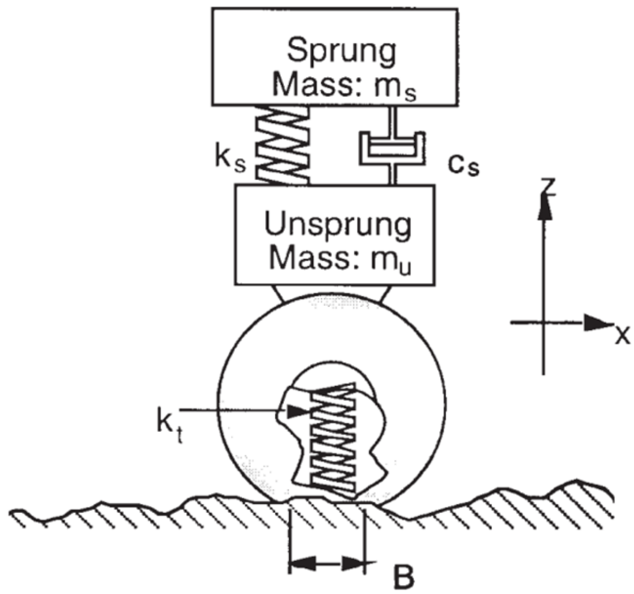

FIGURE 2.2 The Quarter-car Simulation Model (*18*).

In terms of obtaining an accurate profile, ASTM publication E950-9 covers the standard process for measuring the profile of vehicular traveled surfaces with an accelerometer-established inertial reference on a profile-measuring vehicle (*24*). The HPMS Field Manual also gives guidelines for collection of roughness data, including collecting data when pavement is stable (not in a freeze/thaw or wet state), collecting in the outside lane when practical, maintaining constant speeds, and excluding the impacts of bridges, railroad crossings, or other road features which are not representative of the overall roadway (*19*). IRI data on the lower functional systems (rural and urban collector and urban minor arterial) are only “recommended” since it may not be possible to obtain meaningful roughness measurements with profiling equipment due to problems such as low speed (less than 25 mph), traffic congestion and safety (*19*).

2.3 IRI and Body-Vehicle Vibration Response

Road roughness is the main contributor of the experienced in-vehicle vibration, which impacts drivers/passengers' ride quality directly. As a result, people can link IRI closely with body-vehicle vibration. Many studies have been done to quantify the relation between the IRI and measured or simulated body-vehicle vibration response and to identify the IRI limits based on ride quality.

Ahlin and Cranlund derived the analytical relationship between car floor vertical acceleration root mean squared (RMS) value (a_{floor}) and the IRI (*25*). The reference quarter-car model for the IRI computation was used for simulating the car floor acceleration. A velocity of the model and the waviness of the road elevation were concerned in the derived relationship. It was also shown that there can be a difference by a factor of 30 between the worst and best vibration response for the same IRI value. Another study by Magnusson et al. studied the correlation among road roughness indicators (IRI and road profile elevation RMS values in different wave bands) and the front wheel vertical acceleration RMS value (a_{fw}) for field-test measurements on 45 test sections along a 60-km route (*26*). Two instrumented vehicles were used: the Volvo 245 passenger car and the Scania 94 heavy truck. It was found that the acceleration level over all test sections were approximately the same in both vehicles. The regression curves were also generally similar and both had good correlation with IRI. More studies were conducted to examine the relationship between IRI and vehicle vibration response based on simulated vehicle models. Prem and Ayton applied a two-axle longitudinal passenger half-car model with 6 degrees of freedom (DOF) (*27*). They estimated a linear relation between the RMS value of the frequency-weighted vertical acceleration on the driver's seat (a_{wd}) and IRI based on data from 10 test sections. Cantisani and Loprencipe investigated the relationship between IRI and the RMS value of frequency-weighted vertical acceleration on the driver's seat under variant operational speeds (*28*). An 8-DOF full car model of the Fiat Stilo passenger car was used. Profiles of 124 real test sections with a length of 320 m were processed at simulation environments with velocities scaling from 30 to 90 km/h. The results show that although all acceleration levels correlated very well with IRI, their magnitude can vary significantly under variant vehicle speeds.

TABLE 2.4 Probable Reactions in Public Transportation (*25, 26, 27, 28*)

Source	Vehicle/Simulation Model	Velocity (km/h)	Regression Relationship	*R*
Ahlin and Granlund	2-DOF car model	--	$a_{floor} = 0.16(v/80)^{(w-1)/2}$IRI	-
Magnusson et al.	Volvo 245 (Instrumental)	70	a_{fw} = 0.9197IRI+0.0935	0.887
	Scania 64 (Instrumental)	70	a_{fw} = 0.9226IRI+0.0402	0.927
Prem and Ayton	6-DOF passenger half-car	80	a_{wd} = 0.0844IRI+0.0355	0.956
Gantisani and Loprencipe	8-DOF passenger full-car	30	a_{wd} = 0.08IRI	0.866
		50	a_{wd} = 0.11IRI	0.943
		60	a_{wd} = 0.17IRI	0.964
		80	a_{wd} = 0.22IRI	0.949
		90	a_{wd} = 0.27IRI	0.894

Table 2.4 summarizes the models and results in these studies. All models have indicated a good correlation between IRI and vibration-base measurements, with the correlation coefficients ranging from 0.887 to 0.964. Theoretically, the values of speed and vehicle dynamic parameters are unlikely to have significant impacts of the correlation level between IRI and vibration-base measurements. However, they will change the actual relationship. For example, in Gantisani and Loprencipe's study, the coefficient of IRI changed from 0.08 to 0.27 when the simulated speed changed from 30 to 90 km/h. It also indicates that the expected vibration will increase with speed when the roughness level, or IRI, remains the same. According to Ahlin and Granlund's study, it is possible that one can still compare the vibration responses with different travel speeds by calibrating the vibration measurement with a speed factor. This idea will be tested in this dissertation research. It is also important to note that all models in Table 4 were based on a constant speed ranging from 30 to 90 km/h. In real world, the vehicle speed is expected to change even if it travels in a same pavement section. Previous studies did not investigate how the variation of speed will impact the correlation between vibration-base measurement and IRI. When examining the relationship between vibration-based roughness measurement and IRI, the variation of speed will be taken into consideration in this dissertation research.

2.4 Probe-Base Pavement Roughness Assessment

A considerable amount of work has been completed to improve the concept of using inexpensive vehicle or smartphone sensors to assess pavement roughness condition. In 2010, the Michigan Department of Transportation (MDOT) started to demonstrate and evaluate a system to monitor slippery roads and road surface roughness based on probe data (*11*). A Droid phone platform, mounted on the windshield similar to a navigation device, was used to collect vehicle data and transmit it to a backend server. The platform mainly collected four kinds of data: vehicle Controller Area Network (CAN) messages; external road surface temperature and humidity (added external sensors); GPS position (from the Droid phone); and 3-axis accelerometer data (from the Droid phone). The system was installed in two vehicles, driven by MDOT employees over a two year period (from 2010 to 2012). Over 13 giga bytes of data have been accumulated over 30,000 miles. In that project, variance of the vertical accelerometer signal was chosen as the metric to represent pavement roughness. The sample rate of the accelerometer is 100 HZ. After collection, the accelerometer readings were calibrated, using a curve fitting algorithm, to a 10-point scale known as the Pavement Surface Evaluation and Rating (PASER) system. The research team recommended refining the curve fitting algorithm with future data from MDOT's annual PASER rating study.

A research team from Auburn University investigated the application of using vehicle-based sensors assess pavement condition (*12*). The main focus of the study was to utilize vehicular sensors to estimate the IRI. In addition, detection and mapping of potholes was addressed. Several vehicular sensors including accelerometers, gyroscopes, and suspension deflection meters were tested to estimate the IRI. Testing was conducted under controlled speed on a 1.7 mile (2,750 m) long test track at the National Center for Asphalt Technology (NCAT). The team hoped that those sensors could capture the vibrations of a running vehicle, which can represent pavement roughness. The amount of overall vibrations across a given segment was determined by taking the root mean square (RMS) of a signal measurement. The overall vibrations were then compared with the true IRI of the pavement segment. The resulting data indicated that the RMS of vertical accelerations represents the best case scenario to capture the true IRI. It displayed the same trend of the known IRI, with only a few expected differences in magnitude. The study also indicated that the estimation error increases with decreasing window size and thus recommended to use larger windows when possible to assure the most accurate IRI estimates. In conclusion, this study found that the most feasible application to estimate the IRI is to implement a root mean square algorithm on vertical acceleration measurements.

In 2011, Flintsch et al. conducted a pilot study using probe vehicles to measure road ride quality, or roughness (*13*). Again, vertical acceleration data were used as an index of vehicle vibration. A smoothness profile was obtained using an inertial-based laser profiler, while the vertical accelerometer measurements were obtained using a vehicle instrumented with an accelerometer at the Virginia Smart Road facility in Blacksburg, Virginia. The accelerometer operated at a rate of 10 HZ. GPS positions were also recorded. A total of four runs were completed on the test track to collect acceleration data. The study confirmed that the acceleration runs are very repeatable. Analysis using the coherence function indicates that the acceleration data linearly correlate well to road profile between wavelength 50 and 300 m.

Another study conducted by the Center for Transportation Studies at the University of Virginia has extended this work to investigate system-level designs to extend the technical feasibility to a "system" that could support transportation agency pavement management (*3*). This project researched and discussed the technical feasibility and characteristics of three potential probe-based pavement roughness assessment systems: a) a system using intelligent transportation system (ITS) and connected vehicle technology, b) a system using a vehicle-installed accelerometer and communications system instrument package, and c) a system using smartphone devices containing accelerometers. The third approach was identified as the most appropriate system in the near future given the relative easier implementation and a large and expanding market share of smartphone. The study also addressed that such a data-gathering system will increase frequency of pavement roughness data collection, increase the number of lane-miles of monitored roadways, decrease lag time from collection to interpretation, and add to the information available to transportation professionals.

In 2013, a study from North Dakota State University (*29*) derived a theoretical relationship between IRI and accelerometer data for a connected vehicle approach for pavement roughness estimation. The research introduced the road impact factor (RIF) which is derived from vehicle integrated accelerometer data. A time-wavelength-intensity-transform (TWIT) algorithm was also developed to create a wavelength-unbiased measurement based on RIFs from different speed bands. The analysis demonstrates that RIF and IRI are directly proportional. Profile and acceleration data were collected from six runs with a constant speed (55.6 km/h) on a 150-meter pavement section in Minnesota to validate this relationship. The author concluded that the proposed application enables low-cost, network-wide and repeatable performance measures at any speeds. No discussion were provided on sample size and sampling rate for acceleration data collection.

2.5 The Connected Vehicle Program and Basic Safety Message

The connected vehicle program will provide a great opportunity to improve pavement roughness assessment thanks to its data-gathering capability. According to USDOT, the program focuses on "intelligent vehicles, intelligent infrastructure, and the creation of an intelligent transportation system through integration with and between these two components." (*5*) Connected vehicle applications will provide a connected, data-rich travel environment by capturing data from equipments located on-board vehicles and within the infrastructure. As presented in the figure below, there are two basic communications components to the connected vehicle program: Vehicle to Vehicle (V2V) communications and Vehicle to Infrastructure (V2I) communications. V2V uses information contained in a wireless message transmitted from vehicle to vehicle, and helps prevent crashes and injuries by activation of warnings for the driver or other vehicle safety systems. V2I communications require road-based infrastructure, and involve communications from vehicles to fixed-position devices which are in turn connected to a network or the internet.

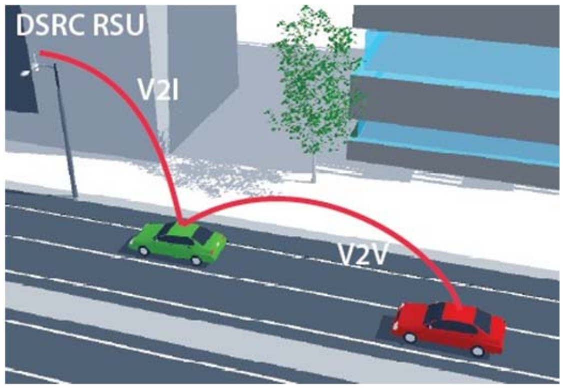

FIGURE 2.3 Connected vehicle application.

Currently, the connected vehicle research primarily focuses on safety, mobility and environmental improvements (*5*). To serve these purposes, standardized communication methodology has been published. The Society of Automotive Engineers (SAE) has published a document which outlines the methodology and data elements for connected vehicle communication: the J2735 Dedicated Short Range Communications (DSRC) Message Set Dictionary. It was found that data from the key data set can also serve for pavement condition monitoring as it includes all data element required for estimating pavement roughness. The building block of safety systems according to J2735 standard message set is the basic safety message (BSM), which is a pre-determined set of elements critical for safety use. Also described as the "Here I Am" message, the BSM contains data from vehicle sensors at an instant in time, and includes information on vehicle position, speed and acceleration, yaw rate, brake status, and vehicle specifications (*6*). The broadcast spatial interval varies with speed or roadway conditions; by default the BSM is broadcast every 0.1 second (100 ms or 10 Hz).

2.6 The Empirical Bayes Method

This section presents an overview of the Empirical Bayes (EB) method, which is the state-of-the-art method for highway safety analysis. Observational before-after studies have been considered the industry standard for the safety evaluation of treatments such as developing Crash Modification Factors (CMFs). Harwood et al. documented that there are three common ways to carry out a before-after study: naïve before-after evaluations, comparison group evaluations, and the EB approach (*30*). Of these three methods, the EB approach was recommended in the first edition of Highway Safety Manual (HSM) (*31*), which provides transportation professionals a guideline of a science-based technical approach to quantitative safety analysis.

According to Hauer, the EB method is able to account for regression-to-the-mean effects, as well as traffic volume and other roadway characteristic changes, by combining safety performance function (SPF) estimates with the observed count of crashes *(32*). Regression-to-the-mean is the natural tendency of observed crashes to regress (return) to the mean in the year following an unusually high or low crash count (*32*). This advantage allows the EB approach to overcome the limitations faced by the other two evaluation methods and provide more accurate estimates of safety effects.

The EB approach precisely predicts the number of crashes that would have occurred at an individual treated site in the after period if a treatment was not implemented (E_A). Safety effectiveness is estimated by comparing the total crash prediction for all treated sites if no treatments applied with the observed number of crashes in the after period (*32*).

A critical step is to predict E_A, which is based on the number of crashes expected in the before period without the treatment (E_B). E_B is a weighted average of information from two sources (*33*):

- The observed number of crashes in the before period at the treated sites (O_B), and
- The crashes predicted at the treated sites based on reference sites with similar traffic and geometric features (N_B).

N_B can be calculated using Safety Performance Functions (SPFs) that indicate crashes' relationships with traffic volume and geometric features. SPFs regressed from information of an untreated "reference" group. Sites in the reference group have similar features as treated sites in the becfore period. As a result, N_B represents the "mean" frequency of crashes of the study sites. Figure 2.4 shows how EB estimation works for a single site.

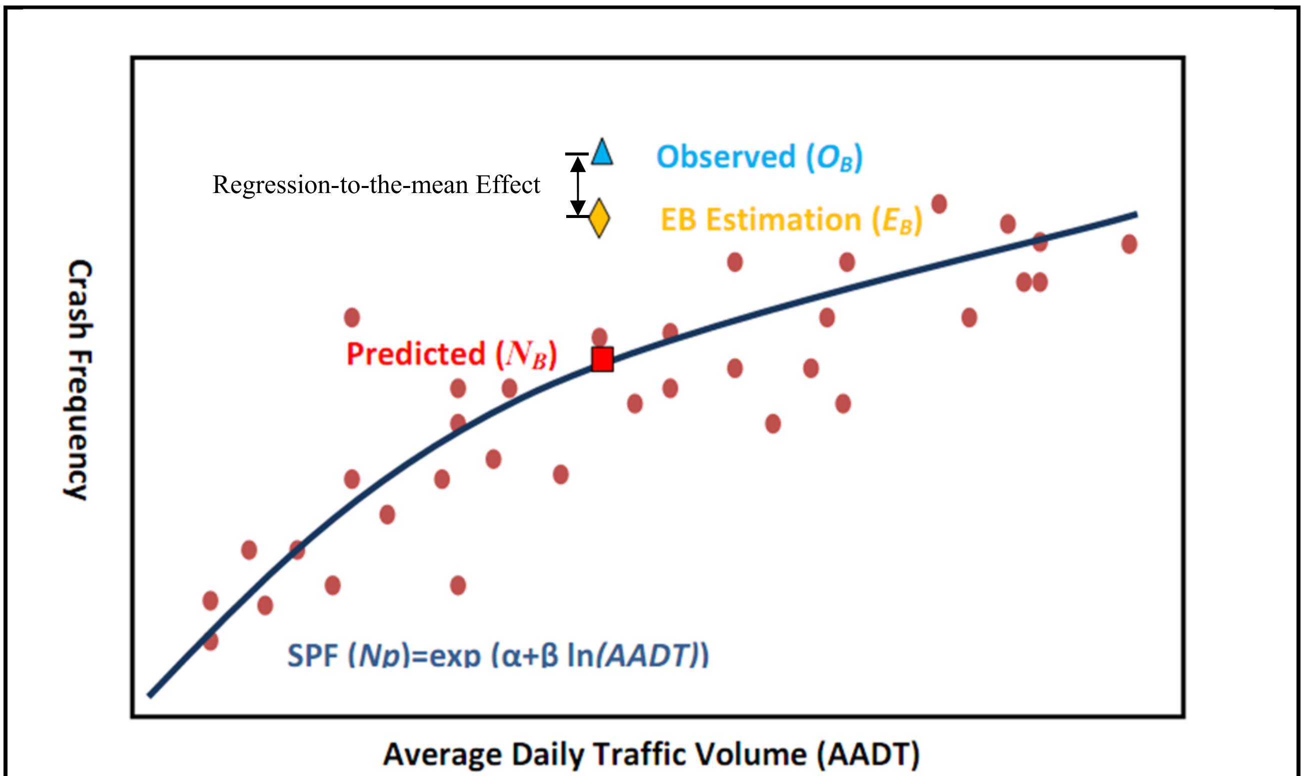

FIGURE 2.4 Illustration of regression-to-the-mean and the EB estimation (*33*).

As shown in Figure 2.4, E_B falls somewhere between the values of O_B and N_B. Regression-to-the-mean effect is the difference between observed crashes and EB estimation. A ratio is calculated by dividing the predicted crash frequency of the treated sites (N_A) in the after period by that in the before period. In order to estimate the expected crashes in the treatment group had no treatment been applied, the EB estimated crash frequency in the before period in a treatment group is multiplied by the ratio. Note that more detail about the EB method will be discussed in Chapter 5.

2.7 Pavement-related Safety Studies

While there has been a longstanding interest in examining the impact of pavement condition on safety, there are relatively few studies that have examined this issue in detail. Initial investigations in the late 1980s examined the effect of resurfacing. A synthesis by Cleveland of published evidence from studies conducted before 1986 found that there was a small, immediate increase in overall crash frequency for rural resurfacing projects conducted to address structural quality or poor ride condition (*34*). On the other hand, it was found that there was an average reduction of about 20 percent in wet pavement crashes for resurfacing projects conducted due to high numbers of wet pavement crashes (*34*). In light of these diverse findings, Cleveland concluded that the detrimental effect of resurfacing on safety, if any, is likely to be small. A related hypothesis was that vehicle speed will increase due to the smoother pavement surface after resurfacing, which, in turn, results in more crashes.

A well cited report by Hauer et al applied the Empirical Bayes (EB) approach to evaluate the safety effectiveness of two types of resurfacing projects undertaken in the early 1980s in New York State (*35*). Crash data and annual average daily traffic (AADT) from 1975 to 1987 were used. The study concluded that non-intersection crashes did increase by 21 percent during the first 30 months after resurfacing on “fast-track” projects in which no safety improvements accompanied the repaving, while non-intersection crashes did not change on reconditioning and preservation (R&P) projects that included geometric safety improvements. Another conclusion was that within the first 6 to 7 years of pavement life, safety improves as the pavement ages. In this study, no pavement condition data were collected and information about NYDOT’s selection criteria regarding the two types of resurfacing projects were not mentioned.

To confirm or refine the Hauer et al study results, a larger study was undertaken in NCHRP project 17-9 (2), which involved five states: Washington, California, Minnesota, New York, and Illinois (*36*). The EB approach was used. Generally, there were five-years of before data and three-years of after data. The results were inconclusive, as there was not a single consistent pattern of safety effectiveness of resurfacing among and within the states. Crashes were found to increase after resurfacing in some states, but to decline in others. In addition, no explanation was found for these state-to-state variations.

Given the hypothesis that smother pavement surfaces following resurfacing lead to higher vehicle speeds, another NCHRP study evaluated the effect of resurfacing, restoration, and rehabilitation (RRR) projects on travel speed (*37*). Speed data were collected before and after resurfacing at 39 sites on rural two-lane highways of five states: Maryland, Minnesota, New Mexico, New York, and West Virginia. The results indicated that overall there was a small but statistically significant increase of approximately 1.6 km/h (1 mph) in both the mean speed and 85^{th} percentile speed after resurfacing. However, this effect varied substantially from site to site. No explanation was found for these site-to-site variations. In addition, no further analysis was conducted regarding the relationship between the change in speed and the change in crashes.

A 2011 study applied the cross-sectional method to investigate the efficacy of roadway improvements in terms of crash reduction on various subclasses of rural two-lane highways (*38*). Data were collected from 540 rural two-lane highway segments in the state of Indiana. The factors in the crash prediction model included lane width, shoulder width, pavement surface friction, pavement condition, and horizontal and vertical alignments. The effect of pavement friction in crash reduction was found to be significant for rural major collectors and rural minor arterials, but insignificant for rural principal arterial two-lane roads. It was also found that increased skid resistance impacted severe crashes more than non-severe crashes as the roadway functional class increased. The Present Serviceability Index (PSI), on a scale of 0 to 5, was used to represent pavement condition. The model results showed that better pavement condition significantly reduced crashes for rural two-lane principal arterials, but the effect was insignificant for the two lower road classes. One concern about this study is that there may be a multicollinearity issue in the models as pavement condition may correlate with pavement friction and this issue was not discussed in the paper.

2.8 Summary of Literature Review

Findings from the literature review have revealed the importance of assessing pavement roughness, limitations of current practices, opportunities from the development of connected vehicle technology, and the possibility of exploring a new way to use pavement condition data.

First, pavement condition assessment is playing an essential role in pavement management system. In network level, it helps to identify deficient pavement sections and support DOTs' maintenance decision making. In project level, DOTs can also award contractor payments according to final project pavement condition data. The two most important pavement condition indexes are CCI and IRI, which represent the general condition and roughness/ride quality, respectively. Due to its need of special data collection equipment and complex data processing mathematical method, transportation agencies cannot afford the time and expense necessary to collect pavement data more frequently than once per year. The connected vehicle program will create a great opportunity to overcome the limitation of current practice. This connected, data-rich environment will allow for innovative connected vehicle applications for transportation infrastructure maintenance. It is possible to collect segment-based pavement roughness information (including all travel lanes) more frequently with a minimum additional cost.

Previous study results reinforce that using a connected vehicle approach for pavement roughness data collection is promising and a cost-effective approach. According to previous research, implementing a root mean square (RMS) algorithm on vertical acceleration measurements could provide the better level of precision. However, it should be noted that most of the studies so far have been conducted based on data collected under controlled and closed environments and very few of them have discussed about the impact of vehicle speed and vehicle dynamic system. In the real world, vehicles will encounter different surface types, change speeds, a good variety of vehicle dynamic systems, and other variant situations, which may cause variations in terms of vehicle-body vibration responses and result in very different acceleration datasets. It is therefore necessary to take this concept to a real world situation to investigate its feasibility.

Traditionally, pavement maintenance is based on assets management condition targets but do not explicitly account for the role of pavement condition in roadway safety. Most of the previous pavement-related safety studies were event-driven, focusing specifically on the activity of resurfacing. The previous studies were not able to quantitatively track the pavement condition before and after the resurfacing projects due to lack of data, so the impact of remediating different levels of pavement distress could not be determined. Instead, some studies assumed the pavement conditions were consistent before the repaving project across sites. Since the pavement condition is sensitive to pavement age, traffic load, and other factors, this assumption could be problematic, especially when the duration of the before period is long. Also some previous studies assumed that the safety effectiveness is the same across facility types. However, the safety effectiveness of a change in pavement condition on rural two-lane highways could be very different with that on urban highways.

Thanks to progress in the automated collection of quantitative pavement condition data, it is now possible to link the pavement condition information to crash history and other roadway features. It provides an excellent opportunity to investigate the safety effectiveness of pavement condition, which could inform many DOT investments in pavement maintenance. Some recent research had examined this topic by including pavement condition as a crash factor in crash prediction models, but this approach cannot account for regression-to-the-mean effects. In addition, inaccurate results may be derived from the regression models due to inappropriate model forms, omitted variable bias, or correlation among variables (*33*).

CHAPTER 3 IDENTIFYING DEFICIENT PAVEMENT SECTIONS USING AN IMPROVED ACCELERATION-BASED METRIC

A paper accepted for presentation in the 2015 Annual Meeting of the Transportation Research Board, and revised and resubmit for publication in *Transportation Research Record*

Huanghui Zeng[1], Hyungjun Park[2], Michael D. Fontaine[3],
Brian L. Smith[4], and Kevin K. McGhee[5]

3.1 Abstract

Transportation agencies devote significant resources towards the collection of highly detailed and accurate pavement roughness data using profiler vans to support pavement maintenance decisions. However, they often cannot afford to measure roughness annually for the whole pavement network. This study introduces an improved acceleration-based metric, an index normalized by vehicle operating speed, to be used on a regular basis to "prescreen" pavement segments that are likely to deficient, and then a profile van can be sent to measure the accurate roughness condition.

A profile van collected pavement profile data on a total of 50 miles (80 km) of roadway, which was then used to calculate the International Roughness Index (IRI). Meanwhile, two tablets were placed on the vehicle floor to collect data, including 3-way accelerations, GPS coordinates, and vehicle speeds. A normalized acceleration-based index was created by incorporating a speed factor. Furthermore, logistic regression models were created to evaluate the effectiveness of the proposed index in identifying deficient pavement sections (IRI ≥ 140 in/mile or 2.21 m/km). It was found that the proposed acceleration-based metric is able to correctly identify between 80 and 93 percent of all deficient pavement sections.

In conclusion, this research points to the feasibility of using a cost-effective acceleration-based application for the purpose of network screening. The network screening process will reduce the total mileage of pavement sections that need to be measured and meanwhile still identify locations where maintenance work is necessary.

1 Graduate Research Assistant, Department of Civil and Environmental Engineering, University of Virginia, Charlottesville, VA22904, E-mail: hz3xm@virginia.edu.
2 Senior Scientist, University of Virginia Center for Transportation Studies, Charlottesville, VA22904, Phone: 434-924-1651, Email: hpark@email.virginia.edu.
3 Associate Principal Research Scientist, Virginia Center for Transportation Innovation and Research, Charlottesville, VA 22903, Phone: 434-293-1980, E-mail: Michael.Fontaine@VDOT.Virginia.gov.
4 Professor and Chair, Department of Civil and Environmental Engineering, University of Virginia, Charlottesville, VA22904, Phone: 434-243-8585, E-mail: briansmith@virginia.edu.
5 Kevin K. McGhee, Associate Principal Scientist,Virginia Center for Transportation Innovation and Research Charlottesville, VA 22903, Phone: 434-293-1956 E-mail: Kevin.McGhee@VDOT.Virginia.gov

3.2 Introduction

Transportation agencies have traditionally depended on measures of pavement roughness to support planning maintenance, repair, and rehabilitation work on the pavement system. Since the 1960s, many measures and measurement techniques have been developed. Currently one of the most commonly used measurements is the International Roughness Index (IRI) which was developed by NCHRP and the World Bank. IRI is computed based on the measured longitudinal profiles of a roadway (*39*). Given the need for specialized equipment and sensors, it is very difficult to collect this data at numerous locations in a timely and cost effective manner. For a large portion of the roadway system (i.e., secondary roadways and local systems), the roughness is usually measured infrequently, often only once every 3 to 5 years.

Highway transportation is undergoing significant technological transformations thanks to the emerging connected vehicle environment which enables vehicles to wirelessly communicate with other vehicles and with the infrastructure (*4*). This connected, data-rich environment will allow for innovative connected vehicle applications for transportation infrastructure maintenance. The use of simple sensors such as accelerometers, already installed either in vehicles or mobile devices, is able to directly measure the vehicle vibration responses, which is believed to highly correlate with pavement roughness. Several past efforts investigated the feasibility of collecting acceleration data to assess pavement roughness at a significantly lower cost and higher level of temporal resolution (*3*, *11*, *12*, *13*). One critical issue about the acceleration-only index is that its value depends on a combined effect of vehicle operating speeds, vehicle dynamic features, and pavement characteristics (i.e., wavelength). Thus, it is hard to generate reproducible roughness measurements under naturalistic driving conditions without considering this combined effect. On the other hand, it is cost prohibitive to develop specific acceleration-based models for each vehicle system and each type of pavement. As a result, totally replacing the current IRI practice with the acceleration-based index is not recommended, especially for applications requiring a high degree of accuracy (i.e., construction). However, if an acceleration-based metric can be developed by incorporating vehicle speed and be used as a supplementary method to current practice, it may help to address some of the current practice's limitations by providing more timely information to decision makers. For example, the acceleration-based metric could be used for network screening, which is a low-level practice that does not require highly accurate and detailed roughness measurements. One of the key concerns about the current IRI practice is that it is too costly to assess the whole system's pavement roughness condition once a year. The acceleration-based metric would help to identify pavement segments that are likely to deficient, and then a profile van can be sent to those flagged sections to measure the accurate roughness condition. Introducing a network screening process should be able to reduce the total mileage of pavement sections that need to be measured and meanwhile still identify locations where maintenance work is necessary.

To complete the network screening process in a cost-effective manner, the data should be generated through people's daily travel in common vehicles. Using smartphone or vehicular sensors appears to be a good way to collect data. A remaining question is whether those data can generate meaningful results for network screening under naturalistic driving conditions. In the real world, vehicles will encounter different surface types, changing speeds, divergent travel paths and other factors which may cause variations in terms of vehicle-body vibration responses and result in very different acceleration datasets. It is therefore necessary to take this concept to a real world situation to investigate its feasibility for identifying deficient pavements.

3.3 Objectives and Scope

The goal of this study is not to propose a new method to replace the current IRI practice, but to improve current practice by introducing a supplemental method for pavement roughness assessment. The focus is to demonstrate the feasibility of using an acceleration-based index to classify pavement roughness levels under "uncontrolled" real world driving conditions. Specifically, two objectives were addressed:

- Developed an acceleration-based metric by incorporating vehicle speeds, and
- Evaluated the effectiveness of using the acceleration-based metric to identify deficient pavement sections.

Note that the vibration response of a running vehicle is influenced by the vehicle operating speed, the vehicle dynamic system, and pavement roughness. This study addressed mainly the impact of vehicle speed, and an ongoing effort will investigate the feasibility of calibrating different vehicle systems in conjunction with the vehicle speed.

The background of current pavement roughness assessment practice, previous studies, methodology for the proposed application, and the analysis results will then be presented. Finally, this paper concludes with a summary of findings and recommendations for future studies.

3.4 Background

By definition, IRI is the accumulated suspension stroke in a mathematical car model divided by the distance traveled by the model during a simulated ride on a pavement section whose profile is measured (*18*). It is recorded in inches per mile (in/mile), or meters per kilometer (m/km). By applying a unit quarter-car model and simulating the vehicle response at a constant speed (80 km/h) on a known profile, the IRI is a reproducible index, making it outperform other pavement roughness measurements. IRI was chosen as the standard reference roughness index of the Highway Performance Monitoring System (HPMS), a national database of roadway information kept by the Federal Highway Administration (FHWA) (*19*).

Pavement condition data in Virginia are collected using an automated method that relies on advanced computing technology and a multitude of sensors and equipment (including high-speed lasers, cameras and accelerometers). To assess the network roughness condition, Fugro Roadware (VDOT's current contractor) uses its instrumented vans to measure roadway profiles every year for the interstate and primary highway systems and every five years for the secondary system. The profiles are later analyzed by a software package to determine the IRI value of the related pavement section. Although the final IRI is reported at every 0.1-mile (163 m), the profile data are recorded at a much smaller interval of less than 6 inches (*3*).

For pavement maintenance purpose, Virginia Department of Transportation (VDOT) uses IRI for overall awareness of road condition in terms of ride quality. Interstate and Primary pavement sections with an average IRI of 140 in/mile (2.2 m/km) or more or a Secondary pavement section with an average IRI of 220 in/mile (3.47 m/km) or more are considered 'deficient' in terms of ride quality (*15*). Every year, VDOT makes its maintenance activity decisions for the pavement system based on IRI and other pavement condition information.

3.5 Literature Review

This section first introduces a previous study regarding the relationship between vehicle vibration response, vehicle speed, and roughness, and then presents several recent studies that used smartphone-based or connected vehicle applications to monitor pavement roughness.

Ahlin and Cranlund derived the analytical relationship between the car floor vertical acceleration root mean squared (RMS) value and the IRI (*25*). The reference quarter-car model for the IRI computation was used for simulating the car floor acceleration. A velocity of the vehicle model and the Power Spectral Density (PSD) of the road profile elevation were taken into account within the derived approximate relationship. It was found that the conversion from IRI (m/km) to vertical vehicle vibration response in a quarter car can often be done using a factor 0.16, but depending on actual roughness wavelength and vehicle speed, the conversion factor ranges from 0.04 to 1.4. This indicates that there can be a difference of a factor 30 between different rides, given the very same IRI value.

A considerable amount of work has been completed recently to improve the concept of using inexpensive vehicle or smartphone sensors to assess pavement roughness conditions. A research team from Auburn University investigated the application of using vehicle-based sensors to assess pavement condition (*12*). The main focus of the study was to utilize vehicular sensors (accelerometers, gyroscopes, and suspension deflection meters) to estimate the IRI. Testing was conducted under controlled speed on a 1.7 mile (2,750 m) long test track at the National Center for Asphalt Technology (NCAT). The amount of overall vibrations across a given segment was determined by taking the root mean square (RMS) of a signal measurement. The overall vibrations were then compared with the true IRI of the pavement segment. The resulting data indicated that the RMS of vertical accelerations represents the best case scenario to capture the true IRI. The study also indicated that the estimation error increases with decreasing window size and thus recommended to use larger windows when possible to assure the most accurate IRI estimates.

In 2011, Flintsch et al. (*13*) conducted a pilot study using probe vehicles to measure road ride quality, or roughness. Again, vertical acceleration data were used as an index of vehicle vibration. A smoothness profile was obtained using an inertial-based laser profiler, while the vertical accelerometer measurements were obtained using a vehicle instrumented with an accelerometer at the Virginia Smart Road facility in Blacksburg, Virginia. The accelerometer operated at a rate of 10 HZ. GPS positions were also recorded. A total of four runs were completed on the test track to collect acceleration data. The study confirmed that the acceleration runs are very repeatable. Analysis using the coherence function indicates that the acceleration data linearly correlate well to smoothness profile between wavelength 50 and 300 m.

Bridgelall derived a theoretical relationship between IRI and accelerometer data for a connected vehicle approach for pavement roughness estimation (*29*). The research introduced the road impact factor (RIF) which is derived from vehicle integrated accelerometer data. A time-wavelength-intensity-transform (TWIT) algorithm was also developed to create a wavelength-unbiased measurement based on RIFs from different speed bands. The analysis demonstrates that RIF and IRI are directly proportional. Profile and acceleration data were collected from six runs with a constant speed (55.6 km/h) on a 150-meter pavement section in Minnesota to validate this relationship. The author concluded that the proposed application enables low-cost, network-wide and repeatable performance measures at any speeds. No discussion was provided on sample size and sampling rate for acceleration data collection.

In summary, the literature review reinforces the possibility of using vehicular or smartphone sensors as a cost-effective approach for pavement roughness data collection. According to previous research, implementing a root mean square (RMS) algorithm on vertical acceleration measurements could provide a better way to quantify the vehicle vibration response, which is believed to correlate with the IRI. However, special attention should be given that most of the studies so far have been conducted based on data collected under controlled and closed environments and therefore did not investigate the effects of vehicle speed, and did not address how DOTs might use the acceleration measurements. In the real world, vehicles will encounter different surface types, changing speeds, divergent travel paths and other conditions which may cause variations in terms of vehicle-body vibration responses and result in very different acceleration datasets. It is therefore necessary to transfer this concept to a real world situation to improve the acceleration-based metric and investigate its feasibility for identifying deficient pavements.

3.6 Methodology

The vibration response of a running vehicle is influenced by the vehicle operating speed, vehicle dynamic system, and pavement roughness. As for this study, an acceleration-based metric was developed by incorporating vehicle speeds so that the metric can account for most of the impact of vehicle speed variations and be applied to roadways with different functional classes and posted speed limits. Data were collected using a same vehicle and thus there were no variations in terms of vehicle dynamic system.

The two objectives were accomplished using the following three steps:

- Data collection on three functional classes of highways near Charlottesville, Virginia;
- Development of an improved acceleration-based metric by incorporating vehicle speed; and
- Develop classification models based on the proposed acceleration-based metric and evaluate their effectiveness in identifying deficient pavement sections.

3.6.1 Data Collection and Pavement Group Identification

A pick-up truck (GMC Sierra 2500 HD) with a RoLine profiler installed was used to collect pavement profile on 50 miles (80 km) of roadway segments. The collected profile was used to calculate the International Roughness Index (IRI). Meanwhile, two tablets (Samsung Galaxy Note 10.1) were placed on the vehicle floor to collect data, including 3-way accelerations, GPS coordinates, and vehicle speeds. The two tablets were placed on the floor in front of the second row seats and close to the two side doors so that both right-wheel-path and left-wheel-path data can be collected. To ensure the tablets do not dislocate themselves when the vehicle is running, they were fit into two boxes attached to the floor with tape.

The acceleration data were updated every 0.02 second, while the GPS and speed data were updated every 1 second. Only the vertical acceleration was used to quantify vehicle vibration responses. Each individual data record was matched to the milepost location through a map-matching process based on the GPS information. Acceleration data were aggregated using the RMS algorithm at the 0.1-mile (0.16-km) interval. It was found that the estimated GPS accuracy was between 4 and 8 meters, which is acceptable for estimating the roughness condition for every 0.1-mile (160-meter) pavement section. Vehicle speeds were also recorded every 1 second, allowing us to address the impact of speed on acceleration readings.

Data collection was conducted on April 22, 2014 near Charlottesville, Virgina. The studied segments contain three different functional classes of highway with asphalt-based surfaces. The roadway designs of these three types of highways are very different in terms of horizontal/vertical curves, grades, traffic control, cross sections, etc. The posted speed limits range from 30 mph to 70 mph (48.3 to 112.6 km/h) and data were collected under reasonable operating speeds. According to the HPMS Field Manual, low vehicle speed will bias the IRI measurements (*8*). As a result, this study only used data that were collected at a speed higher than 30 mph (48.3 km/h). The final dataset contained data on 35.7miles (57.5 km) of interstate freeways (IS-64 W/E), a 3.5-mile (5.6-km) primary highway segment (US-15) and 10.8 miles (17.4 km) of secondary roadway (SR) segments.

The collected IRI data were used as the reference value of pavement roughness. For general classification of road condition, VDOT identifies different roughness levels using corresponding quantitative IRI values (*9*). Note that transportation agencies may have different definitions for deficient pavement and thus may not have identical threshold values. As for this study, pavement sections with an IRI greater or equal to 140 in/mile (2.2 m/km) were marked as deficient sections. Table 3.1 summarizes the number of 0.1-mile sections in each roughness category according to VDOT's current policy. Of the total of 500 0.1-mile (0.16 km) pavement sections, there were 81 deficient sections. The IRI values range from 37.3 in/mile to 267.45 in/mile (0.59 to 4.22 m/km), while the speed ranges from 32 mph to 67.5 mph (51.5 to 108.6 km/h). The speeds measured from the two tablets were very similar, and thus the speed information was extracted from only one of the tablets.

TABLE 3.1 Data Summary based on Routes

Route	IRI Summary (in/mile)			Speed (mph)			Number of Sites		Length (mile)
	Med.	Min.	Max.	Med.	Min.	Max.	Deficient	Non-Def.	
IS-64E	75.5	45.5	256.8	65.9	63.9	67.5	16	162	17.8
IS-64W	76.9	37.3	267.5	64.8	64.0	74.3	17	162	17.9
US-15	82.6	63.4	125.5	52.4	50.2	54.1	0	35	3.5
SR-616	124.7	86.1	172.0	45.4	41.2	47.8	6	15	2.1
SR-600	121.2	85.7	219.3	40.8	34.0	50.4	9	25	3.4
SR-799	87.4	123.9	228.5	39.3	32.0	49.3	8	20	2.8
SR-676	189.9	151.8	248.2	40.5	33.5	45.8	25	0	2.5
Total	85.0	37.3	267.5	64.8	32.0	67.5	81	419	50

To investigate how the proposed methods will generalize to an independent data set, the whole dataset was divided randomly into a training dataset and a testing dataset, as suggested by Hastie et al. (*40*). The training dataset containing two-thirds of the data (335 observations) was used to develop the acceleration-based metric and the classification model; while the testing dataset (165 observations) validated the results. Figure 3.1 compares the box-plot of the three datasets in terms of IRI (in/mile), RMS acceleration (m/second^2), and speed (m/second). The Kolmogorov-Smirnov (K-S) test was applied to test whether the training and testing datasets were drawn from the same distribution (*41*), as shown in the right bottom of the figure. The box-plots and K-S test results indicate that there are no significantly different central tendency features between the training and testing datasets.

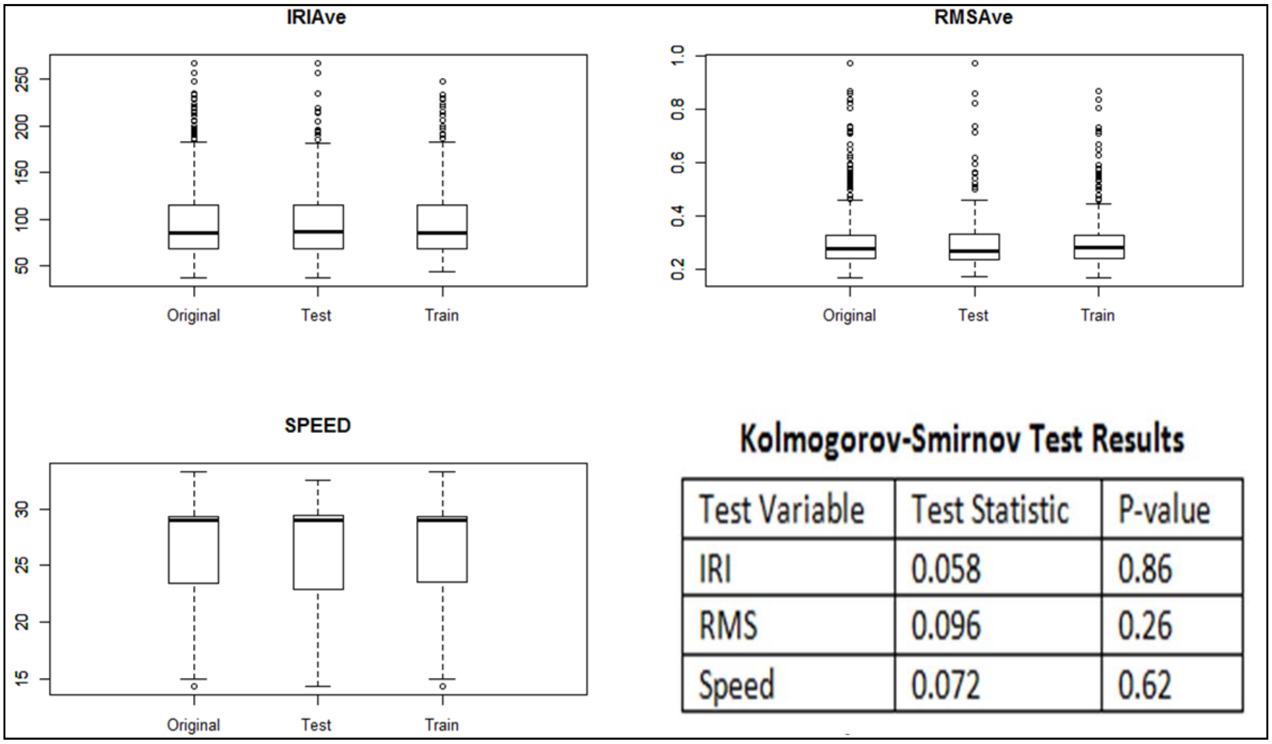

Test Variable	Test Statistic	P-value
IRI	0.058	0.86
RMS	0.096	0.26
Speed	0.072	0.62

FIGURE 3.1 Comparison of IRI, RMS and Speed Data in the Test and Train Datasets.

<u>3.6.2 Normalized Root Mean Squared Acceleration</u>

According to previous studies, root mean squared (RMS) vertical acceleration, which is calculated with the equation below, represents a better scenario for matching the IRI with acceleration measurements under a constant speed (*12*).

$$a_{z,RMS} = \sqrt{\frac{1}{N}\sum_{i=1}^{N}(a_{z,i} - g)^2} \qquad (12)$$

Where:

$a_{z,\,RMS}$ = the RMS vertical acceleration for the studied pavement section;
N = the number of acceleration readings among the studied pavement section;
$a_{z,i}$ = the i^{th} vertical acceleration reading among the studied section;
g = the contribution of the force of gravity.

As a result, we use RMS vertical acceleration to quantify the vehicle floor vibration level. It is important to note that the value of RMS acceleration also relates to vehicle speed. For instance, the RMS accelerations may be very different between those on a freeway section with a speed limit of 70 mph and on a secondary roadway section with a speed limit of 35 mph, even though they have very similar IRI values. According to Ahlin and Cranlund's study, the approximation relationship is shown as the following equation between IRI, vehicle speed (v) and vehicle floor vibration (vib), assuming the reference quarter-car model. Vehicle floor vibration is usually quantified as the RMS vertical acceleration (*25*). The value of the PSD exponent (n) is low for roads where the dominating roughness amplitudes have short wavelengths, such as on a modern designed highway with a deteriorated surface with plenty of potholes, etc. The value of n is high for roads where the dominating roughness amplitudes have long wavelengths, such as on an older rural low volume road, just after an 1–2 inch asphalt overlay has been placed.

$$\frac{vib}{IRI} = 0.16(v/80)^{(n-1)/2} \qquad (25)$$

According to the approximation relationship, for a given pavement section, the floor vibration or the RMS vertical acceleration is directly proportional to vehicle operation speed. The value of the proportion factor is determined by the ratio of vehicle speed to 80 km/h (the simulation speed when calculating IRI). A normalized floor vibration, or normalized RMS vertical acceleration (*NRMS*), is defined by incorporating vehicle speed, as shown in the following equation.

$$NRMS = (80/v)^{w} a_{z,RMS}, \text{ where } w = (n-1)/2.$$

NRMS indicates the vibration level that a vehicle is expected to experience at the speed of 80 km/h.

The next question is how to determine the value of the exponent w. Theoretically, each pavement section has its own PSD characteristics and thus a unit w. However, it will be cost prohibitive to calculate the value of *w* for each individual pavement section. For network screening purposes, a general value of *w* can be used by assuming that there is a typical value for most roads. The authors applied 3-fold cross-validation with logistic regression to determine the approximate exponent value (*w*) that should be used in the acceleration-based metric. Cross-validation is a popular data mining method that helps to find the optimal tuning parameter (*w* in this case) that minimizes prediction error (*40*). In 3-fold cross-validation, the original sample is randomly partitioned into three equal size subsamples. Of the three subsamples, a single subsample is retained as the validation data for testing the model, and the remaining two subsamples are used as training data. The next step is to fit a model based on the training data and a candidate value of the tuning parameter, and then use the validation data to calculate prediction error (i.e., MSE). The cross-validation process is then repeated three times (the folds), with each of the three subsamples used exactly once as the validation data. The three prediction error results from the folds can then be averaged to produce a single estimation. Repeating this process for every possible value of the tuning parameter provides an estimate of the test error curve, which can be used to find the tuning parameter that minimizes it.

3.6.3 Pavement Classification Model Development and Evaluation

To investigate the effectiveness of the proposed acceleration-based metric, a logistic regression method was created and then evaluated. Logistic regression is used here because it not only can help approximate the actual pavement roughness level using acceleration and speed data, but also is able to indicate the likelihood of correct estimation. Knowing the likelihood of correct estimation is useful for pavement maintenance decision making (i.e., prioritizing repaving projects). In addition, there are mature tools to evaluate and validate logistic regression models.

After the *NRMS* accelerations were calculated, logistic models were developed to predict a pavement section's roughness level based on its *NRMS* value. The important outputs include a threshold *NRMS* value ($NRMS_0$) and a probability function. The following section will describe the technical detail of model development and validation.

The model setup is as follows. For pavement section i, define

$$Y_i = \begin{cases} 1 & If\ the\ section's\ IRI\ value\ is\ greater\ or\ equal\ to\ IRI_0 \\ 0 & If\ the\ section's\ IRI\ value\ is\ less\ than\ IRI_0 \end{cases}$$

Where IRI_0 is the threshold value in the model that defines whether a pavement section is deficient or not, its default value is 140 in/mile.

Let p_i be the probability of being a deficient pavement (IRI $\geq IRI_0$ in/mile) for section i. The observed Y_i is assumed to follow a Bernoulli distribution ($Y_i \sim$ Bernoulli (p_i)).

As a key parameter, p_i is associated with the *NRMS* acceleration of section i ($NRMS_i$) by a logit link function (or by a probability function).

$$logit(p_i) = \log\left(\frac{p_i}{1-p_i}\right) = \alpha + \beta NRMS_i, \quad \text{or}$$

$$p_i = \frac{\exp(\alpha + \beta NRMS_i)}{1 + \exp(\alpha + \beta NRMS_i)}$$

Where α and β are regression coefficients. The exponential of regression coefficients, $exp(\beta)$, is the odds ratio (OR) for the *NRMS* acceleration. The regression model will estimate the probability of being a deficient pavement, given the section's *NRMS* acceleration. A section will be predicted as a deficient section if this probability is greater than a predefined threshold value p_0 (default value is 0.5). Mean squared error (MSE), as shown below, can be used as an estimation of the prediction error.

$$MSE = \frac{1}{N}\sum_{i=1}^{N}(p_i - Y_i)^2$$

Once the logistic model is developed, the related threshold value of normalized RMS acceleration ($NRMS_0$) can be determined by the following equation.

$$NRMS_0 = \frac{1}{\beta}(log\left(\frac{p_0}{1-p_0}\right) - \alpha)$$

A section will be identified as rough section if its *NRMS* acceleration is higher than $NRMS_0$, and the probability function will inform the likelihood of correct classification. To ensure the probability function and threshold value can work properly, the logistic model needs to be evaluated and validated.

The model performance was evaluated mainly by the receiver operating characteristic (ROC) curve, which measures model sensitivity and specificity (*42*). In the case of this study, the sensitivity is the probability of correctly predicting a deficient pavement section, and the specificity is the probability of correctly predicting a non-deficient section.

Both indexes are related to the threshold value p_0 and there is a tradeoff between sensitivity and specificity. The ROC curve is a plot of sensitivity versus false positive rate (i.e., 1-Specificity) for all possible thresholds (p_0). The prediction performance of the model can be measured by the area under the curve (AUC), with a higher AUC value indicating better predictive power. A perfect prediction method would yield the maximum AUC of 1. A completely random guess would result in an AUC of 0.5.

3.7 Analysis Results

This section presents the results from data analysis. The analysis first presents the proposed acceleration-based metric from the cross-validation result, then introduces the development of logistic models, and finally evaluates the model performance.

3.7.1 Acceleration-based Metric

Figure 3.2 shows the scatter plots of IRI with RMS acceleration or NRMS acceleration when the exponent *w* values are 0.5 and 1.3, respectively. The 3-fold cross-validation curve based on the training data was also shown in the bottom right of Figure 2, indicating how the value of MSE changes when the value of the exponent *w* changes from 0.5 to 2.0.

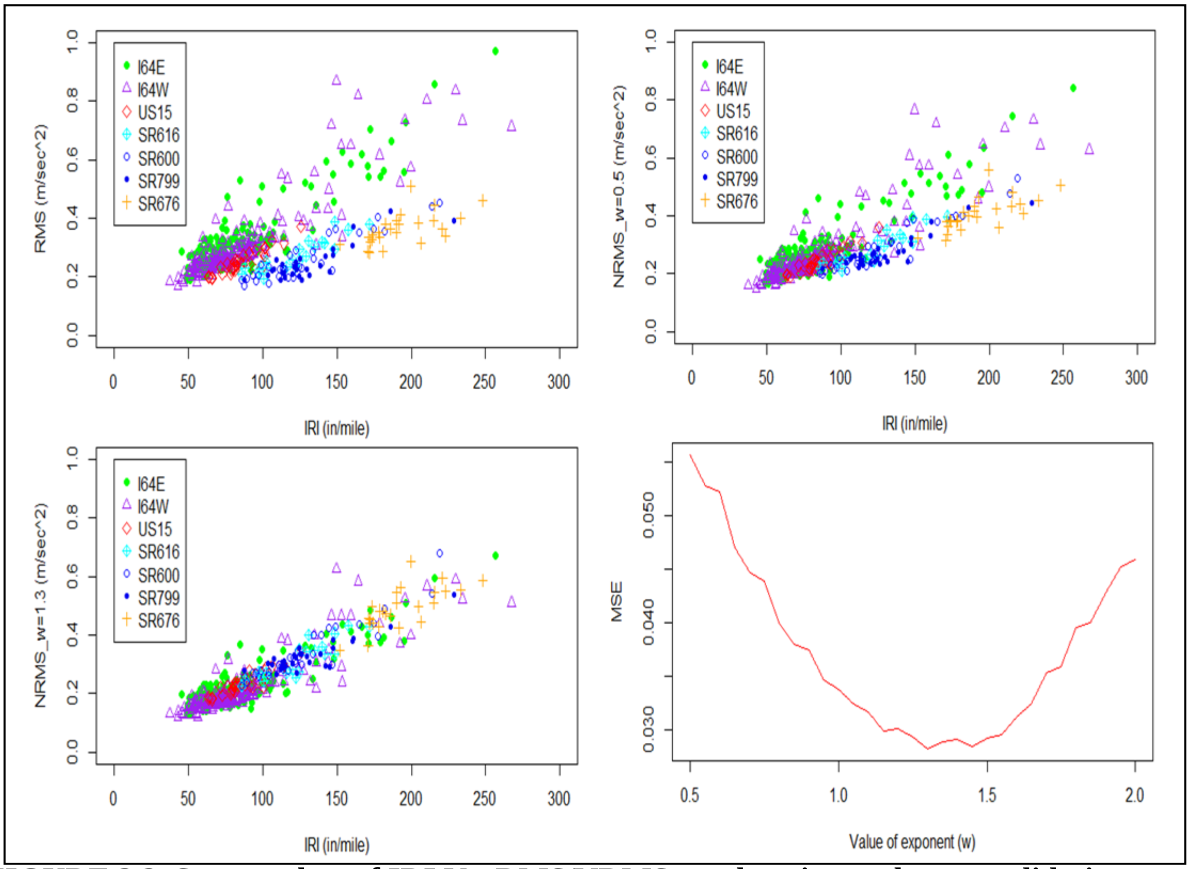

FIGURE 3.2 Scatter plots of IRI Vs. RMS/NRMS acceleration and cross-validation result.

According to Figure 3.2, the RMS accelerations before normalization did not show consistent relationships with the IRI values between different routes. However, after normalization, the NRMS values appear to share a similar relationship with the IRI between different routes. It indicates that incorporating vehicle speed in the acceleration-based metric is possible to generalize results to different functional classes of highway.

The 3-fold cross-validation result indicates that the optimal value of w is 1.3, and the related *NRMS* can minimize the MSE of the prediction model to 0.028. It also illustrates that the MSE is stable when the exponent value is between 1.1 and 1.6. In other words, selecting different values within this range is not expected to change the effectiveness of *NRMS* significantly. As for this study, the *NRMS* was determined with 1.3 as the exponent value (as shown in the following equations).

$$NRMS = (80/v)^{1.3} a_{z,RMS}$$

<u>3.7.2 Logistic Regression Models</u>

For network screening, the key interest is whether DOTs can use the proposed acceleration-based metric to identify deficient pavement sections. Logistic models were developed to demonstrate this feasibility by classifying pavement sections into deficient and non-deficient categories based on their *NRMS* values. Note that the training dataset was used to develop the models. A default model was first developed with IRI_0 equaling to current VDOT threshold value (140 in/mile) for deficient pavement. Three shifted models were also created with IRI_0 values (112, 119, and 126 in/mile, respectively) that are lower (10%, 15%, and 20% lower, respectively) than the current VDOT threshold value. All models' ability to flag deficient pavement (IRI ≥ 140 in/mile) sections were evaluated using the testing dataset. Compared with the default model, the shifted models are expected to perform better in capturing deficient sections, but at the expense of misclassifying more non-deficient pavement sections. . It was found that the 15%-shifted model performed better in balancing this tradeoff than the other two shifted models. As a result, the 15%-shifted model was selected and presented here as a comparison model of the default model. The tradeoffs between these models will be further discussed later in the paper. The model outputs are summarized in Table 3.2.

TABLE 3.2 Logistic Model Results Summary

Model	Variable	Coefficient	S.E.	Significant	Odds Ratio[1]	Nagelkerke R Square[2]	AIC	$NRMS_0$
Default Model	Intercept	-14.20	2.16	0.000	1.48	0.84	69.46	0.36
	NRMS	39.04	6.16	0.000				
Shifted Model	Intercept	-11.78	1.42	0.000	1.46	0.82	115.00	0.31
	NRMS	38.12	4.91	0.000				

Note: 1. Odds ratio was scaled for every 0.01 unit increase in RMS acceleration, *Exp (0.01*β);*
2. A surrogate R square for logistic models given by SPSS.

As expected, the *NRMS* value is a significantly important indicator for a deficient pavement in both models. A scaled odds ratio (OR) was calculated to quantitatively evaluate the impact of *NRMS* acceleration. It represents the relative odds of being a deficient pavement for every 0.01 unit increase in *NRMS* acceleration. The default model results indicate that, for every 0.01 m/sec^2 increase in *NRMS* acceleration, the relative odds of being a deficient pavement will increase by 48% (OR=1.48). The predictive models (probability functions) are as follows:

Default Model: $Probability(deficient\ pavement) = \frac{\exp(-14.2+39.04NRMS)}{1+\exp(-14.2+39.04NRMS)}$

Shifted Model: $Probability(deficient\ pavement) = \frac{\exp(-11.78+38.12NRMS)}{1+\exp(-11.78+38.12NRMS)}$

Where *NRMS* is the normalized RMS acceleration of the target section.

With these models, the probability of being a deficient pavement section can be predicted based on the acceleration and vehicle speed data collected on the target section. Generally speaking, a higher *NRMS* acceleration results in a higher probability of being a deficient pavement section. Assuming that the threshold probability between deficient and smooth pavement is 0.5 ($p_0 = 0.5$), the corresponding *NRMS* acceleration threshold ($NRMS_o$) values for the default and shifted models are 0.36 m/sec^2 and 0.31 m/sec^2, respectively.

In the network screening process, a pavement section's roughness level can be estimated simply by comparing the *NRMS* value with the threshold value. For example, if a pavement section has a *NRMS* value of 0.42 m/sec^2 (greater than 0.36 m/sec^2), its estimated classification will be a deficient section according to the default model and thus it is recommended to further investigate its roughness condition (i.e., collect its profile or IRI data). Furthermore, there is a probability of 0.90 that the classification is correct according to the probability function. This probability information is useful in the decision making of pavement maintenance (i.e., prioritizing pavement treatment projects).

3.7.3 Model Evaluation and Validation

The models were evaluated based on both training data (the original data for model development) and testing data (the additional data for model validation). As a result, two ROC curves were generated for each model, as shown in Figure 3.3. To better examine the effecitiveness of incorporating vehicle speed into the acceleration-based metric, Figure 3.3 also shows the ROC curves of a logistic regression model based on the RMS vertical acceleration that did not take speed into account.

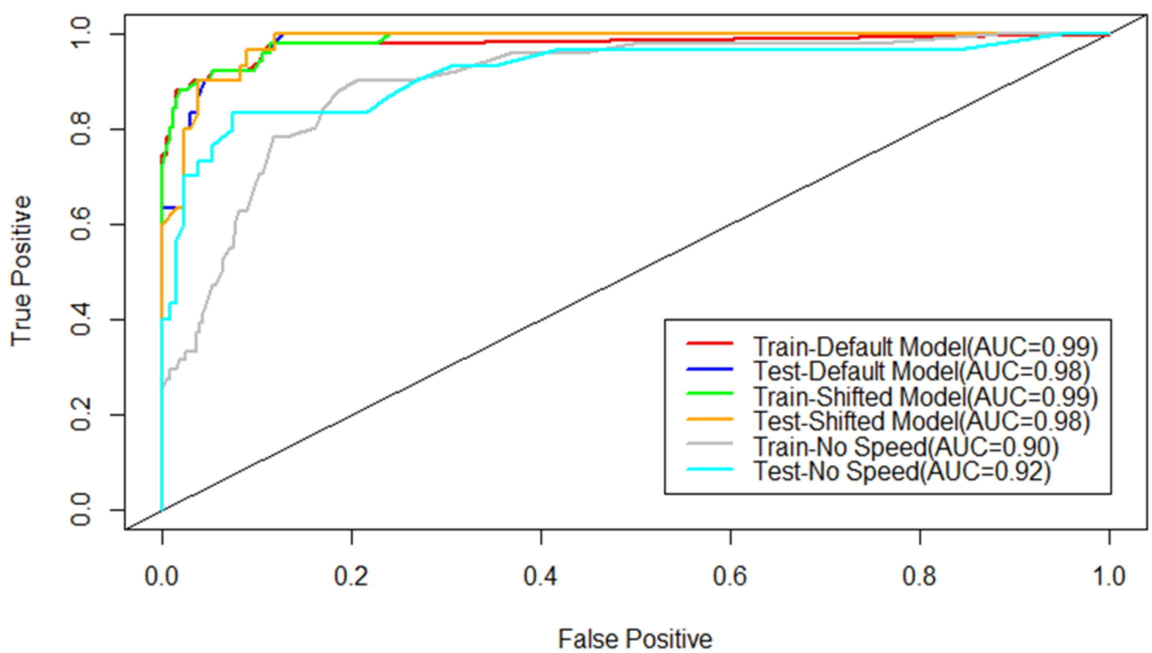

FIGURE 3.3 ROC curves for the training and testing datasets.

The default model had very similar ROC curves with the shifted model. According to the ROC curves, the logistic regression model based on the proposed metric (*NRMS*) has a high predictive power. The AUCs are 0.99 for the training dataset and 0.98 for the testing dataset, both close to the perfect AUC value of 1. This result indicates that using the proposed acceleration-based metric to identify the deficient pavement sections is statistically highly effective and transferable. Both the default model and the shifted model performed significantly better than the model without speed. It indicates that incorporating vehicle speed in the acceleration-based metric is much more effective than the acceleration-only metric.

To further evaluate the models, classification tables were created by showing the number of sections by observed roughness level and predicted roughness level (assuming $p_0 = 0.5$), as well as the percentage of correct prediction (Table 3.3). Note that the disaggregated numbers are listed in parentheses, with the first value for interstate sections (IS-64E/W) and the latter value for non-interstate sections. As a comparison, the classification results were also shown for the model that did not incorporate vehicle speed.

TABLE 3.3 Classification Results Summary

		Testing Data Predicted		
Model	Observed	Non-Def.	Deficient	Correct Percentage
Default Model	Non-Def.	132 (99, 33)[1]	3 (0, 3)	97.78 (100.00, 91.67)
	Deficient	6 (3, 3)	24 (13, 11)	80.00 (81.25, 78.57)
Shifted Model	Non-Def.	123 (96, 27)	12 (3, 9)	91.11 (96.97, 75.00)
	Deficient	2 (1, 1)	28 (15, 13)	93.33 (93.75, 92.86)
No Speed	Non-Def.	133 (98, 34)	2 (1, 1)	98.51 (98.99, 97.14)
	Deficient	13 (7, 6)	17 (9, 8)	56.66 (56.25, 57.14)

Note: 1. The first value in the parenthesis indicates the number of interstate sections and the latter the number of non-interstate sections.

Overall, the percentages of correct classification from both the default and shifted models are greater than 92 percent on the testing dataset. This result is consistent with the ROC curve results. The default model was able to correctly identify 80 percent of the deficient pavement sections and only mis-identified about two percent of those non-deficient sections. The shifted model can capture more deficient sections (93%) but also mis-identfied more non-deficient sections (8.9%). Generally speaking, lowering the IRI threshold value in the development of classification models increases the accuracy of identifying deficient sections, but also harms its ability to correctly identify non-deficient pavements. The model based on the RMS acceleration without incorporating vehicle speed can only correctly identify 57 percent of deficient sections. As a result, there is a significant improvement regarding correctly identifying deficient pavements by incorporating vehicle speed into the acceleration-based metric.

Figure 3.4 provides more insights for the classification results by showing each pavement section's IRI value and estimated probability from the probability function. All 165 observations in the testing dataset were colored and marked according to the four classification outcomes.

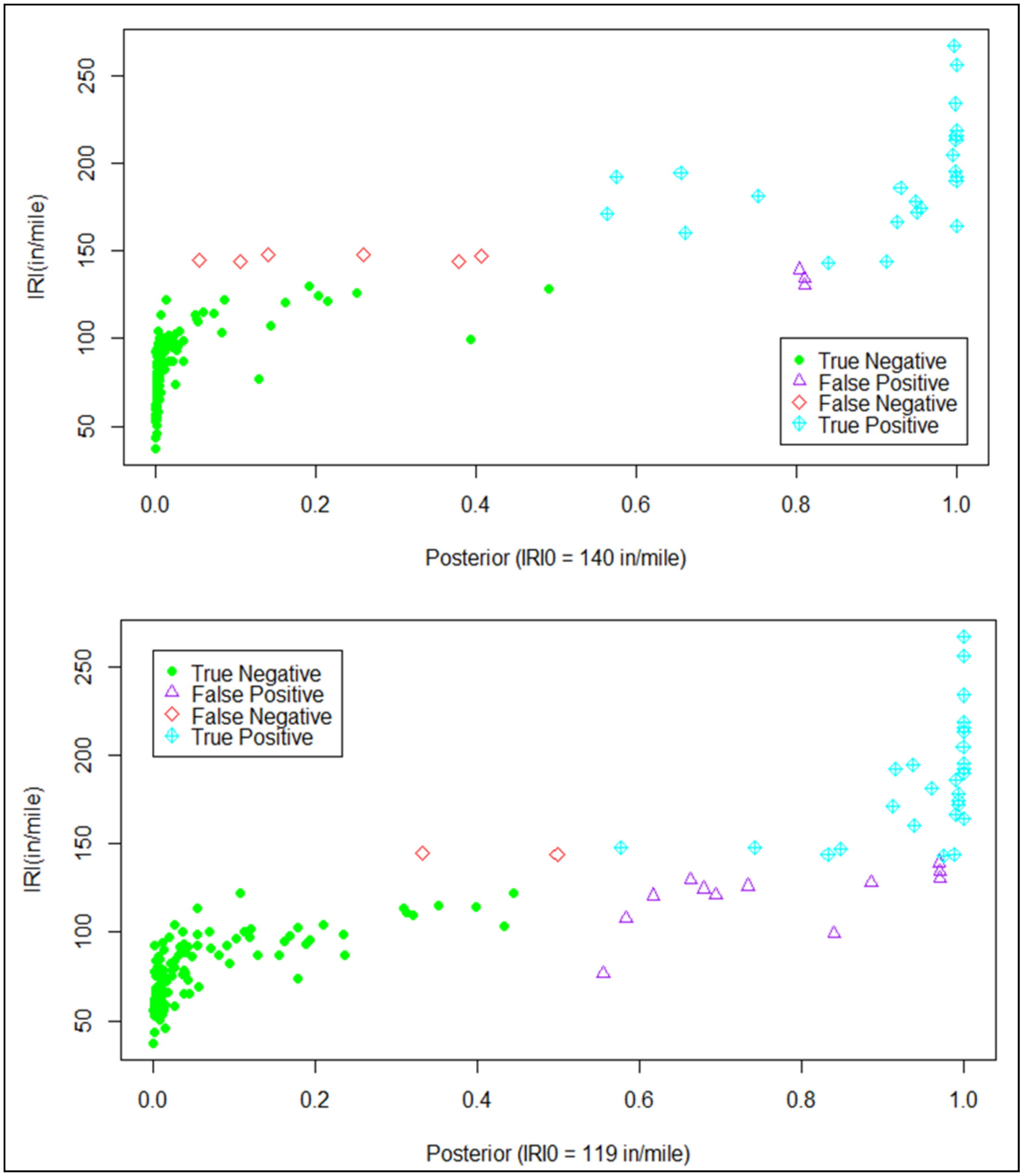

FIGURE 3.4 IRI values and the estimated probability.

It was found that all nine sections that were mis-classified by the default model (top of Figure 3.4) had IRI values between 130 and 150 in/mile. Specifically, this model missed six sections that were near the deficient threshold while picking up three sections that soon would be deficient. The shifted model (bottom of Figure 4.4) missed only two sections that were at the early stage of being deficient, but picked up 12 non-deficient sections (9 of them had IRI values greater than 120 in/mile). It is clear that there are advantages and disadvantages in selecting either model for network screening. The default model will identify fewer pavement sections for further investigation. This will require fewer resources, but it will miss some sections that are at the early stage of being deficient. The shifted model will identify relatively more pavement sections, including sections that are close to being deficient. However, it means an increase in further investigation on non-deficient sections. Transportation agencies are recommended to select the model based on their own pavement maintenance goals and available resources. In summary, the evaluation results indicate that estimating the roughness level based on *NRMS* acceleration can achieve a high accuracy level that is feasible for network screening. It is expected that the predictive power is transferable across different functional classes of highways in Virginia. The results show a promising effectiveness of using the proposed acceleration-based metric to identify deficient pavement sections.

3.8 Conclusions

This study developed a normalized acceleration-based metric (*NRMS*) that can generalize to different functional classes of highway by incorporating vehicle speed. This proposed metric was trained and tested on data collected from three functional classes of highway and illustrated a promising performance in identifying deficient pavement sections. It is expected the proposed acceleration-based metric to be used in a network screening process.

In conclusion, this research points to the feasibility of using a cost-effective application for the purpose of network screening. The network screening process will reduce the total mileage of pavement sections that need to measure and meanwhile still identify locations where maintenance work is necessary.

There are several opportunities to expand this research to further validate this approach. First, it is recommended to design filters to remove invalid data by identifying situations where the acceleration-based metric can not work. With the help of filters, only valid data points will remain. Due to the requirement of vehicle speed for IRI data collection, this research did not investigate acceleration data collected under 30 mph. However, it is plausible that the acceleration-based metric has a lower speed requirement than IRI. As a result, future research can examine the minimum speed for valid data. Also, this study did not investigate the identification of pavement sections with IRI values greater than 220 in/mile given a lack of data. This could be another area for future research. Last but not least, a prototype system can be developed using state-owned vehicles as probe vehicles to collect data. With the prototype system, a more comprehensive dataset can be generated by collecting data on more routes and in a wider area. It can be used to validate previous findings, address issues regarding implementation, assess the network benefit of this system, and explore the possibility of measuring other pavement condition data using a similar approach.

ACKNOWLEDGMENTS

This research was funded by the Connected Vehicle Infrastructure University Transportation Center (CVI-UTC). The authors wish to thank Edgar de León Izeppi and Samer Katicha of Virginia Tech Transportation Institute for their help in data collection.

CHAPTER 4 THE IMPACT OF VEHICLE DYNAMIC SYSTEM ON THE ACCELERATION-BASED METRIC FOR PAVEMENT ROUGHNESS

A paper prepared for submission to the *International Journal of Pavement Engineering*

Huanghui Zeng[1], Brian L. Smith[2], and Hyungjun Park[3]

4.1 Abstract

Transportation agencies devote significant resources towards the collection of highly detailed and accurate pavement roughness data using profiler vans to support pavement maintenance decisions. Thanks to the progress of wireless communication and sensor technology, numerous studies were conducted to investigate the feasibility of using probe vehicle data (i.e., Vehicle floor acceleration) for pavement condition assessment. One challenge of this concept is that there are a huge variety of vehicle dynamic systems which can directly impact the resulting probe data. This study investigated the impact of vehicle dynamic systems on vehicle vibration response, which directly affects the acceleration-based metric for pavement roughness measurements.

Profile and probe data were collected on a total of 10.8 mile segments using three different vehicles. The sensitivity analysis and relationship analysis based on quarter-car model simulations found that variations in vehicle dynamic parameters can result in a significantly different magnitude of vibration response. The magnitude of vehicle vibration response is most sensitive to the spring stiffness of the sprung mass and least sensitive to the loading of the vehicle. Furthermore, the relationship analysis shows that the vibration responses are linearly correlated between different vehicle systems, which were illustrated in both the quarter-car simulations and the probe data collected under naturalistic driving conditions.

These findings help transportation agencies better understand the probe data generated from different vehicle systems in the real world, and thus could use the related acceleration-based metric properly for pavement condition network screening. Assuming that transportation agencies will use agency-owned vehicles to build a pavement condition network screening system, a vehicle calibration procedure was developed to help them calibrate vehicles in the fleet. Case studies based on the probe data collected from different vehicles were also presented and demonstrated that the calibration improved system performance.

1 Graduate Research Assistant, Department of Civil and Environmental Engineering, University of Virginia, Charlottesville, VA22904, E-mail: hz3xm@virginia.edu.
2 Professor and Chair, Department of Civil and Environmental Engineering, University of Virginia, Charlottesville, VA22904, Phone: 434-243-8585, E-mail: briansmith@virginia.edu.
3 Senior Scientist, University of Virginia Center for Transportation Studies, Charlottesville, VA22904, Phone: 434-924-1651, Email: hpark@email.virginia.edu.

4.2 Introduction

Transportation agencies have traditionally depended on measures of pavement roughness to support planning maintenance, repair, and rehabilitation work on the pavement system. Since the 1960s, many measures and measurement techniques have been developed. Currently one of the most commonly used measurements is the International Roughness Index (IRI) which was developed by NCHRP and the World Bank. IRI is computed based on the measured longitudinal profiles of a roadway (*39*). Given the need for specialized equipment and sensors, it is very difficult to collect this data at numerous locations in a timely and cost effective manner.

Highway transportation is undergoing significant technological transformations thanks to the emerging connected vehicle environment which enables vehicles to wirelessly communicate with other vehicles and with the infrastructure (*4*). This connected, data-rich environment will allow for innovative connected vehicle applications for transportation infrastructure maintenance. The use of simple sensors such as accelerometers, already installed either in vehicles or mobile devices, is able to directly measure the vehicle vibration responses, which is believed to highly correlate with pavement roughness. Several past efforts investigated the feasibility of collecting acceleration data to assess pavement roughness at a significantly lower cost and higher level of temporal resolution (*3*, *11*, *12*, *13*). One critical issue about the acceleration-only index is that its value depends on a combined effect of vehicle operating speeds, vehicle dynamic features, and pavement characteristics (i.e., wavelength). Thus, it is hard to generate reproducible roughness measurements under naturalistic driving conditions without considering this combined effect. On the other hand, it is cost prohibitive to develop specific acceleration-based models for each vehicle system and each type of pavement. As a result, totally replacing the current IRI practice with the acceleration-based index is not recommended, especially for applications requiring a high degree of accuracy (i.e., construction). However, if an acceleration-based metric can be used as a supplementary method to current practice, it may help to address some of the current practice's limitations by providing more timely information to decision makers. For example, the acceleration-based metric could be used for network screening, which is a low-level practice that does not require highly accurate and detailed roughness measurements. One of the key concerns about the current IRI practice is that it is too costly to assess the whole system's pavement roughness condition once a year. The acceleration-based metric would help to identify pavement segments that are likely to be deficient, and then a profile van can be sent to those flagged sections to measure the accurate roughness condition. Introducing a network screening process should be able to reduce the total mileage of pavement sections that need to be measured and meanwhile still identify locations where maintenance work is necessary.

To complete the network screening process in a cost-effective manner, the data should be generated through people's daily travel in common vehicles. Using smartphone or vehicular sensors appears to be a good way to collect data. A remaining question is whether this data can generate meaningful results for network screening under naturalistic driving conditions from numerous vehicles. In the real world, vehicles will encounter different dynamic systems, different surface types, changing speeds, divergent travel paths and other factors which may cause variations in terms of vehicle-body vibration responses and result in very different acceleration datasets. It is therefore necessary to take this concept to a real world situation to investigate its feasibility for identifying deficient pavements.

4.3 Objectives and Scope

Note that the vibration response of a running vehicle is influenced by the vehicle operating speed, the vehicle dynamic system, and pavement roughness. A previous study (*43*) was able to develop an improved acceleration-based metric by incorporating vehicle speed. As a follow-up project, this study addressed mainly the impact of vehicle systems. The goal of this study is to understand the data generated from different vehicle dynamic systems so that transportation agencies can use this data properly in pavement roughness assessment. Specifically, two objectives were addressed:

- Investigate the impacts of vehicle dynamic parameters on the acceleration-based metric, and
- Develop a procedure for calibrating data from different vehicle systems and provide a case study.

It is important to know that this study does not intend to propose a new method to replace the current IRI practice, but to improve current practice by introducing a supplemental method for pavement roughness assessment. The background of current pavement roughness assessment practice, previous studies, methodology for the proposed application, and the analysis results will then be presented. Finally, this paper concludes with a summary of findings and recommendations for future studies.

4.4 Background

By definition, IRI is the accumulated suspension stroke in a mathematical car model divided by the distance traveled by the model during a simulated ride on a pavement section whose profile is measured (*23*). It is recorded in inches per mile (in/mile), or meters per kilometer (m/km). By applying a unit quarter-car model and simulating the vehicle response at a constant speed (80 km/h) on a known profile, the IRI is a reproducible index, making it outperform other pavement roughness measurements. IRI was chosen as the standard reference roughness index of the Highway Performance Monitoring System (HPMS), a national database of roadway information kept by the Federal Highway Administration (FHWA) (*19*).

Pavement condition data in Virginia are collected using an automated method that relies on advanced computing technology and a multitude of sensors and equipment (including high-speed lasers, cameras and accelerometers). To assess the network roughness condition, Fugro Roadware (VDOT's current contractor) uses its instrumented vans to measure roadway profiles every year for the interstate and primary highway systems and every five years for the secondary system. The profiles are later analyzed by a software package to determine the IRI value of the related pavement section. Although the final IRI is reported at every 0.1-mile (163 m), the profile data are recorded at a much smaller interval of less than 6 inches (*3*).

For pavement maintenance purpose, Virginia Department of Transportation (VDOT) uses IRI for overall awareness of road condition in terms of ride quality. Interstate and Primary pavement sections with an average IRI of 140 in/mile (2.2 m/km) or more or a Secondary pavement section with an average IRI of 220 in/mile (3.47 m/km) or more are considered 'deficient' in terms of ride quality (*15*). Every year, VDOT makes its maintenance activity decisions for the pavement system based on IRI and other pavement condition information.

4.5 Literature Review

A considerable amount of work has been completed recently to improve the concept of using inexpensive vehicle or smartphone sensors to assess pavement roughness conditions. A research team from Auburn University investigated the application of using vehicle-based sensors to assess pavement condition (*12*). The main focus of the study was to utilize vehicular sensors (accelerometers, gyroscopes, and suspension deflection meters) to estimate the IRI. Testing was conducted under controlled speed on a 1.7 mile (2,750 m) long test track at the National Center for Asphalt Technology (NCAT). The amount of overall vibrations across a given segment was determined by taking the root mean square (RMS) of a signal measurement. The overall vibrations were then compared with the true IRI of the pavement segment. The resulting data indicated that the RMS of vertical accelerations represents the best case scenario to capture the true IRI. The study also indicated that the estimation error increases with decreasing window size and thus recommended to use larger windows when possible to assure the most accurate IRI estimates.

In 2011, Flintsch et al. (*13*) conducted a pilot study using probe vehicles to measure road ride quality, or roughness. Again, vertical acceleration data were used as an index of vehicle vibration. A smoothness profile was obtained using an inertial-based laser profiler, while the vertical accelerometer measurements were obtained using a vehicle instrumented with an accelerometer at the Virginia Smart Road facility in Blacksburg, Virginia. The accelerometer operated at a rate of 10 HZ. GPS positions were also recorded. A total of four runs were completed on the test track to collect acceleration data. The study confirmed that the acceleration runs are very repeatable. Analysis using the coherence function indicates that the acceleration data linearly correlate well to smoothness profile between wavelength 50 and 300 m.

Bridgelall derived a theoretical relationship between IRI and accelerometer data for a connected vehicle approach for pavement roughness estimation (*29*). The research introduced the road impact factor (RIF) which is derived from vehicle integrated accelerometer data. A time-wavelength-intensity-transform (TWIT) algorithm was also developed to create a wavelength-unbiased measurement based on RIFs from different speed bands. The analysis demonstrates that RIF and IRI are directly proportional. Profile and acceleration data were collected from six runs with a constant speed (55.6 km/h) on a 150-meter pavement section in Minnesota to validate this relationship. The author concluded that the proposed application enables low-cost, network-wide and repeatable performance measures at any speeds. No discussion was provided on sample size and sampling rate for acceleration data collection.

A recent study was conducted by Center for Transportation Studies (CTS) at the University of Virginia to address the impact of vehicle speed on vehicle vibration response (*43*). This study developed a normalized acceleration-based metric (*NRMS*) that can generalize to different functional classes of highway by incorporating vehicle speed. Vehicle speed and vertical acceleration were both included to calculate *NRMS*. Pavement roughness condition classification models were created using a logistic regression method, based on the proposed metric (*NRMS*). It was found that the model can correctly identify between 80 to 93 percent of deficient pavement sections. It is expected the proposed acceleration-based metric to be used in a network screening process.

In summary, the literature review reinforces the possibility of using vehicular or smartphone sensors as a cost-effective approach for pavement roughness data collection. However, special attention should be given that very few studies so far have been conducted to investigate the impact of variation in vehicle dynamic system. In the real world, probe data will come from numerous vehicles, which could have a good variety of dynamic characteristics. It is possible that the variations of vehicle dynamic system result in very different acceleration datasets. It is therefore necessary to extend this concept to a real world situation where data are collected from numerous probe vehicles and investigate the feasibility of identifying deficient pavements using a connected vehicle-enabled pavement network screening system.

4.5 Methodology

Figure 4.1 shows the workflow of this project from data collection to final conclusion.

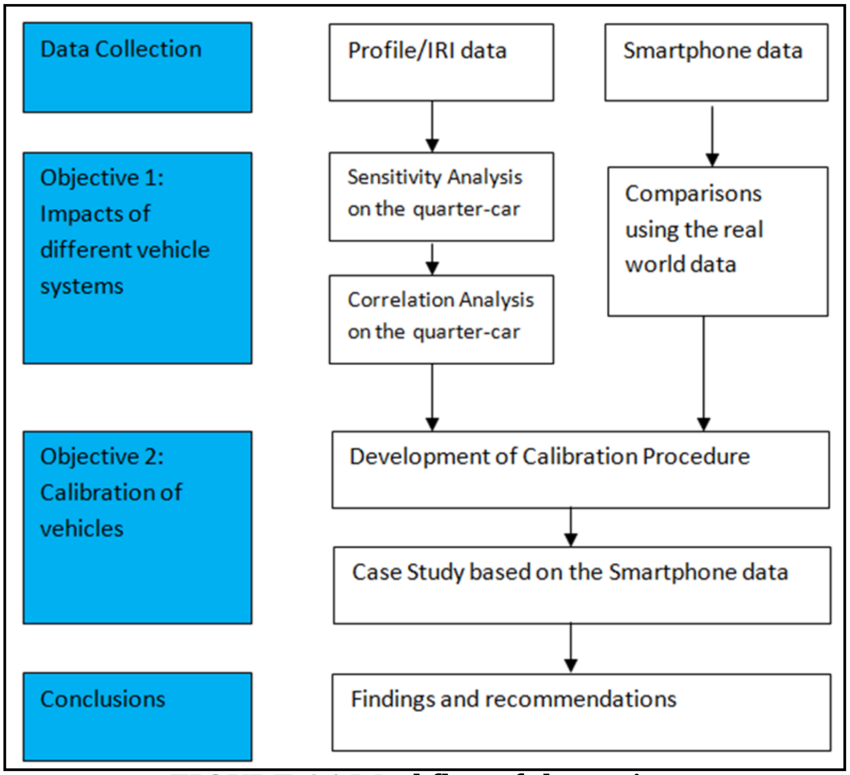

FIGURE 4.1 Workflow of the project.

As mentioned in the Objective section above, two primary objectives were addressed in this study. For the first objective, to investigate the impacts of different vehicle dynamic systems, two types of analyses were conducted. Firstly, a quarter-car model was applied to simulate the sensitivity of the vehicle vibration response when several key vehicle dynamic parameters change. The relationship of vibration responses between a variety of vehicle systems were further examined. Secondly, real world data collected from several pavement sections using three different types of vehicles were compared to validate the results from the simulation analysis.

The second objective was addressed based on the better understanding of the vehicle dynamic system's impacts on vibration response. The findings from addressing the first objective inspired a possible solution for vehicle calibration, and thus a standard procedure was introduced to calibrate data from different vehicle systems. Finally a case study illustrated how transportation agencies can apply the procedure.

The following section presents the method of using the quarter-car model to simulate vehicle vibration response, followed by a description of the real world data collection and the quantification of vehicle vibration response.

4.5.1 Vehicle Vibration Response Simulation

Researchers have used the quarter-car model to simulate the vibration response of vehicle body for a long time. According to Jazar, the quarter car model is the most employed and useful model of a vehicle suspension system (*44*). Although the quarter car model contains no representation of the geometric effects of the full car and offers no possibility of studying longitudinal and lateral interconnections, it represents well the vertical variance of vehicle movement and thus contains the most basic features of the real problems and representation of the problem of controlling wheel and wheel-body variations (*44*). During the development of IRI, the World Bank compared a variety of models and the quarter car model (Figure 5.2) with Golden Car parameters was found to have the best correlations between a profile index and the response-type systems (*23*). As a result, this study applied the same quarter car model to simulate the car floor acceleration responses. Since this study focus primarily on the impact of vehicle dynamic system, the simulation analysis was conducted based on a constant speed (50 mph) to simplify the model. The following section will describe how the quarter-car model can be applied to simulate vehicle vibration responses.

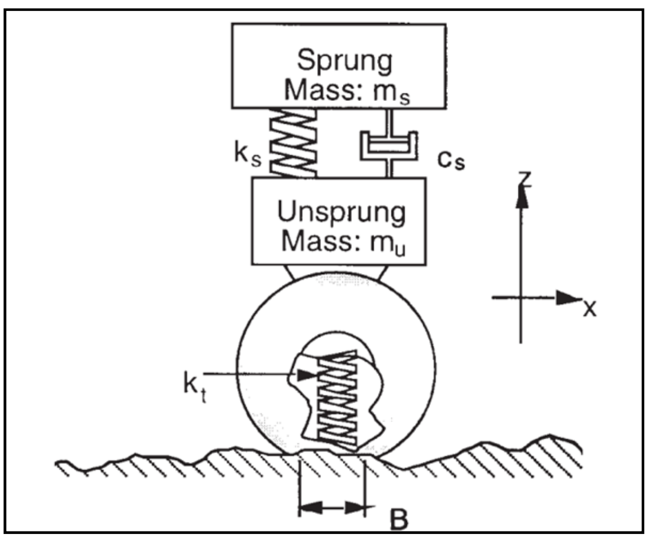

FIGURE 4.2 The Quarter-car Simulation Model (*39*).

Figure 4.2 shows the quarter-car model as in the IRI calculation. It represents the major dynamic effects that determine how pavement roughness causes vehicle vibration. This model includes two masses (m_s and m_u), two springs (k_s and k_t) and one damper (c_s). One could add another damper to the unsprung mass. However, compared with the suspension damper, it is very small and it could be ignored. To simplify the equations the parameters are normalized by the sprung mass, m_s. The parameters (normalized to m_s = 1) for the Golden Car are (*23*):

c_s = 6. [1/s], k_t = 653 [1/s2],

k_s = 63.3 [1/s2], $\mu = m_u/m_s$ = 0.15.

Necessary notation is introduced below to simulate the quarter-car model's vibration response by modifying the method for calculating the IRI, as presented in Sayer's study (*23*). Let p be the raw profile measured by the high speed laser profiler. Before simulating the quarter-car's response to it, the raw profile needs to be preprocessed using a moving average algorithm for two reasons: to simulate the enveloping behavior of pneumatic tires on highway vehicles, and to reduce the sensitivity of the vibration response algorithm to the sample interval, Δ. A moving average smoothing filter is defined as below:

$$p_s(i) = \frac{1}{k}\sum_{j=1}^{i+k-1} p(j)$$

$$k = max(1, [\frac{w_B}{\Delta}])$$

Where:

p = measured profile elevation,

p_s = smoothed profile elevation,

w_B = moving average base length, 250 mm,

Δ = sample interval, 1 inch for a typical high-speed laser profiler, and

$[w_B/\ \Delta]$ = the smallest integer that is greater than $w_B/\ \Delta$.

Theoretically, the quarter car model is described by four first-order ordinary differential equations that can be written in matrix form:

$$\dot{\mathbf{X}} = \mathbf{AX} + \mathbf{B}p_s$$

Where the **X**, **A**, and **B** arrays are defined as follows:

$$\mathbf{X} = [\mathbf{z_s}, \dot{\mathbf{z}}_\mathbf{s}, \mathbf{z_u}, \dot{\mathbf{z}}_\mathbf{u}]^\mathrm{T}$$

$$\boldsymbol{A} = \begin{bmatrix} 1 & 0 & 0 & 0 \\ -k_2 & -c & k_2 & c \\ 0 & 0 & 1 & 0 \\ k_2/\mu & c/\mu & -(k_1+k_2)/\mu & -c/\mu \end{bmatrix}$$

$$\mathbf{B} = [0,0,0,\mathrm{k}_1/\mu]^\mathrm{T}.$$

Where:

T = transpose operation of matrixes/vectors,

$\boldsymbol{z_s}$ = height of sprung mass,

$\boldsymbol{z_u}$ = height of unsprung mass, and

$\dot{\boldsymbol{z}}_{\boldsymbol{s}}$ and $\dot{\boldsymbol{z}}_{\boldsymbol{u}}$ **=** time derivatives of the heights of sprung mass and unsprung mass, respectively.

Time is related to longitudinal distance by the simulated speed of the vehicle. For the calculation of IRI, one can accumulate the differences between the time derivatives of sprung mass height and unsprung mass height, as presented in the following equation.

$$IRI = \frac{1}{L}\int_0^{L/V} |\dot{\boldsymbol{z}}_{\boldsymbol{s}} - \dot{\boldsymbol{z}}_{\boldsymbol{u}}|dt$$

Where:

L = length of the segment where the IRI is calculated on;

V = vehicle speed, the default value is 50 MPH, or 22.22 meter/second.

According to Hartman (*45*), the solution for a general differential equation $\dot{\mathbf{x}} = \mathbf{Ax} + \mathbf{Bu}$ will be better approximated when $\boldsymbol{u}$ is a vector of constants over interval i-1 to i. The closed-form solution is known as below:

$$x_i = e^{\boldsymbol{A}\Delta/V} x_{i-1} + \boldsymbol{A}^{-1}\left(e^{\frac{\boldsymbol{A}\Delta}{V}} - \boldsymbol{I}\right)\boldsymbol{Bu}$$

According to a Taylor series expansion (*46*):

$$e^{\boldsymbol{A}\Delta/V} = \boldsymbol{I} + \sum_{i=1}^{N} \frac{\boldsymbol{A}^i (\frac{\Delta}{V})^i}{i!}$$

This solution is accurate to the extent that the input $\boldsymbol{u}$ is actually constant over the interval from point i-1 to i. Also previous research shows that the best approximation of the sampled profile to a continuous one is that the profile slope is constant between samples. This indicates that the profile slope should be applied as the assumed constant input $\boldsymbol{u}$ to obtain the best accuracy. As a result, the quarter car differential equation is transferred as below, for the purpose of getting an accurate solution. In addition, the transferred format will have the capability to simulate acceleration response.

$$\dot{\boldsymbol{x}} = \boldsymbol{Ax} + \boldsymbol{Bs_{p_s}}$$

Where the profile slop $\boldsymbol{s_{ps}}$ can be calculated using the following equation:

$$s_{p_s}(i) = \frac{p_s(i+k) - p_s(i)}{k\Delta};$$

The $\boldsymbol{A}$ and $\boldsymbol{B}$ arrays are defined the same ways as before, and a new state variable vector $\boldsymbol{x}$ was defined based on the slope of the original state variables, as indicated below:

$$\boldsymbol{x} = [\boldsymbol{s_{z_s}}, \dot{\boldsymbol{s}}_{\boldsymbol{z_s}}, \boldsymbol{s_{z_u}}, \dot{\boldsymbol{s}}_{\boldsymbol{z_u}}]^T$$

Note that the new state variables were generated by the same way as the profile slope.

With the new differential equation, the IRI can also be defined as below:

$$IRI = \frac{1}{n}\sum_{i=1}^{n} |\, s_{z_s}(i) - s_{z_u}(i)|$$

By solving the differential equation, the resulting sprung mass vertical acceleration (car floor vertical acceleration) value can be approximated as:

$$a(i) = \frac{\dot{z}_s(i+k) - \dot{z}_s(i)}{k\Delta/V} = \dot{s}_{z_s}(i)V$$

The RMS acceleration can also be calculated accordingly.

$$a_{RMS} = \sqrt{\frac{1}{n}\sum_{i=1}^{n} a(i)^2} = \sqrt{\frac{1}{n}\sum_{i=1}^{n} (V\dot{s}_{z_s}(i))^2}$$

This study used Matlab, a powerful tool for numerical computing, to conduct vehicle vibration response simulations. A Matlab function was created with the ability to calculate the simulated RMS acceleration at every 0.1 mile interval given the pavement profile and values of the four vehicle dynamic parameters. Simulation runs were conducted by changing the parameter values.

4.5.2 Data Description

A pick-up truck (GMC Sierra 2500 HD) with a RoLine profiler installed was used to collect pavement profile on 10.8 miles (17 km) of roadway segments. The collected profile was used to calculate the International Roughness Index (IRI) and simulate RMS acceleration of the quarter-car model. Meanwhile, two tablets (Samsung Galaxy Note 10.1) were placed on the vehicle floor to collect data, including 3-way accelerations, GPS coordinates, and vehicle speeds, which were applied to calculate the acceleration-based metric. The two tablets were placed on the floor in front of the second row seats and close to the two side doors so that both right-wheel-path and left-wheel-path data could be collected. To ensure the tablets did not dislocate themselves when the vehicle was running, they were fit into two boxes attached to the floor with sticky tape.

The acceleration data were updated every 0.02 second, while the GPS and speed data were updated every 1 second. Only the vertical acceleration was used to quantify vehicle vibration responses. Each individual data record was matched to the milepost location through a map-matching process based on the GPS information. Acceleration data were aggregated using the RMS algorithm on the 0.1-mile (0.16-km) interval. It was found that the estimated GPS accuracy was between 4 and 8 meters, which is acceptable for estimating the roughness condition for every 0.1-mile pavement section. Vehicle speeds were also recorded every 1 second, allowing us to address the impact of speed on acceleration readings.

Data collection was conducted on April 22, 2014 near Charlottesville, Virginia. The studied segments contain 10.8-mile segments from four secondary routes: SR-600, SR-616, SR-676, and SR-799. The collected IRI data were used as the reference value of pavement roughness. For general classification of road condition, VDOT identifies different roughness levels using corresponding quantitative IRI values (*15*). Note that transportation agencies may have different definitions for deficient pavement and thus may not have identical threshold values. As for this study, pavement sections with an IRI greater or equal to 140 in/mile (2.2 m/km) were marked as deficient sections. Table 4.1 summarizes the number of 0.1-mile sections in each roughness category according to VDOT's current policy. Of the total of 108 0.1-mile (0.16 km) pavement sections, there were 48 deficient sections. The IRI values range from 85.7 in/mile to 248.2 in/mile (0.59 to 4.22 m/km).

TABLE 4.1 Data Summary based on Routes

Route	IRI Summary (in/mile)			Number of Sites		Length (mile)
	Med.	Min.	Max.	Deficient	Non-Def.	
SR-616	124.7	86.1	172.0	6	15	2.1
SR-600	121.2	85.7	219.3	9	25	3.4
SR-799	87.4	123.9	228.5	8	20	2.8
SR-676	189.9	151.8	248.2	25	0	2.5
Total	94.6	85.7	248.2	48	60	10.8

Besides the GMC pickup truck, two other vehicles (a 2001 Volvo S60 and a 2012 Subaru Forester) were also used to collect GPS, vehicle acceleration and speed data using the same tablets on the same segments in April 2014. The vehicle speeds range from 31 mph to 56 mph.

4.5.3 Quantification of Vehicle Vibration Response

Most previous studies used root mean squared (RMS) vertical acceleration, which is calculated with the equation below, to represent the vehicle vibration response under a constant speed (*12*).

$$a_{z,RMS} = \sqrt{\frac{1}{N}\sum_{i=1}^{N}(a_{z,i} - g)^2} \qquad (12)$$

Where:
$a_{z,\ RMS}$ = the RMS vertical acceleration for the studied pavement section;
N = the number of acceleration readings among the studied 0.1-mile pavement section;
$a_{z,i}$ = the i^{th} vertical acceleration reading among the studied section;
g = the contribution of the force of gravity.

One limitation of the RMS is that it can not account for the changing speeds in the real world. To address this limitation, a UVA CTS study developed and evaluated an improved acceleration-based metric, the normalized RMS vertical accelerations (*NRMS*s). According to the study, *NRMS* is defined by incorporating vehicle speed, as shown in the following equation (*43*).

$$NRMS = (80/V)^{1.3} a_{z,RMS},$$

Where V = vehicle speed in km/h.

NRMS indicates the vibration level that a vehicle is expected to experience at the speed of 80 km/h. Unlike the *RMS*, the *NRMS* can generalize to different functional classes of highway thanks to the incorporation of vehicle speed. Once the tablet data were collected, they were aggregated to calculate the *NRMS* at a 0.1-mile interval on the study routes.

4.6 Analysis Results

4.6.1 Sensitivity Analysis

The purpose of sensitivity analysis is to understand whether and how different vehicle dynamic systems will impact the vibration responses. As described above, there are four important parameters in a quarter-car model: tire stiffness, sprung mass stiffness, sprung mass damping, and the ratio of unsprung mass to sprung mass. It is useful to learn how the vibration response changes accordingly when these parameters change. Simulations were conducted based on quarter-car models with changing dynamic parameters. Table 4.2 summarized the values of the Golden-Car parameters, the coefficients of variation (CV, ratio of standard deviation to the mean value) for typical vehicles (*47*), and the simulation intervals.

TABLE 4.2 Summary of Golden-car Dynamic Parameters and Simulation Intervals

Parameter	Golden-car	CV[1]	Intervals[2]
k_t (1/s^2)	653	21.7	[300, 1006]
k_s (1/s^2)	63.3	27.4	[29, 97]
c_s (1/s)	6	18.1	[2.76, 9.24]
μ	0.15	-	[0.07, 0.23]

Note: 1. Data came from Bridgelall's recent study (*47*);
2. Determined as $basicvalue * (1 \pm z_{\alpha=0.05} * 27.4\%)$.

The simulation intervals were the intervals within which the values of the dynamic parameters change. It was determined in a way that they could cover most of the vehicles in the market. It was found that the sprung mass stiffness has the largest coefficient of variation (CV) value. As a result, its value (27.4%) was used to decide to what extend the dynamic parameters need to fluctuate and the upper/lower bound of the simulation intervals were calculated by increasing/decreasing the original parameter by 54% (1.96*27.4%).

The quarter-car simulations at the speed of 50 mph (80 km/h) were conducted on the four collected profiles with the dynamic parameters fluctuating within the simulation intervals. The resulting RMS accelerations were recorded for each simulation. Figures 4.3 to 4.6 show the sensitivity analysis results with shape areas indicating the fluctuations in the RMS acceleration.

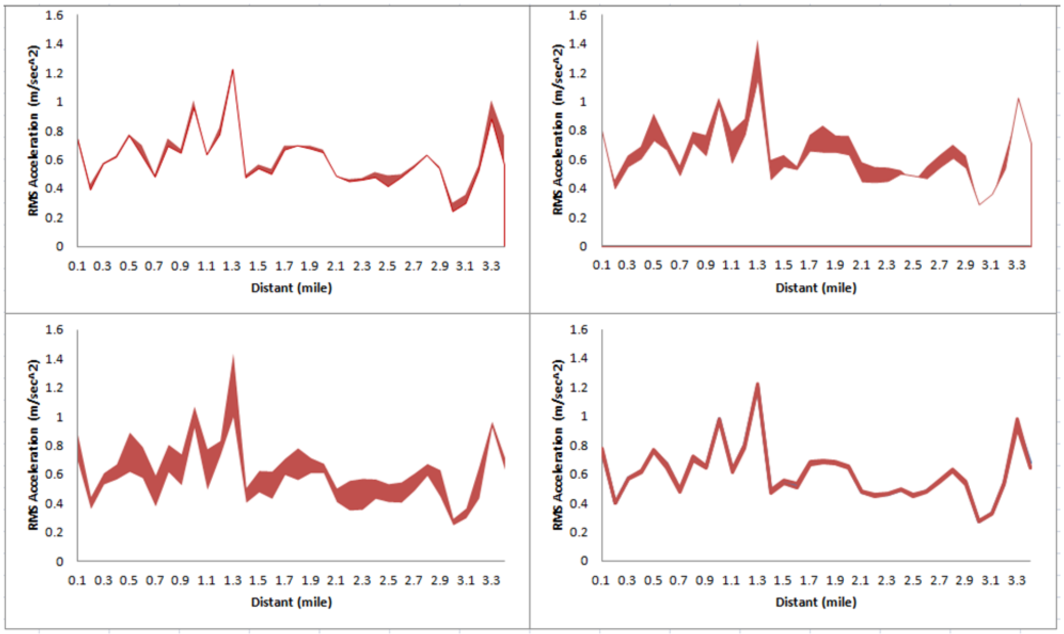

FIGURE 4.3 Effect of quarter car parameters on RMS on SR-799;
Top Left k_t; Top Right:C_s; Bottom Left: k_s; Bottom Right:μ.

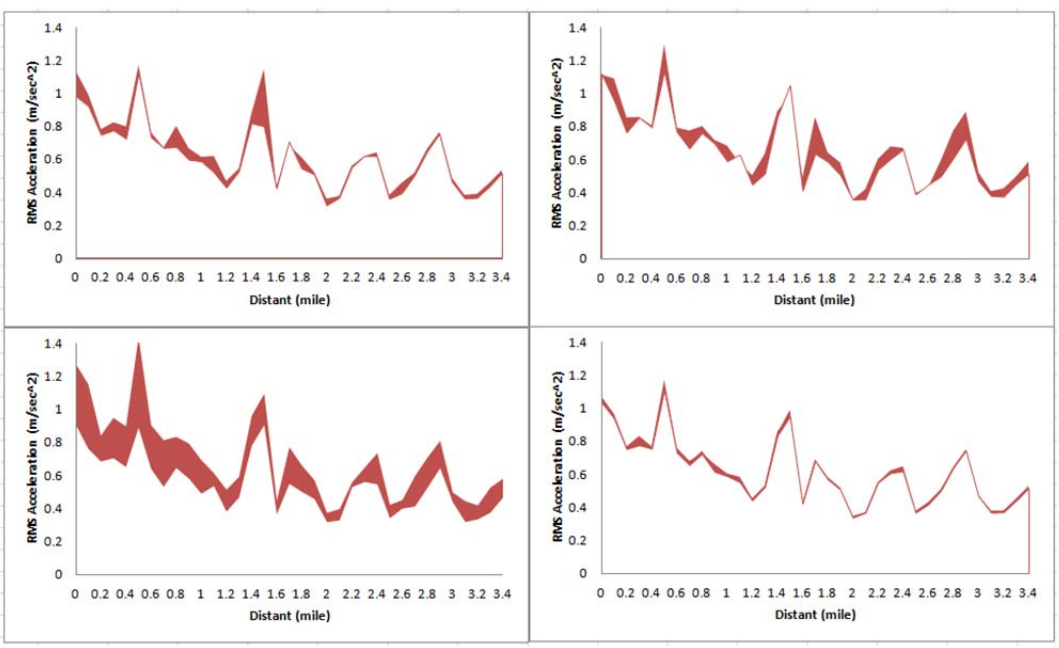

FIGURE 4.4 Effect of quarter car parameters on RMS on SR-600;
Top Left k_t; Top Right:C_s; Bottom Left: k_s; Bottom Right:μ.

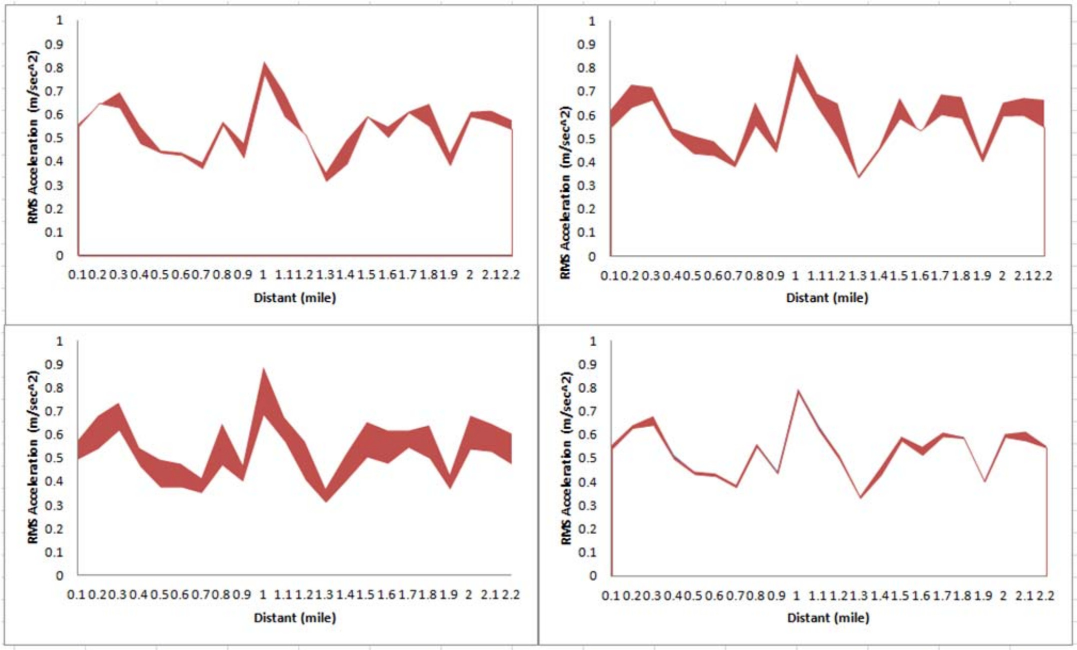

FIGURE 4.5 Effect of quarter car parameters on RMS on SR-616;
Top Left k_t; Top Right:C_s; Bottom Left: k_s; Bottom Right:μ.

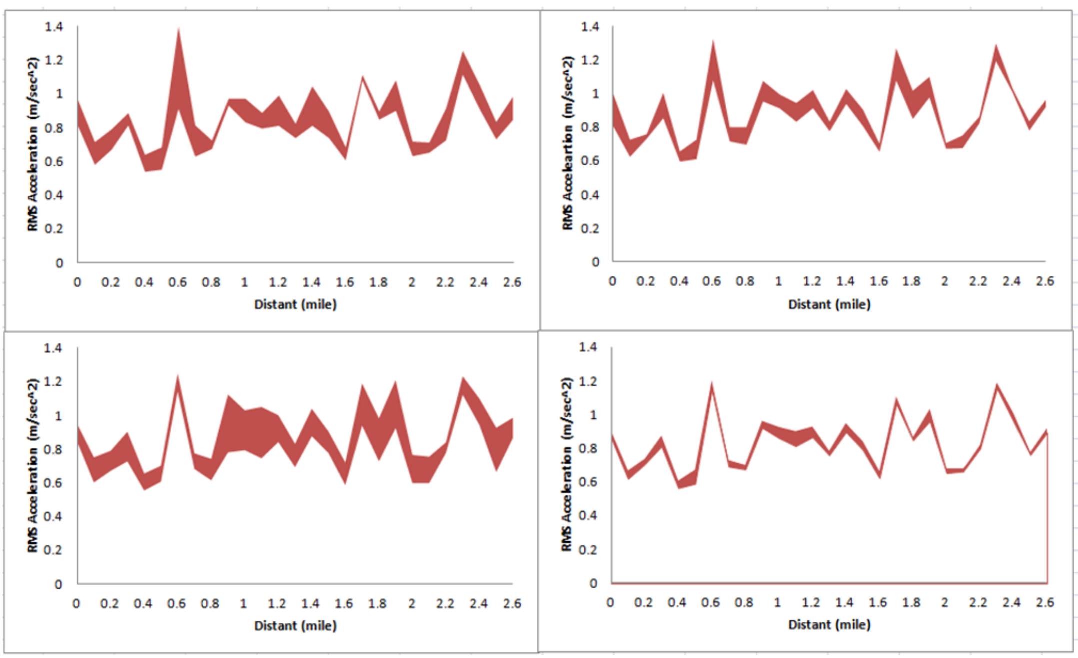

FIGURE 4.6 Effect of quarter car parameters on RMS on SR-676;
Top Left k_t; Top Right:C_s; Bottom Left: k_s; Bottom Right:μ.

According to the figures above, it appears that the spring stiffness of the sprung mass (k_s) most affects the vehicle floor RMS acceleration, followed by the damping of the sprung mass and tire stiffness. On the other hand, the fluctuations of the ratio of the unsprung mass to the sprung mass have very small impact on the final RMS acceleration.

To quantify the sensitivity of the parameter change, a sensitivity rate (*SR*) is defined as the mean of the ratios of the upper limits of the RMS accelerations to their related lower limits, as shown in the equation below.

$$SR = \frac{1}{N}\sum_{i=1}^{N}\frac{a_{RMS}(i)^{+}}{a_{RMS}(i)^{-}}$$

Where $a_{RMS}(i)^{+}$ and $a_{RMS}(i)^{-}$ are the upper and lower limits of the RMS acceleration for the i^{th} observation, and *N* is the number of observations. The *SR* is an index with a value that is always higher than 1. The higher SR value indicates a higher level of sensitivity.

Table 4.3 summarizes the SR and the standard deviation (STD) of those related ratios for each dynamic parameter.

TABLE 4.3 SR and its Standard Deviation according to Individual Dynamic Parameter

	k_t (1/s^2)	k_s (1/s^2)	c_s (1/s)	μ
SR	1.09	**1.27**	1.12	1.03
STD	0.09	**0.12**	0.08	0.02

Note: A SR numbers in bold indicate that it is significantly larger than 1 at the 0.05 confidence level.

According to the table above, only the *SR* of the sprung mass stiffness is significantly larger than 1 at the 0.05 confidence level, indicating that the variation in sprung mass stiffness could have a statistically significant impact on vehicle vibration response. On average, changing the sprung stiffness from one end to the other end can increase the RMS acceleration by 27%. On the other hand, the *SR* for the ratio of unsprung mass to sprung mass is only slightly larger than 1, indicating that the loading of the vehicle is not expected to have much influence on the resulting RMS acceleration.

The results of sensitivity analysis indicate that people could obtain significantly different acceleration results from two vehicle systems when their spring stiffness of the sprung mass is not similar to each other. Considering that transportation agencies could use a fleet that contains a variety of vehicle systems, it is necessary to explore the relationship between acceleration data from different vehicles, which could lead to a solution to calibrate vehicle systems.

4.6.2 Relationship Analysis

This section will first show visually the relationship between accelerations from any two of the nine simulated vehicle dynamic systems (as listed in the following table).

TABLE 4.4 Simulation Scenarios with Different Dynamic Parameters

Sim ID	k_t (1/s^2)	k_s (1/s^2)	c_s (1/s)	μ
1	653	63.3	6	0.15
2	940.32	63.3	6	0.15
3	365.68	63.3	6	0.15
4	653	97.482	6	0.15
5	653	29.118	6	0.15
6	653	63.3	9.24	0.15
7	653	63.3	2.76	0.15
8	653	63.3	6	0.23
9	653	63.3	6	0.07

Figure 4.7 shows a scatter plot matrix of the simulated RMS accelerations, which is able to indicate the relationship of RMS accelerations between any two simulation scenarios.

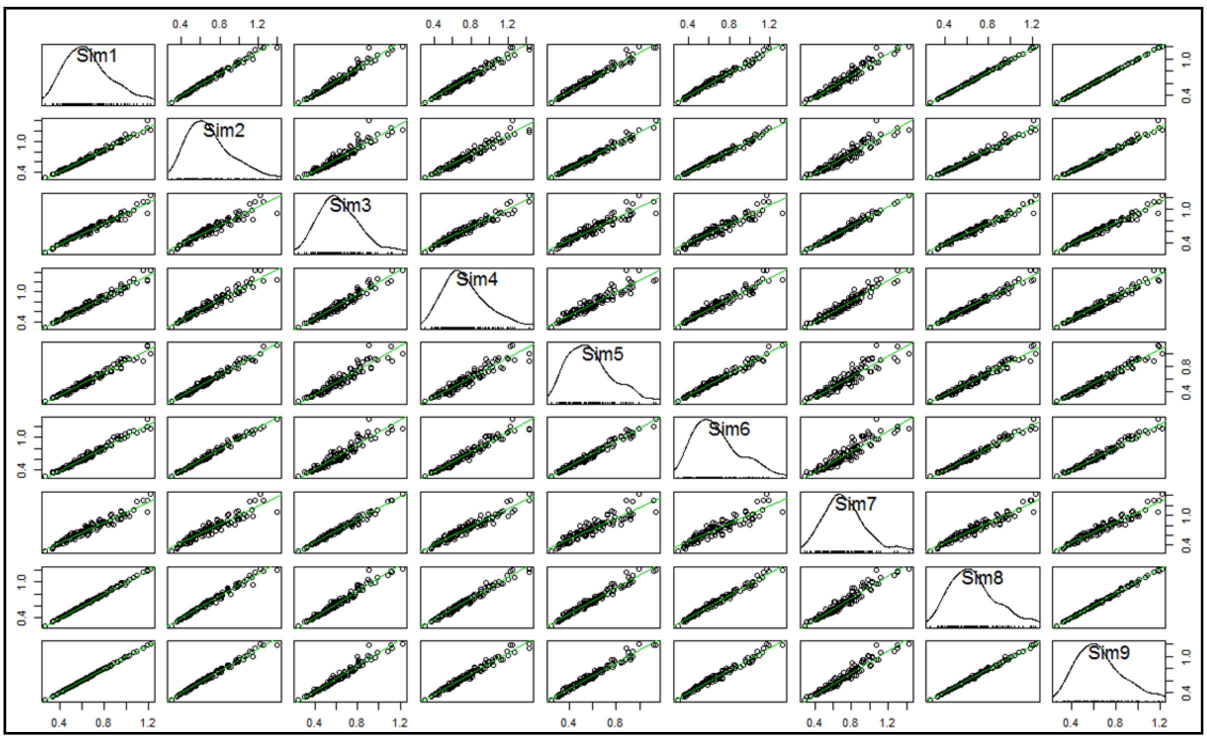

FIGURE 4.7 Scatter plot matrix for the nine simulation scenarios.

Visually, the scatter plot matrix illustrates a very good linear relationship for each pair of simulation scenarios. The following correlation table tells a similar story.

TABLE 4.5 Correlation Coefficient Table

	Sim 1	*Sim 2*	*Sim 3*	*Sim 4*	*Sim 5*	*Sim 6*	*Sim 7*	*Sim 8*	*Sim 9*
Sim 1	1.00								
Sim 2	0.99	1.00							
Sim 3	0.98	0.95	1.00						
Sim 4	0.98	0.97	0.97	1.00					
Sim 5	0.98	0.99	0.94	0.94	1.00				
Sim 6	0.99	0.99	0.95	0.97	0.99	1.00			
Sim 7	0.97	0.94	0.99	0.96	0.92	0.92	1.00		
Sim 8	1.00	0.99	0.98	0.99	0.98	0.99	0.97	1.00	
Sim 9	1.00	0.99	0.99	0.98	0.98	0.98	0.97	1.00	1.00

It was found that the RMS accelerations from each individual simulation scenario correlated very well with those from other simulation scenarios. The correlation coefficients in most cases are higher than 0.95, with the smallest value of 0.92.

With the results from the quarter car simulation, it is reasonable to assume that the relationship of vibration response between two different vehicle systems is linear. This assumption was tested using real world tablet data.

4.6.3 Real World Data Comparison

This section compares the tablet data from three different vehicles to see whether the linear relationship holds up in the real world. Two linear regression models were created based on the tablet data collected on the same four routes where the profile data were collected, with *NRMS* from the GMC Sierra 2500 HD as the dependent variable and *NRMS*s from the Subaru Forester and the Volvo S60 as the independent variable, respectively. Note that *NRMS* was used here because in naturalistic driving situation vehicle speeds change between different drives and it is recommended to normalize the RMS acceleration with vehicle speed.

The following figures show the scatter plots of NRMS data from each pair of vehicles. Visually, linear trends appear in both scatter plots.

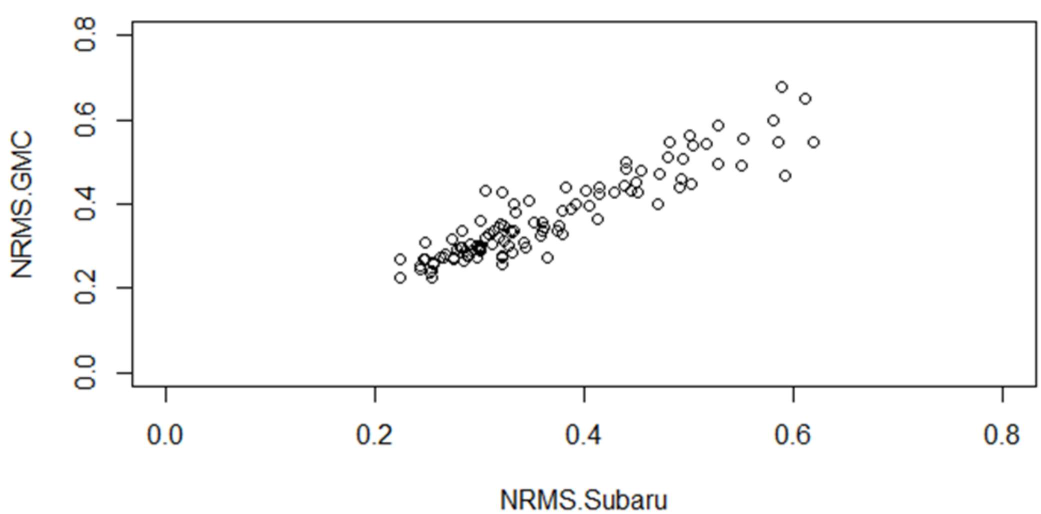

FIGURE 4.8 Scatter plot: NRMS.GMC Vs. NRMS.Subaru.

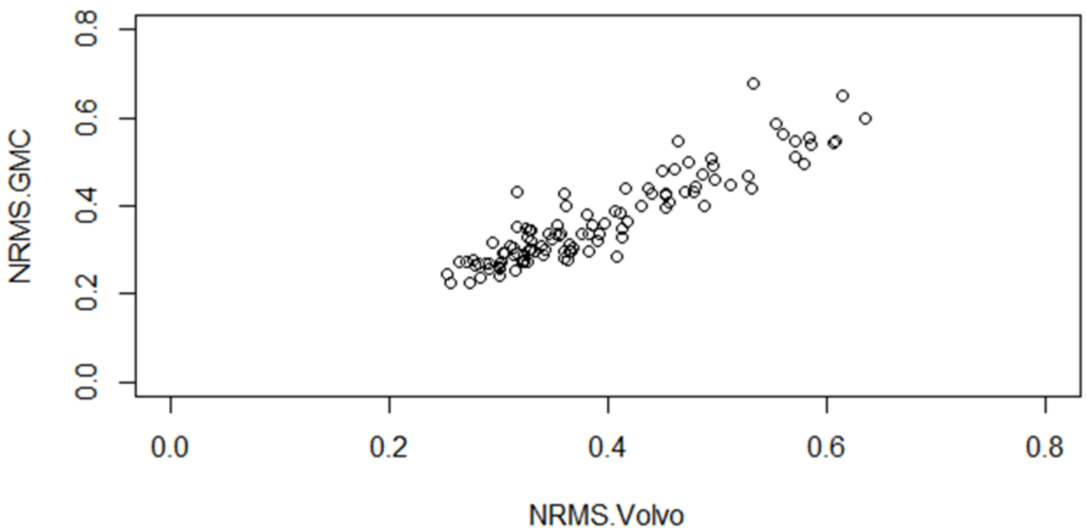

FIGURE 4.9 Scatter plot: NRMS.GMC Vs. NRMS.Volvo.

Table 4.6 summarizes the results for the two linear models.

TABLE 4.6 Linear Regression Model Results

<table>
<tr><th>Model</th><th>Parameter</th><th>Coefficient</th><th>Std. Error</th><th>t value</th><th>Pr(>|t|)</th></tr>
<tr><td rowspan="4">GMC-Subaru</td><td>Intercept</td><td>0.022</td><td>0.014</td><td>1.49</td><td>0.138</td></tr>
<tr><td>NRMS.Subaru</td><td>0.948</td><td>0.038</td><td>24.78</td><td><0.0001</td></tr>
<tr><td>R-squared</td><td>0.85</td><td></td><td></td><td></td></tr>
<tr><td>F-statistic</td><td>614.2</td><td></td><td></td><td></td></tr>
<tr><td rowspan="5">GMC-Volvo</td><td>Parameter</td><td>Coefficient</td><td>Std. Error</td><td>t value</td><td>Pr(>|t|)</td></tr>
<tr><td>Intercept</td><td>-0.016</td><td>0.017</td><td>-0.95</td><td>0.138</td></tr>
<tr><td>NRMS.Volvo</td><td>0.977</td><td>0.042</td><td>23.34</td><td><0.0001</td></tr>
<tr><td>R-squared</td><td>0.84</td><td></td><td></td><td></td></tr>
<tr><td>F-statistic</td><td>544.7</td><td></td><td></td><td></td></tr>
</table>

According to the linear regression analysis, the linear models fitted the data well, with both R-squared values at around 0.84. The independent variable from both models is statistically significant at the 0.01 level. To examine whether there are any non-linear relationships existing in the data, more plots are presented in Figures 4.10 and 4.11. These include plots of fitted values versus residuals/standardized residuals, Q-Q plot, and residuals versus leverage plot.

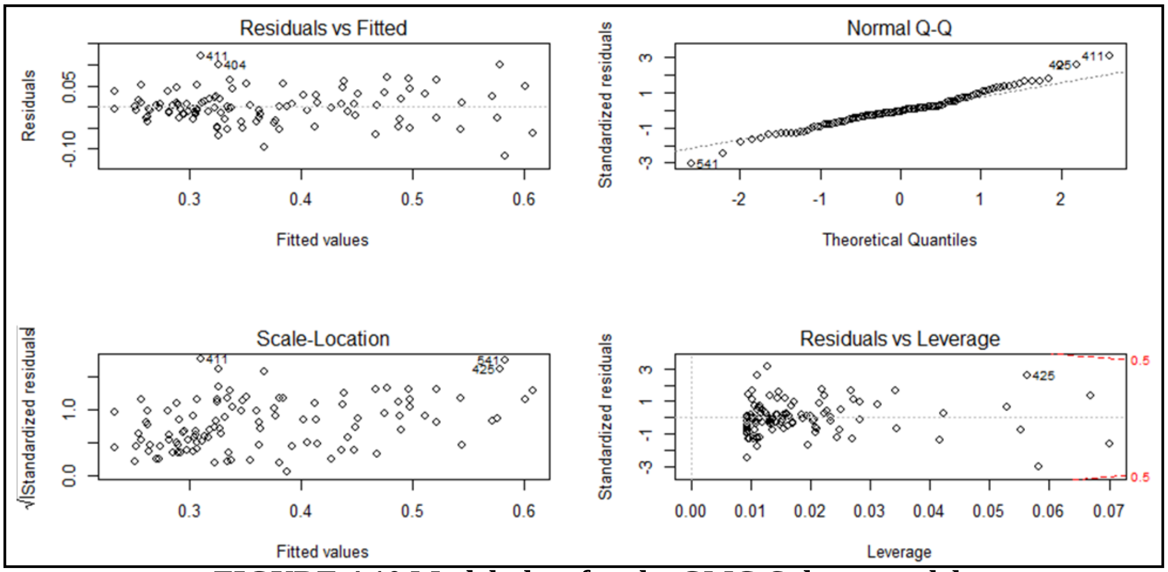

FIGURE 4.10 Model plots for the GMC-Subaru model.

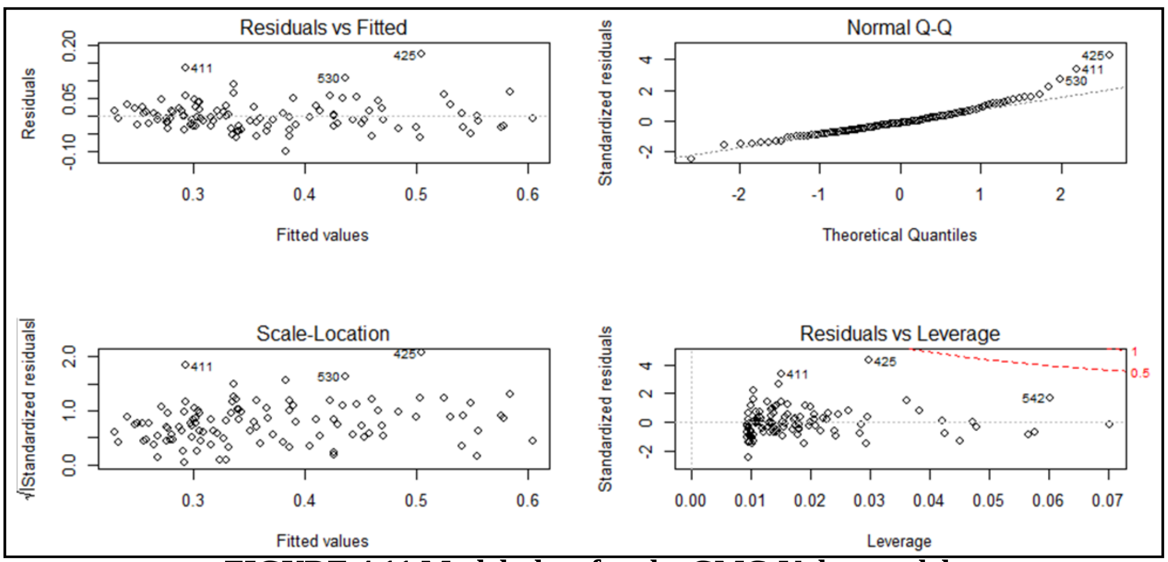

FIGURE 4.11 Model plots for the GMC-Volvo model.

There are no obvious curvilinear trends in the residuals across the fitted values. In other word, the real world tablet data also show a linear relationship between NRMS results from different vehicles.

In summary, the sensitivity analysis and relationship analysis provide a better insight regarding the imparts of vehicle dynamic system on vibration response and the relationship between vibration results from different vehicle systems. It was found that variations in vehicle dynamic parameters can result in a significantly different magnitude of vibration response. The magnitude of vehicle vibration response is most sensitive to the spring stiffness of the sprung mass and the vibration responses on the same pavement segment can fluctuate by an average of 27% under extreme cases. Furthermore, the relationship analysis shows that the vibration responses are linearly correlated between different vehicle systems, which were illustrated in both the quarter-car simulations and the tablet data collected under naturalistic driving conditions.

4.7 Probe System Calibration

Assuming that transportation agencies will use agency-owned vehicles to build a pavement condition network screening system, it is possible that the fleet includes some vehicles that have a good variety of dynamic systems. The findings above indicate that the acceleration-based indexes on a typical pavement section from different vehicle systems can be calibrated to a reference value using a linear model, as presented in the following equation.

$$NRMS_{reference} = \alpha + \beta NRMS_{non-reference}$$

Where:
$NRMS_{reference}$ = the calibrated/reference *NRMS* value, it represents the *NRMS* result of the reference vehicle on the same pavement section;
$NRMS_{non\text{-}reference}$ = the *NRMS* value before calibration; and
α, β = coefficients for the linear model.

The purpose of the calibration process is to determine proper coefficients for each type of vehicles in the fleet. This section introduces a vehicle calibration procedure to help them calibrate vehicles in the fleet. The procedure includes data and system requirement for calibration, the criteria regarding the necessity of the calibration, the criteria regarding the success of the calibration, and a step by step process description. A case study based on smartphone data collected from three vehicles were also presented and demonstrated that the calibration improved system performance.

4.7.1 System Requirement

For calibration purposes, at lease two elements are required, including an agency-owned fleet and a reference vehicle.

The agency-own fleet contains vehicles that will be used as probes to collect data for pavement roughness assessment. There are no restrictions on the types of vehicle. However, it is expected that wider vehicle system diversity requires more efforts for calibration. The probe data can come from mobile devices such as smartphones and tablets, or vehicular sensors that already installed in the vehicle. Required data elements include GPS location, vehicle body vertical acceleration, vehicle speed, as well as vehicle ID that allows people to identify which vehicle the data come from.

A reference vehicle is a vehicle whose roughness measurement will be used as the target variable in calibrating other non-reference vehicles. Generally, a pavement classification model has been developed based on the reference vehicle data to identify deficient pavement sections.

4.7.2 Calibration Procedure

The flowchart presents a recommended calibration procedure, followed by a detailed description for each step. It is important to note that it may not be necessary to calibrate each individual vehicle in the fleet as some vehicles could have very similar dynamic systems. For example, vehicles of the same model or vehicles that have been shown to have very similar vibration responses could result in NRMS results with only marginal varieties. In this case, transportation agencies can only calibrate a representative vehicle and apply the resulting model to the whole group.

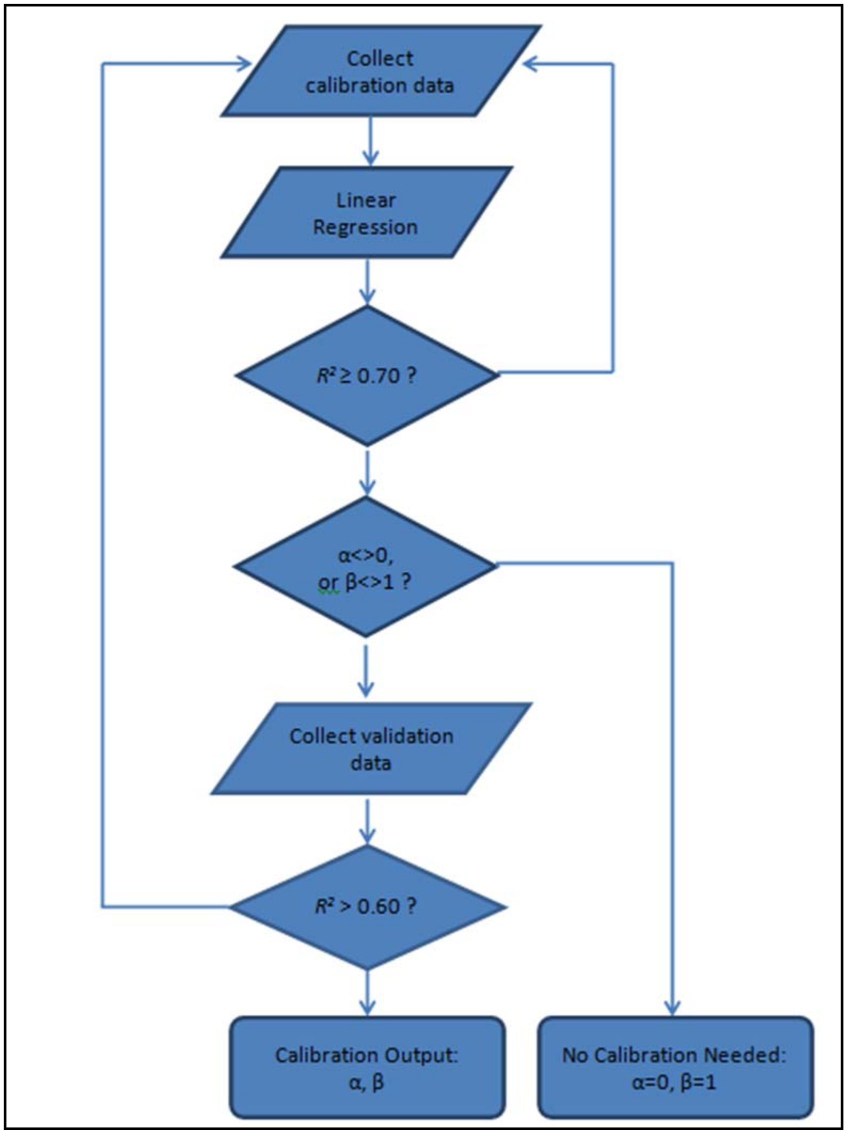

FIGURE 4.12 Calibration flowchart.

The steps for calibrating a non-reference vehicle is described below:

1. **Collect data on a set of selected pavement sections for initial calibration**

   Both the reference vehicle and the non-reference vehicle should collect GPS information, acceleration, and vehicle speed data on the selected pavement sections. For better performance of the calibration model, it is recommended to include the most typical types of pavements with a good variety of roughness level. To facilitate the calibration process, the locations should be carefully selected so that both the reference vehicle and non-reference vehicles can easily collect data there. Also, the difference of data collection time between the reference vehicle and the non-reference vehicle should be less than one month.

2. **Develop a linear regression model to find out the coefficients**

   A linear regression model can be created using the NRMS from the reference vehicle as the dependent variable and the NRMS from the non-reference vehicle as the independent variable.

$$NRMS_{reference} = \alpha + \beta NRMS_{non-reference}$$

3. Check the goodness of fit of the regression model

This step is optional. The goodness of fit of the regression model can be impacted by the variations between the reference vehicle data collection and the non-reference vehicle data collection, in terms of time, weather condition, driving path and other conditions. Idearly the data from reference vehicle and non-reference vehicle should be collected under similar conditions, which may be hard to achieve in some naturalistic driving condition. Checking the goodness of fit (*R* squared value) is a good way to help users decide whether or not to accept the regression model. The default threshold R squared value is set to 0.7. Note that people can adjust this value based on specific condition given more available data. If the goodness of fit meets the criteria, the regression model can be applied to the next step; if not, it is recommended to select a new set of calibration sections and restart from Step 1. This step can be skipped if there is a good reason to believe in the regression model.

4. Compare the coefficients with calibration criteria

Some vehicles may share similar dynamic systems. It is possible that some vehicles can generate very similar roughness measurements even without calibration. There are two criteria to determine whether calibration work is needed. Hypothesis test should be conducted to see whether the criteria are met. The null hypothesis is that the roughness measurement of the reference vehicle is similar to that from the non-reference vehicle ($NRMS_{reference} = NRMS_{non-reference}$). It can also be stated based on the coefficient values.

H_0: $\alpha = 0$, and $\beta = 1$.

If the hypothesis is rejected, it indicates that calibration is necessary and the calibration process should continue. Otherwise, it is not worth to calibrate the studied vehicle and the original data from the non-reference vehicle can be used directly.

5. Collect data on a set of selected pavement sections for validation of the model

The step collects data on a separate set of pavement sections for validation purpose. Again, both the reference vehicle and the non-reference vehicle should collect data for these sections.

6. Calculate the validation result and compare it with validation criteria

The calibrated NRMS for the non-reference vehicle can be calculated using the linear model developed from Step 2.

$$NRMS_{calibrated} = \alpha + \beta NRMS_{non-reference}$$

The NRMS from the reference vehicle can be treated as ground truth to test the performance of the calibration model. The coefficient of determination (*41*), or R squared, is applied as the validation criteria and defined by the following equation. Here the R squared value shows the similarity between the calibrated NRMS values and the reference NRMS values.

$$R^2 = 1 - \frac{\sum_{i=1}^{n}(NRMS_{reference,i} - NRMS_{calibrated,i})^2}{\sum_{i=1}^{n}(NRMS_{reference,i} - \overline{NRMS})^2}$$

Where:
$\overline{NRMS}$ = the average NRMS of the reference vehicle,and
n = number of observations in the validation dataset.

A typical value of R squared ranges from 0 to 1, with higher value indicating better performance of the calibrated value. As a result, people can set up validation criteria based on the R squared value. As a default case, here the threshold R squared value is set to 0.6. Note that this threshold value can be adjusted based on specific cases. If the result meets the criteria ($R^2 > 0.6$), accept the calibration model and use it to calibrate data on new pavement sections; if not, selected a new set of calibration pavement sections and restart the process from Step 1.

4.7.3 Case Studies

This section presents two case studies regarding calibrating probe vehicle systems. The first case tried to calibrate the Volvo S60 based on the data collected on secondary roads, with the GMC pickup truck as the reference vehicle. First, the data collected on SR-600 are used here as the initial calibration data. The next step is to develop a regression model with the GMC truck NRMS and the Volvo NRMS as the dependent and independent variables, respectively. The table below summarizes the model results.

TABLE 4.7 Linear Calibration Model Results for Case #1

Parameter	Coefficient	Std. Error	t value	Pr(>|t|)
Intercept	-0.07	0.04	-1.76	0.09
NRMS.Volvo	1.09	0.10	11.11	<0.001
R-squared	0.79			
F-statistic	123.5			
DOF	32			

The R-squared value is higher than 0.7 and the regression model is applied to the next step, which will test whether there are statistical evidence to reject the hypothesis that the NRMSs from the reference vehicle and the non-reference vehicle are similar.

TABLE 4.8 Hypothesis Test Results

Hypothesis	t value	Pr(>|t|)
α=0	-1.76	0.09
β=1	0.90	0.37

According to the hypothesis test results, both *t* values are not significant at the 0.05 confidence level. In other words, there is no significant statistical evidence to reject the null hypothesis. It indicates that it may not worth to calibrate the NRMS results from the Volvo S60 and its NRMS result can be used directly as the reference vehicle.

To identify deficient pavement sections, the UVA CTS study developed a pavement classification model based on the data from GMC pickup truck (*43*). This model was applied in this case study. The NRMS threshold value was found to be 0.36 m/sec^2 to separate deficient pavement and non-deficient pavement. Assume that VDOT wants to screen the pavement condition on SR-616, SR-676, and SR-799, the original NRMS values calculated from the Volvo S60 data can be directly applied to the classification model to identify deficient pavement sections. Table 4.9 summarizes the classification results from both the reference vehicle (GMC) and the non-reference vehicle (Volvo).

TABLE 4.9 Pavement Roughness Classification Results for Case #1

Vehicle	Observed	Testing Data Predicted		
		Non-Def.	Deficient	Correct Percentage
GMC	Non-Def.	34	1	97.14
	Deficient	7	32	82.05
Volvo	Non-Def.	33	2	94.29
	Deficient	7	32	82.05

According to Table 4.9, the performance of Volvo data is very close to that from the reference vehicle. Both of them can identify correctly 82 percent (32 out of 39) of those deficient sections. This also shows that it is not necessary to calibrate the Volvo S60 data if the GMC pickup truck is treated as the reference vehicle.

The second case shows another scenario in which calibration is necessary in order to improve the network screening performance. Data were collected on I-64 in October 2013, using two vehicles, a 2001 Volvo S60 and a 2003 Toyota Corolla. The initial calibration dataset includes a 5.8-mile freeway segment, from milepost 118.3 to milepost 124 on I-64 E, and the testing dataset includes a 5.2-mile freeway segment, from milepost 124.1 to milepost 119 on I-64 W.

The table below summarizes the model results, with the Volvo and Corolla data as the dependent and independent variables, respectively.

TABLE 4.10 Linear Calibration Model Results for Case #2

Parameter	Coefficient	Std. Error	t value	Pr(>|t|)
Intercept	0.019	0.012	1.57	0.12
NRMS.Corolla	0.709	0.038	18.72	0.00
R-squared	0.86			
F-statistic	350.5			
DOF	56			

The R-squared value (0.86) is higher than 0.7 and the regression model is applied to the next step, which will test whether there are statistical evidence to reject the hypothesis that the NRMSs from the reference vehicle and the non-reference vehicle are similar.

TABLE 4.11 Hypothesis Test Results

Hypothesis	t value	Pr(>|t|)
α=0	1.57	0.12
β=1	**7.70**	0.00

According to the hypothesis test results, the t value for β=1 is significant at the 0.05 confidence level. In other words, there is a significant statistical evidence to reject the null hypothesis. It indicates that it may worth to calibrate the NRMS results from the 2003 Toyota Corolla.

The next step is to test whether the same calibration model (as presented in the following equation) holds up using a separate dataset. In this case, the I-64 W data were applied to test the calibration model.

$$NRMS_{calibrated} = 0.019 + 0.709NRMS_{Corolla2003}$$

Since no classification model based on the Volvo data is available, the second case study can not compare the classification results between the reference vehicle data and non-reference vehicle data. Instead, plots and R squared values were used to evaluate the calibration effectiveness. Figure 4.13 shows the plots of NRMS results according to mileposts for Volvo S60, Corolla, and calibrated Corolla data. For comparison purpose, both I-64 E and I-64 W data were shown here.

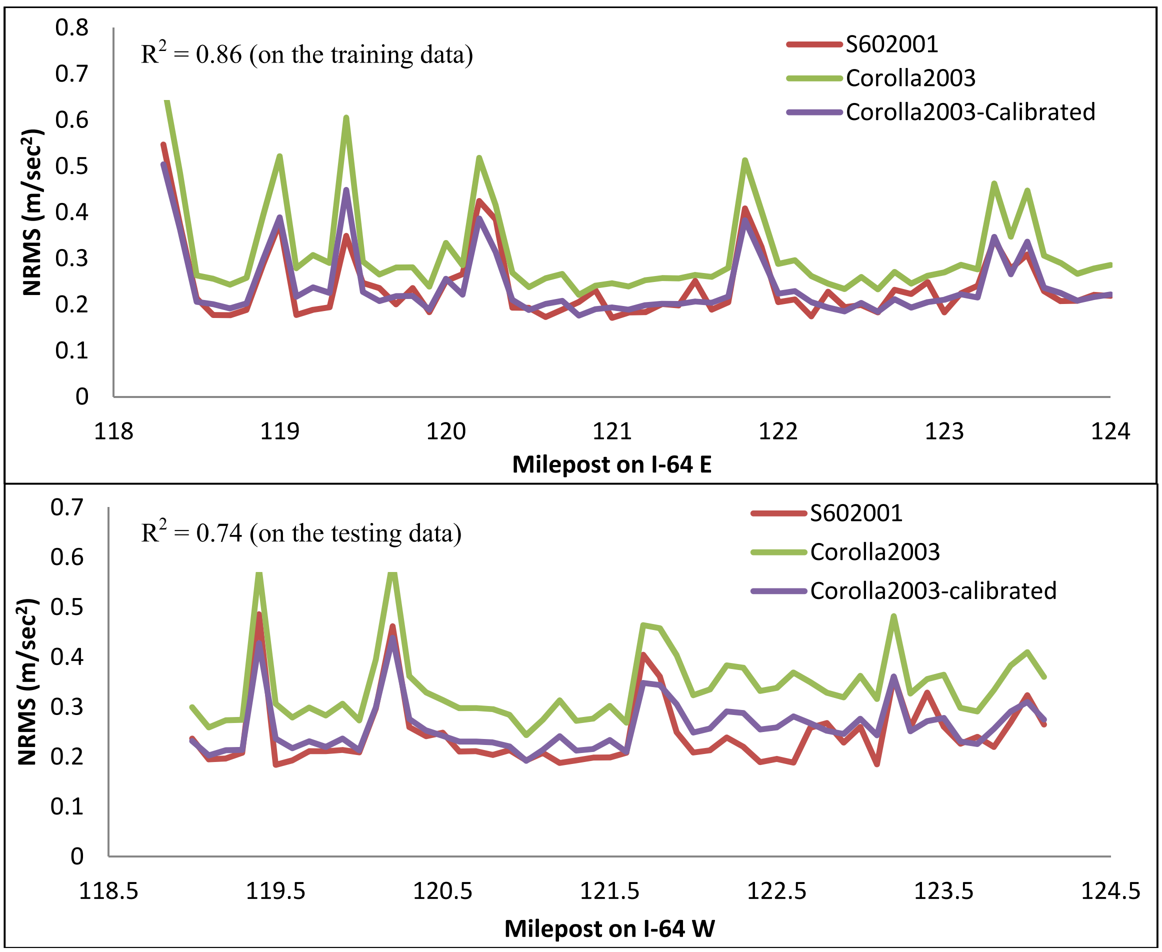

FIGURE 4.13 NRMS according to milepost on I-64 E/W.

Visually, the calibrated Corolla data were much more similar to the reference vehicle (Volvo S60) data for both the calibration and testing datasets. Before calibration, the NRMSs from the Corolla were about 41% higher than the reference vehicle, while the calibrated NRMSs has a significantly better similarity with the reference data, with a coefficient of determination (R^2) value of 0.74 on the testing dataset. The R squared value is higher than the threshold value (0.60) set for the acceptance of the calibration model. As a result, if a transportation agency uses the 2001 Volvo S60 as the reference vehicle, the calibration model developed here should be applied to calibrate data from a 2003 Toyota Corolla or other vehicles with a similar dynamic system.

4.7.4 Discussion

Before the full implementation of the connected vehicle program, it is likely that only a limited number of vehicles (i.e., agency-owned vehicles) are capable of sending out probe data for pavement network screening. It is expected that the calibration procedure can help to reduce impacts of the variety of vehicle dynamic systems and thus still obtain robust results with small sample size of data. The calibration procedure is only applicable in situations when transportation agencies know which type of vehicle the probe data come from. This information will allow transportation agencies to create and select proper calibration models. As a result, it is recommended that vehicle identification or vehicle type to be included in the probe data elements, along with accelerations, vehicle speeds and GPS locations. In addition, it is cost prohibitive and unnecessary to calibrate each individual vehicle in the fleet. Since some vehicles have very similar dynamic systems (i.e., vehicles of the same model), they are likely to share similar NRMS results on a same pavement segment. In this case, transportation agencies can only calibrate a representative vehicle and apply the resulting model to the whole group. Transportation agencies are recommended to select the most common vehicle type as the reference vehicle to minimize the need of vehicle calibration. It is also recommended that the calibration models be updated in a proper time interval (i.e., every five years) for the reason that vehicle' dynamic characteristics may change with its age.

When most of the vehicles are connected in the future, transportation agencies may not be able to access to the general vehicles' identification information for calibration due to privacy concerns. In that case, averaging the NRMS results from numerous vehicles on the same section could be a more proper approach to reduce the impact of vehicle dynamic systems. Continuous research regarding this approach and sampling methods is strongly recommended once there are available data on the field.

4.8 Conclusions

This study investigated the impact of vehicle dynamic systems on vehicle vibration response, which directly affects the acceleration-based metric for pavement roughness measurements. The sensitivity analysis and relationship analysis based on quarter-car model simulations provide a better insight regarding the imparts of vehicle dynamic systems and the relationship between vibration results from different vehicle systems. It was found that variations in vehicle dynamic parameters can result in a significantly different magnitude of vibration response. The vehicle vibration response is most sensitive to the spring stiffness of the sprung mass and least sensitive to the loading of the vehicle. Furthermore, the relationship analysis shows that the vibration responses are linearly correlated between different vehicle systems, which were illustrated in both the quarter-car simulations and the probe data collected under naturalistic driving conditions.

These findings help transportation agencies better understand the probe data generated from different vehicle systems in the real world, and thus use the related acceleration-based metric properly for pavement condition network screening. Assuming that transportation agencies will use agency-owned vehicles to build a pavement condition network screening system, a vehicle calibration procedure was developed to help them calibrate vehicles in the fleet. The procedure includes data and system requirements for calibration, the criteria regarding the necessity of the calibration, the criteria regarding the success of the calibration, and a step by step process. Two case studies based on probe data collected from different vehicles were also presented and demonstrated that the calibration improved system performance.

There are several opportunities to expand this research to further validate this approach. For example, a prototype system can be developed using state-owned vehicles as probe vehicles to collect data. With the prototype system, a more comprehensive dataset can be generated by collecting data on more routes and in a wider area. It can be used to validate previous findings, address issues regarding implementation and assess the network benefit of this system. Also, it is recommended to design filters to remove invalid data by identifying situations where the acceleration-based metric can not work. For example, when a vehicle stops before a traffic light, the data do not contain useful information regarding pavement roughness. With the help of filters, only valid data points will remain.

ACKNOWLEDGMENTS

This research was funded by the Connected Vehicle Infrastructure University Transportation Center (CVI-UTC). The authors wish to thank Edgar de León Izeppi and Samer Katicha of Virginia Tech Transportation Institute for their help in data collection.

CHAPTER 5 ESTIMATION OF THE SAFETY EFFECT OF PAVEMENT CCONDITION ON RURAL TWO-LANE HIGHWAYS

A paper accepted for publication in *Transportation Research Record*

Huanghui Zeng[1], Michael D. Fontaine[2], and Brian L. Smith[3]

5.1 Abstract

The condition of the pavement surface can have an important effect on highway safety. For example, skidding crashes are often related to pavement rutting, polishing, bleeding, and dirty pavements. When transportation agencies develop paving schedules for their roadways, they often make decisions based on asset management condition targets but do not explicitly account for the role of pavement condition in roadway safety.

The Virginia Department of Transportation (VDOT) began automated pavement condition data collection using digital images and an automated crack detection methodology in 2007. This development enabled the DOT to track historical pavement condition information, and thus facilitates research regarding pavement condition impacts on safety. Information on how pavement condition influences safety could be used to inform paving decisions and better set priorities for maintenance.

The objective of this study is to quantitatively evaluate the safety effectiveness of good pavement conditions versus deficient pavement conditions on rural two-lane undivided highways in Virginia. Using the Empirical Bayes method, it was found that good pavements are able to reduce fatal and injury (FI) crashes by 26 percent over deficient pavements, but do not have a statistically significant impact on overall crash frequency. Further analysis indicated that the safety benefit of pavement condition improvement on FI crashes does not statistically significantly change as the lane or shoulder width increases. In conclusion, improving pavement condition from deficient to good can offer a significant safety benefit in terms of reducing crash severity.

1 Graduate Research Assistant, Department of Civil and Environmental Engineering, University of Virginia, Charlottesville, VA22904, Phone: 434-924-6362, E-mail: hz3xm@virginia.edu.
2 Associate Principal Research Scientist, Virginia Center for Transportation Innovation and Research, Charlottesville, VA 22903, Phone: 434-293-1980, E-mail: Michael.Fontaine@VDOT.Virginia.gov.
3 Professor and Chair, Department of Civil and Environmental Engineering, University of Virginia, Charllottesville, VA22904, Phone: 434-243-8585, E-mail: briansmith@virginia.edu.

5.2 Introduction

Pavement condition can have an important effect on highway safety. According to the American Association of State Highway and Transportation Official's (AASHTO) *A Policy on Geometric Design of Highways and Streets*, pavements should enable drivers to steer easily, keep their vehicles moving in the proper path, and provide a level of skid resistance that will accommodate the braking and steering maneuvers that can reasonably be expected for a particular site (*7*). Skidding crashes, a major concern in highway safety, are usually related to pavement rutting, polishing, bleeding, and dirty pavements (*7*). Previous research regarding the safety effect of pavement condition usually focused on either maintenance activities such as resurfacing or a certain type of pavement distress. Few studies were able to evaluate the safety effect of the general pavement condition, due in part to a lack of systematic data on overall pavement condition across the roadway network. If this information were available, it could be used for a variety of applications, including prioritizing sites for the agency's annual paving program or quantifying the benefits of preventative maintenance treatments.

Historically, it has been difficult to evaluate the safety effect of pavement conditions because of the lack of robust and consistent pavement condition measures. The Virginia Department of Transportation (VDOT) began automated pavement condition data collection using digital images and an automated crack detection methodology in 2007, which led to significant improvements in the consistency and efficiency of pavement condition data assessments. Since then, pavement condition information has been updated annually for the entire interstate and primary highway systems and every five years for the secondary system (*2*). This development has enabled engineers to track historic pavement condition information, and thus facilitates safety research regarding the effect of pavement conditions on crash frequency and severity.

5.2 Objectives and Scope

The intent of this paper is to provide DOTs with information that will allow them to include safety in the pavement management decision making process. It is not intended to be used as a justification to repave a road section that has a demonstrated pavement friction problem. The objective is to quantitatively evaluate the safety effectiveness of good pavement conditions versus deficient pavement conditions. The effect of pavement condition on both overall crash frequency and crash severity was examined. The targeted facility type is segments on rural two-lane primary highways in the Commonwealth of Virginia. The Empirical Bayes (EB) approach was applied using information from VDOT databases containing roadway inventory information, crash history, and pavement condition between 2007 and 2011.

5.3 Literature Review

While there has been a longstanding interest in examining the impact of pavement condition on safety, there are relatively few studies that have examined this issue in detail. Initial investigations in the late 1980s examined the effect of resurfacing. A synthesis by Cleveland of published evidence from studies conducted before 1986 found that there was a small, immediate increase in overall crash frequency for rural resurfacing projects conducted to address structural quality or poor ride condition (*34*). On the other hand, it was found that there was an average reduction of about 20 percent in wet pavement crashes for resurfacing projects conducted due to high numbers of wet pavement crashes (*34*). In light of these diverse findings, Cleveland concluded that the detrimental effect of resurfacing on safety, if any, is likely to be small. A related hypothesis was that vehicle speed will increase due to the smoother pavement surface after resurfacing, which, in turn, results in more crashes.

A well cited report by Hauer et al applied the Empirical Bayes (EB) approach to evaluate the safety effectiveness of two types of resurfacing projects undertaken in the early 1980s in New York State (*35*). Crash data and annual average daily traffic (AADT) from 1975 to 1987 were used. The study concluded that non-intersection crashes did increase by 21 percent during the first 30 months after resurfacing on "fast-track" projects in which no safety improvements accompanied the repaving, while non-intersection crashes did not change on reconditioning and preservation (R&P) projects that included geometric safety improvements. Another conclusion was that within the first 6 to 7 years of pavement life, safety improves as the pavement ages. In this study, no pavement condition data were collected and information about NYDOT's selection criteria regarding the two types of resurfacing projects were not mentioned.

To confirm or refine the Hauer et al study results, a larger study was undertaken in NCHRP project 17-9 (2), which involved five states: Washington, California, Minnesota, New York, and Illinois (*36*). The EB approach was used. Generally, there were five-years of before data and three-years of after data. The results were inconclusive, as there was not a single consistent pattern of safety effectiveness of resurfacing among and within the states. Crashes were found to increase after resurfacing in some states, but to decline in others. In addition, no explanation was found for these state-to-state variations.

Given the hypothesis that smother pavement surfaces following resurfacing lead to higher vehicle speeds, another NCHRP study evaluated the effect of resurfacing, restoration, and rehabilitation (RRR) projects on travel speed (*37*). Speed data were collected before and after resurfacing at 39 sites on rural two-lane highways of five states: Maryland, Minnesota, New Mexico, New York, and West Virginia. The results indicated that overall there was a small but statistically significant increase of approximately 1.6 km/h (1 mph) in both the mean speed and 85^{th} percentile speed after resurfacing. However, this effect varied substantially from site to site. No explanation was found for these site-to-site variations. In addition, no further analysis was conducted regarding the relationship between the change in speed and the change in crashes.

A 2010 study applied the cross-sectional method to investigate the efficacy of roadway improvements in terms of crash reduction on various subclasses of rural two-lane highways (*38*). Data were collected from 540 rural two-lane highway segments in the state of Indiana. The factors in the crash prediction model included lane width, shoulder width, pavement surface friction, pavement condition, and horizontal and vertical alignments. The effect of pavement friction in crash reduction was found to be significant for rural major collectors and rural minor arterials, but insignificant for rural principal arterial two-lane roads. It was also found that increased skid resistance impacted severe crashes more than non-severe crashes as the roadway functional class increased. The Present Serviceability Index (PSI), on a scale of 0 to 5, was used to represent pavement condition. The model results showed that better pavement condition significantly reduced crashes for rural two-lane principal arterials, but the effect was insignificant for the two lower road classes. One concern about this study is that there may be a multicollinearity issue in the models as pavement condition may correlate with pavement friction and this issue was not discussed in the paper.

In summary, most of the previous studies were event-driven, focusing specifically on the activity of resurfacing. The previous studies were not able to quantitatively track the pavement condition before and after the resurfacing projects due to lack of data, so the impact of remediating different levels of pavement distress could not be determined. Instead, some studies assumed the pavement conditions were consistent before the repaving project across sites. Since the pavement condition is sensitive to pavement age, traffic load, and other factors, this assumption could be problematic, especially when the duration of the before period is long. Also some previous studies assumed that the safety effectiveness is the same across facility types. However, the safety effectiveness of a change in pavement condition on rural two-lane highways could be very different with that on urban highways. Thanks to progress in the automated collection of quantitative pavement condition data, it is now possible to link the pavement condition information to crash history and other roadway features. It provides an excellent opportunity to investigate the safety effectiveness of pavement condition, which could inform many DOT investments in pavement maintenance. Some recent research had examined this topic by including pavement condition as a crash factor in crash prediction models, but this approach cannot account for regression-to-the-mean effects. In addition, inaccurate results may be derived from the regression models due to inappropriate model forms, omitted variable bias, or correlation among variables (*33*).

5.4 Methodology

Observational before-after studies have been considered the industry standard for the safety evaluation of treatments such as developing Crash Modification Factors (CMFs). Harwood et al. documented that there are three common ways to carry out a before-after study: naïve before-after evaluations, comparison group evaluations, and the Empirical Bayes (EB) approach *(30).* Of these three methods, the EB approach was recommended in the first edition of *Highway Safety Manual* (HSM) *(31).*

According to Hauer, the EB method is able to account for regression-to-the-mean effects, as well as traffic volume and other roadway characteristic changes, by combining safety performance function (SPF) estimates with the observed count of crashes *(32, 33*). Regression-to-the-mean is the natural tendency of observed crashes to regress (return) to the mean in the year following an unusually high or low crash count. This advantage allows the EB approach to overcome the limitations faced by the other two evaluation methods and provide more accurate estimates of safety effects. Moreover, VDOT conducts many pavement rehabilitation/resurfacing projects every year and maintains a comprehensive pavement condition database. Generally, the pavements before the rehabilitation/resurfacing projects are deficient while the conditions become good after the project is completed, allowing the research team to find an adequate sample of sites to study. Because of these factors, the EB method was selected as the most suitable approach for this study.

The methodology for this project consisted of three major phases, which are discussed below:

- Data collection and treatment group identification
- SPF development
- EB analysis of pavement condition effect

5.4.1 Data Collection

The most recent five years of data available were used, from 2007 to 2011. Two data sets were created: one for the reference group and another for the treatment group. The reference group included segments of rural two-lane undivided highways that did not have major construction, alignment changes, or resurfacing during the study period, while the treatment group included rural two-lane undivided segments that had been resurfaced but also did not have major construction or alignment changes in the study period. Also, no safety improvements were included in any treatment group projects examined. Information from the reference group was used to develop the SPFs, and information from the treatment group was used to conduct the before-after studies.

The data were mainly obtained from two separate data systems, both of which are maintained by VDOT. The pavement condition data were from pavement management system, while roadway inventory, AADT, and crash history information were from the VDOT Roadway Network System (RNS). These data elements were collected on all rural two-lane undivided segments in Virginia. Note that crashes reported within 250 ft of an intersection were excluded from this study because of the differing characteristics of intersection crashes and road segment crashes. Also, segments were excluded if they were shorter than 0.1 mile or longer than 10 miles. The pavement condition index used by VDOT is called the Critical Condition Index (CCI), first derived in 1998 by the US Army Corps of Engineers (*15*). CCI is represented on a scale of 0 to 100, with 100 representing a pavement with no visible distress. For asphalt pavements, the CCI is calculated based on alligator cracking, longitudinal cracking, transverse cracking, patching, potholes, delaminations, bleeding, and rutting (*2*). The details of the CCI calculation methodology are provided in a VDOT report published in 2002 (*17*). VDOT does not collect friction data on a systematic basis at this time, although that capability is under investigation. Friction may or may not be correlated with the CCI. If cracking is driving CCI at a site, then friction factor and CCI may be correlated. If rutting is driving CCI, then friction may not be correlated with CCI. As shown in Table 5.1, CCI values are grouped into five condition categories: excellent, good, fair, poor and very poor.

TABLE 5.1 Pavement Condition Category Based on CCI (*15*)

Pavement Condition	CCI Scale
Excellent	90 and above
Good	70-89
Fair	60-69
Poor	50-59
Very Poor	49 and below

In VDOT's pavement maintenance practice, pavement sections with a CCI value below 60 (poor and very poor) are considered "deficient" and will be further evaluated for maintenance and rehabilitation actions (*15*). In other words, it is expected that a pavement section should have a CCI value below 60 before being resurfaced, and a CCI value above 90 immediately after the project. To ensure that the EB approach has sufficient data, only sites with at least two years of before data and two years after data were examined. Since VDOT CCI data are only available between 2007 and 2011 when this research was conducted, the range of the "before" period was limited. As a result, pavement sections that rehabilitated/resurfaced in 2009 were picked as the initial set for examination. The process to select the treatment group sites was as follows:

1. Select pavement sections on rural two-lane undivided roads that were rehabilitated in 2009;

2. Check the CCI of the selected sites and remove sites that have a CCI value higher than 60 in 2007 and 2008 or have a CCI value lower than 70 in 2010 and 2011;
3. To ensure that the selected sites did not experience changes in geometric or traffic control conditions, remove sites where one or more of the following features were changed between 2007 and 2011: shoulder width, lane width, posted speed limit, surface type, number of lanes, and facility type;
4. Remove segments with a length less than 0.1 mile (0.161 km) or greater than 10 miles (16 km).

Once the study sites were selected, their roadway features, AADT, pavement condition, and crash information were matched. In addition, 2009 data were excluded in the treatment group data as it was the year when pavements were resurfaced.

In summary, 5,723 segments with a total centerline mileage of 3,504 miles (5,639 km) were identified as the reference group and 131 segments with a total centerline mileage of 76.12 miles (122.5 km) were selected as the treatment group. The before period is 2007 and 2008, while the after period is 2010 and 2011. Table 5.2 shows descriptive statistics for the reference group, as well as for the before and after periods for the treatment group.

As shown in Table 5.2, in total of 17,074 crashes, including 7,183 FI crashes, were recorded on segments in the reference group from 2007 to 2011. Based on the crash history, the after period experienced 3 fewer total crashes and 15 fewer FI crashes than the before period. This indicates that there was an increase of 15-3 =12 in PDO crash frequency in the after period. It was also found that the proportion of total crashes constituted by the FI crashes changed from 0.39 in the before period to 0.29 in the after period. Among the treatment group segments, the average pavement conditions of the selected segments improved from very poor to excellent. The average AADT trend was found to be consistent with economic trends, dropping from 4,303 vehicles per day in the before period to 4,115 vehicles per day in the after period. The reference group sites had wider range of AADT but a smaller average AADT than the treatment sites.

TABLE 5.2 Descriptive Statistics of Continuous Variables for Segments in the Reference and Treatment Groups

Groups	Variable	Mean	Min.	Max.	Std. Deviation	Sum
Reference Group (2007-2011)	*Total crashes*	0.60	0	18	1.10	17,074
	FI crashes	0.25	0	8	0.61	7,183
	Length (miles)	0.61	0.1	10	0.60	3,504[A]
	AADT	3,529	76	29,142	2,773	--
	Lane width (ft)	10.54	9	15	0.91	--
	Shoulder size (ft)	4.66	0	10	1.86	--
Treatment Group -Before (2007-2008)	*Total crashes*	0.56	0	9	1.70	146
	FI crashes	0.22	0	7	1.03	57
	Length (miles)	0.58	0.1	2.58	0.51	76.12[A]
	AADT	4,303	410	25,739	3,757	--
	Lane width (ft)	10.34	10	12	0.64	--
	Shoulder size (ft)	4.45	2	8	1.26	--
	CCI	44.79	13	59	9.81	--
Treatment Group -After (2010-2011)	*Total crashes*	0.55	0	10	1.62	143
	FI crashes	0.16	0	4	0.68	42
	Length (miles)	0.58	0.1	2.58	0.51	76.12[A]
	AADT	4,115	430	26,943	3,578	--
	Lane width (ft)	10.34	10	12	0.64	--
	Shoulder size (ft)	4.45	2	8	1.26	--
	CCI	95.75	85	100	4.69	--

[A.] Sum of segment length in one year.

TABLE 5.3 Distribution of Lane/Shoulder Width of the Reference and Treatment Groups

Lane Width	Site Numbers (Percentages)		Shoulder Width	Site Numbers (Percentages)	
	Reference Group	*Treatment Group*		*Reference Group*	*Treatment Group*
10 ft	3,211 (56.1%)	96 (73.3%)	2 ft	509 (8.9%)	4 (3.1%)
10.5 ft	269 (4.7%)	5 (3.8%)	3 ft	1,047 (18.3%)	31 (23.7%)
11 ft	1,133 (19.8%)	17 (13.0%)	4 ft	1,294 (22.6%)	37 (28.2%)
11.5 ft	97 (1.7%)	1 (0.7%)	5 ft	607 (10.6%)	24 (18.3%)
12 ft	692 (12.1%)	12 (9.2%)	6 ft	1,568 (27.4%)	33 (25.2%)
Other	320 (5.6%)	0 (0.0%)	Other	698 (12.2%)	2 (1.5%)
Sum	5,723 (100%)	131 (100%)	Sum	5,723 (100%)	131 (100%)

Table 5.3 summarizes the distribution of lane/shoulder width of the reference and treatment groups. Overall, the treatment group has a similar trend in the distribution, although there are some magnitude differences. For example, in both groups the most common lane width is 10 ft (3.0 m), followed by 11 ft (3.3 m) and 12 ft (3.6 m) and the most common shoulder widths are 4 ft (1.2 m) and 6 ft (1.8 m), followed by 3 ft (0.9 m) and 5 ft (1.5 m). The large size of the reference group allows the diversity of lane/shoulder width combinations to be

incorporated into the SPF development, thereby permitting an evaluation of the interactions of lane/shoulder width with pavement condition.

5.4.2 Safety Performance Functions

The general EB procedure has been studied or described by many authors, and is summarized in the HSM (*31*). One key step for the EB procedure is to develop or select a SPF. A well-developed SPF will properly account for traffic volume and other changes. In addition, developing SPFs based on crash types and severities is necessary since most treatments affect various crash and severity types differently. In 2010, VDOT developed a set of SPFs for two-lane roads in Virginia based on data from 2003 to 2007 (*48*). Considering that the 2007-2011 period saw systematic reductions in crashes across Virginia due in part to the economic downturn, the existing SPFs may not represent our study period well. As a result, the authors developed two new Virginia-specific SPFs for total and fatal and injury (FI) crashes for rural two-lane undivided highways. The traffic, geometric, and crash data from 2007 to 2011 collected for the reference group discussed earlier were used to develop these new SPFs.
Many SPF forms were studied by other authors. The most commonly used is a negative binomial regression model with the form as follows:

$$n = \alpha(SegmentLength)^{\beta_1}(AADT)^{\beta_2}e^{(\beta_3 x_1 + \beta_4 x_2 + \ldots)}\text{, or}$$

$$\ln(n) = \alpha + \beta_1 \ln(SegmentLength) + \beta_2 \ln(AADT) + \beta_3 x_1 + \beta_4 x_2 + \ldots$$

Where:

n = the predicted annual crash number,
α and βi = coefficients, and
x_i = explanatory variables other than segment length and AADT.

Besides segment length and AADT, lane and shoulder width are factors that have been shown to be significantly correlated with crash frequency in previous research [e.g., Zegeer et al. (*49*), Gross et al. (*50*), and Zeng and Schrock (*51*)]. As a result, lane and shoulder width were also included in the SPF models. In addition, *year* and *district* were treated as two categorical variables in the model to account for yearly variation and differences in topography and driver behavior in different parts of the state. The variable of year also acts as a surrogate for declining CCI if no paving occurs since the reference group should theoretically have had declining pavement conditions throughout the after period. VDOT has 9 construction districts: Bristol, Culpeper, Fredericksburg, Hampton Roads, Lynchburg, Northern Virginia, Richmond, Salem, and Staunton Districts. Including district information will at least partially account for the differing characteristics across Virginia. For example, rural two-lane highways in the Bristol, Salem, and Staunton Districts tend to occur in mountainous regions of the state with significant horizontal and vertical curvature, while the Hampton Roads and Northern Virginia areas tend to have a more aggressive driving population.

The SPSS statistical software was used to develop SPFs by regressing collected data to negative binomial models. Table 5.4 shows the result of the developed SPFs, as well as their goodness of fit information. Both SPFs have the expected positive or negative coefficients. *Ln AADT* and *Ln Length* have positive coefficients, indicating that the crash frequency increases with traffic volume and segment length, while negative coefficients for shoulder size and lane width show that crash frequency decreases as the width of the lane and shoulder increases. According to the results, most variables have coefficients that are significant at the 0.01 level.

The coefficients of *Years* address that year 2007 and 2008 experienced significantly higher (at the 0.01 level) crashes than year 2011, which is representative of the general downturn in crash frequency observed in Virginia and in many other states during this period. The coefficients of Districts show that rural two-lane undivided roads in mountainous districts (Bristol and Salem) tend to experience significantly higher crashes than other districts, given the same conditions in terms of AADT, lane and shoulder width, year, and segment length. Ideally, horizontal and vertical curvature would have been included in this model as well, but VDOT lacks a systematic inventory of that information.

It is necessary to discuss the transferability of these SPFs. The models developed are applicable to two-lane undivided roads in Virginia, and calibration procedures from the HSM are recommended to gain a more accurate estimation if they are used in other states due to differences in crash reporting and roadway characteristics.

TABLE 5.4 Safety Performance Functions for Rural Two-lane Highways in Virginia

Variable	SPF for Total Crashes		SPF for FI Crashes	
	Coefficient (Std. Error)	*Wald Chi-Square* [E]	*Coefficient (Std. Error)*	*Wald Chi-Square*
Intercept	-3.770 (0.159)	563.2*** [A]	-4.230 (0.230)	338.2***
Ln AADT	0.620 (0.013)	2,133.8***	0.570 (0.019)	883.2***
Ln Length	0.952 (0.012)	6,764.5***	0.974 (0.017)	3,369.5***
Shoulder size	-0.026 (0.006)	21.7***	-0.045 (0.008)	30.7***
Lane width	-0.104 (0.012)	72.2***	-0.100 (0.018)	30.6***
Year 2007	0.213 (0.028)	60.1***	0.249 (0.040)	38.6***
Year 2008	0.093 (0.028)	10.8***	0.184 (0.041)	20.4***
Year 2009	-0.020 (0.029)	0.5	-0.001 (0.043)	0.0
Year 2010	-0.090 (0.029)	9.5***	-0.065 (0.043)	2.283
Year 2011	0.000 [B]	--	0.000 [B]	--
Bristol	0.253 (0.056)	20.1***	0.312 (0.081)	14.8***
Salem	0.229 (0.055)	17.3***	0.288 (0.079)	13.1***
Lynchburg	-0.137 (0.058)	5.7**	-0.196 (0.084)	5.4**
Richmond	-0.217 (0.058)	14.0***	-0.200 (0.084)	5.6**
Hampton Roads	-0.111 (0.065)	3.0*	-0.097 (0.094)	1.1
Fredericksburg	-0.134 (0.058)	5.4**	-0.280 (0.085)	10.8***
Culpeper	-0.035 (0.055)	0.4	-0.021 (0.079)	0.1
Staunton	-0.107 (0.057)	3.5*	-0.091 (0.082)	1.2
Northern VA	0.000 [B]	--	0.000 [B]	--
k	0.358 (0.018)		0.438 (0.036)	
Log-likelihood ratio Chi-Square [C]	7,848.3***		4,129.6***	
AIC	52,358		31,650	
Pseudo R Square [D]	0.75		0.75	

[A] * indicates statistically significant at the 0.1 level; ** indicates statistically significant at the 0.05 level; and *** indicates statistically significant at the 0.01 level;
[B] Set to zero as it is the basic condition of this category valuable;
[C] Given by SPSS, it compares the fitted model against the intercept-only model;
[D] Pseudo R^2= 1-k/k_{max}, where k_{max} is the estimated overdispersion parameter in the intercept-only model *(52) (53);*
[E] Wald Chi-Square is the default test statistic for coefficients in negative binominal regression models in SPSS.

5.4.3 Empirical Bayes Analysis and Results

For every individual treated segment, the next step was to combine the sum of initial predictions (N_B) with the sum of observed count of crashes (O_B) through the use of an overdispersion parameter (k) to generate an acceptable estimate (E_B) for the expected number of crashes in the before period. The related variance ($Var(E_B)$) was also estimated. The calculation process is indicated by the equations below (*31*):

$$N_{i,total} = SPF_{i,total}$$

$$N_{i,FI} = SPF_{i,FI}$$

$$N_B = \sum N_i$$

$$E_B = wN_B + (1-w)O_B \,, \quad w = \frac{1}{1+kN_B}$$

$$Var(E_B) = (1-w)E_B$$

Where:

$N_{i,total}$, $N_{i,FI}$ = predicted total crash or FI crash frequency for the segment in year i of the before period;

N_B = sum of predicted crash frequency of the segment in the before period;

w = weight factor;

E_B = expected crash frequency for the before period;

k = overdispersion parameter;

O_B = sum of observed crash number for the study segment.

With the above results and the predicted sum of number of crashes (N_A) for the same segment, the expected number of crashes in the after period (E_A) without upgrading the pavement condition could be estimated by the following equation:

$$E_A = E_B \frac{N_A}{N_B}$$

To estimate the index of safety effectiveness, or CMF, one needs to sum E_A over all road segments in the treatment group (E_{Asum}) and then compare with the total observed crash number (O_{Asum}) during the after period in the same group. The standard deviation (σ) of CMF is determined by another equation.

$$CMF = \frac{O_{Asum} / E_{Asum}}{1 + Var(E_{Asum}) / E_{Asum}^{\ 2}}$$

$$\sigma = \sqrt{\frac{CMF^2 (Var(E_{Asum}) / E_{Asum}^{\ 2} + Var(O_{Asum}) / E_{Asum}^{\ 2})}{(1 + Var(E_{Asum}) / E_{Asum}^{\ 2})^2}}$$

The EB analysis was conducted using several different scenarios to investigate whether the safety effect of pavement condition varied with different lane and shoulder width combinations. First, the aggregated CMFs were calculated based on all 131 sites' data. Then the sites were divided into two groups based on lane width and CMFs were produced for 10-ft-lane segments and for segments with a lane width from 11 ft to 12 ft. Since a majority of the segments had 10-ft lanes, further evaluation was conducted for these segments based on shoulder width. Two additional CMFs were developed for segments with 10 ft lanes: one for segments with 3 or 4 ft shoulders, and a second one for segments with 5 or 6 ft shoulders.

Table 5.5 summarizes these CMF results and their standard deviations, as well as sample size of each scenario.

TABLE 5.5 CMF Results and Standard Deviations

Scenarios	Sample Size	Total Crash (Std Dev.)	FI Crash (Std. Dev.)
Aggregated results	131	1.03 (0.100)	0.74 (0.123)**[A]
Segments with 10 ft lanes	96	1.03 (0.112)	0.74 (0.138)**
Segments with 11 ft, 11.5 ft, or 12 ft lanes	35	0.98 (0.218)	0.74 (0.279)
Segments with 10 ft lanes and 3 ft or 4 ft shoulders	69	1.04 (0.134)	0.77 (0.161)*
Segments with 10 ft lanes and 5 ft or 6 ft shoulders	27	1.26 (0.259)	0.78 (0.321)

[A] ** indicates significance at the 0.05 level; * indicates significant at the 0.1 level.

According to the aggregated results, improving pavement condition from poor or very poor to excellent or good for rural two-lane highways does not have statistically significant effect on reducing total crashes. However, the improvement is able to reduce FI crashes by an average of 26 percent. The disaggregated analysis has similar results across different lane width and shoulder size. Because of the lack of sites, not all CMFs are significant at the 0.05 level.
One important question is whether there are significant differences in the safety effect of pavement conditions among different lane and shoulder width combinations. A t-test for two samples with unequal variances, indicated by the equation below, was conducted (*54*). The null hypothesis was that the CMFs for segments with different lane width or shoulder width were the same.

$$t = \frac{|CMF_1 - CMF_2|}{\sqrt{\sigma_1^2/n_1 + \sigma_2^2/n_2}}$$

$$DF = \frac{(\sigma_1^2/n_1 + \sigma_2^2/n_2)^2}{(\sigma_1^2/n_1)^2/(n_1-1) + (\sigma_2^2/n_2)^2/(n_2-1)}$$

Where:
t = t test statistic;

CMF_1, CMF_2 = CMF values for the two compared groups;
σ_1, σ_2 = related standard deviations of the tested CMFs;
n_1, n_2 = number of sites in the two compared groups; and
DF = degree of freedom.

Table 5.6 shows the test results, with the number in bold indicating that the t statistic is large enough to reject the null hypothesis.

TABLE 5.6 Statistical Test Results

Scenarios	*t*-Value for Total Crash	*t*-Value for FI Crash
Segments with 10 ft lanes Vs. Segments with 11 ft, 11.5 ft, or 12 ft lanes	1.38	0.02
Segments with 10 ft lanes and 3 ft or 4 ft shoulders Vs. Segments with 10 ft lanes and 5 ft or 6 ft shoulders	4.06**[A]	0.19

[A] ** indicates significance at the 0.05 level.

The results indicated that the safety benefits of repaving pavement are not expected to change statistically significantly as the lane width increase from 10 ft to 11, 11.5, or 12 ft. However, disaggregated analysis for the 10-ft lane segments shows that segments with wider shoulders is expected to have statistically higher overall crash frequency than segments with narrow shoulders after repaving, although no significant difference is expected regarding FI crash frequency. Considering that the sample size is only 27 sites for segments with 10 ft lanes and 3 ft or 4 ft shoulders, the t-test may not truly represent the real situation. Since only sites that were resurfaced in 2009 were examined, sample sizes could not be increased further. Also, it should be noted that the CMFs for both of these scenarios were not significant different from 1.0. As a result, this analysis indicates that there may be a differential impact of pavement condition by shoulder width when lane widths are 10 ft, but the impact on CMF was not statistically significant with this data set. Future study that includes more sample size for this segment type should be able to draw a more robust conclusion.

5.5 Discussion

Generally speaking, two direct outcomes are created by a pavement resurfacing project: improved pavement conditions and new pavement markings. According to previous research, better pavement condition may impact highway safety in two ways. On one hand, it can create faster vehicle operating speeds, which is linked to higher crash severity; on the other hand, it provides better roadway friction and decreases the risk of skidding crashes. Many previous research studies have also shown a positive safety impact of new markings [e.g., Smadi et al. (*55*), Carlson et al. (*56*)]. New markings are usually tied to reduction in nighttime, run of the road, or sideswipe crashes.

The EB results show that the FI crashes were reduced by 26 percent and the overall crash frequency did not change significantly after pavement resurfacing. To better interpret this result, a breakdown of crash types was conducted for the before and after periods. Table 5.7

summarizes observed crash types, the number of nighttime crashes, and the number of wet pavement crashes during the before and after period for the treatment group.

TABLE 5.7 Frequency (Percentage) of Crash Types of the Treatment Group

Crash Type	Total Crash Before	Total Crash After	FI Crash Before	FI Crash After
Rear End	26 (17.8%)	31 (21.7%)	10 (17.5%)	9 (21.4%)
Angle	6 (4.1%)	12 (8.4%)	4 (7.0%)	3 (7.1%)
Sideswipe (same direction)	4 (2.7%)	1 (0.7)	3 (5.3%)	0 (0.0%)
Sideswipe (opposite direction)	6 (4.1%)	0 (0.0%)	3 (5.3%)	0 (0.0%)
Non-collision	9 (6.2%)	6 (4.2%)	5 (8.8%)	1 (2.4%)
Run off the road	51 (34.9%)	56 (39.2)	25 (43.9%)	25 (59.5%)
Animal	37 (25.3%)	32 (22.4)	5 (8.8%)	1 (2.4%)
Other	7 (4.8%)	5 (3.5%)	2 (3.5%)	3 (7.1%)
Sum	146 (100.0%)	143 100.0%)	57 (100.0%)	42 (100.0%)
Night time crash	50 (34.2%)	57 (39.9%)	16 (28.1%)	10 (23.8%)
Night time ROR crash	6 (4.1%)	7 (4.9%)	--	--
Wet pavement crash	32 (21.9%)	33 (23.1%)	12 (21.1%)	7 (16.7%)
Wet pavement ROR crash	5 (3.4%)	5 (3.5%)	--	--

According to the summary, the most common crash type was run off the road (ROR), and it accounted for 35 percent (51 out of 146) and 39 percent (56 out of 143) of overall crashes in before and after periods, respectively. Both the before and after periods had 25 ROR FI crashes. The number of sideswipe crashes was reduced significantly (overall: from 10 to 1; FI: from 6 to 0). Animal related crashes were also reduced. For other crash types, there were increases in rear end and angle crashes, although the FI crashes of the two types did not change much. The frequency of total night time crashes increased by 14 percent in the after period. However, the night time FI crashes decreased by 37.5 percent. The after period had a similar number of wet pavement crashes and wet pavement ROR crashes with the before period, but had five, or 41.7 percent, less wet pavement FI crashes. In general, diverse changes were found between overall and FI crashes for most crash types except sideswipe crashes.

Although resurfacing projects had diverse safety impacts on overall crash frequency by type, they had positive impacts on most types of FI crashes, with sideswipe FI crashes and animal FI crashes, night time FI crashes or wet pavement FI crashes receiving the largest safety benefits. To conclude, improving pavement condition from deficient to good appears to have a neutral impact on frequency of overall crashes. However, it can offer significant safety benefit in reducing crash severity. Specifically, the new pavement markings associated with the repaving likely help reduce nighttime and sideswipe FI crashes, while the new pavement surface likely creates positive impacts on wet weather crashes and helps reduce severity across all crash types.

5.6 Conclusions and Future Research

Given the historical pavement condition data, as well as roadway and crash information, this study was able to quantitatively evaluate the safety effectiveness of good pavement conditions versus deficient pavement conditions. According to the Empirical Bayes analysis, it was found that compared with deficient pavements, good pavements are able to reduce the fatal and injury crashes by 26 percent but do not have a statistically significant impact on overall crash frequency. Further analysis indicated that the safety benefit of pavement improvement does not statistically significantly change as the lane or shoulder width increases. The results of this study could be used for a variety of applications, including prioritizing sites for the agency's annual paving program or quantifying the benefits of preventative maintenance treatments.

One limitation of this study is a lack of before and after data. Since the pavement condition data has only been available since 2007 and crash data have only been updated through 2011 so far, the research could only use segments that were resurfaced in 2009 as the study sites. As a result, the selected sites only had two years before and after data available.

Also, this study focuses specifically on rural two-lane undivided roads. Future research could expand this analysis to other facility types such as freeways or urban/rural multi-lane roads. This would give DOTs an idea whether these findings are transferable to other locations. Another direction could be to research the safety effect of pavement treatments other than resurfacing after which pavement condition could be improved from fair to good or from deficient to fair/good. With these information, DOTs could quantify the safety benefit of most pavement treatments across the entire network. However, it may be hard to find adequate before-after data to conduct the EB study, so a cross-sectional study design could be used to investigate these trends.

ACKNOWLEDGMENTS

The authors wish to thank Raja Shekharan and Liliya Fedzhora of VDOT for providing pavement condition data for this study.

CHAPTER 6 GENERAL CONCLUSIONS AND RECOMMENDATIONS

6.1 General Conclusions and Discussions

Thanks to more than 100 years of investment in infrastructure, the current highway systems play a significant role in supporting the economic activities and the mobility of people and goods throughout the whole country. Given the progress in pavement assessment method and connected vehicle technology, the goal of this dissertation is to improve the pavement management and assessment activities to enhance the returns of transportation agencies' investments in highway infrastructure. Specifically, this research investigated a connected vehicle-enabled application to prescreen pavement segments (i.e., identify deficient pavement) based on roughness, and quantified the safety effect of the general pavement conditions based on data that became available recently. Three related studies were conducted, with the first study proposing and evaluating an acceleration-based metric with vehicle speeds incorporated for pavement roughness measurement, the second study investigating the impact of vehicle dynamic systems and designing a calibration procedure and the third study quantifying the safety effectiveness of good pavement conditions versus deficient conditions.

Paper 1 in Chapter 3 developed a normalized acceleration-based metric (*NRMS*) that can generalize to different functional classes of highway by incorporating vehicle speed. This proposed metric was trained and tested on data collected from three functional classes of highway and illustrated a promising performance in identifying deficient pavement sections (between 83% and 93% correct rate). It is expected that the proposed acceleration-based metric be used in a network screening process. This finding points to the feasibility of a connected vehicle-enabled pavement network screening application.

As a follow-up work of the previous study, Paper 2 in Chapter 4 investigated the impact of vehicle dynamic systems on vehicle vibration response, which directly affects the acceleration-based metric for pavement roughness measurements. It was found vehicle vibration response is most sensitive to the spring stiffness of the sprung mass and the least sensitive to the loading of the vehicle. Furthermore, the relationship analysis shows that the vibration responses are linearly correlated between different vehicle systems.

Assuming that transportation agencies will use agency-owned vehicles to build a pavement condition network screening system, a vehicle calibration procedure was developed to help them calibrate vehicles in the fleet. The procedure includes data and system requirement for calibration, criteria regarding the necessity of the calibration, criteria regarding the success of the calibration, and a step by step process. Two case studies based on probe data collected from different vehicles were also presented and demonstrated that the calibration improved system performance.

Given the historical pavement condition data, as well as roadway and crash information, Paper 3 presented in Chapter 5 applied the Empirical Bayes analysis for evaluating pavement condition safety effect on rural two-lane highways in Virginia. It was found that compared with deficient pavements, good pavements are able to reduce the fatal and injury crashes by 26 percent but do not have a statistically significant impact on overall crash frequency. Further analysis indicated that the safety benefit of pavement improvement does not statistically significantly change as the lane or shoulder width increases. The results of this study could be used for a variety of applications, including prioritizing sites for the agency's annual paving program or quantifying the benefits of preventative maintenance treatments.

6.2 Contributions and Recommendations

This research resulted in several significant contributions in pavement management and assessment, connected vehicle research, and highway safety research. The specific contributions include, but are not limited to:

- **This study provided and evaluated an approach to collect pavement roughness data from the general vehicles under naturalistic driving environments**

  Although numerous previous studies have investigated the relationship between the IRI and vehicle vibration response, most of them did not address the impacts of vehicle speeds and dynamic systems as they were conducted under controlled environments. This dissertation extended the concept to the real world situation where data are collected under a good variety of driving speeds and vehicle systems. It developed methodologies to address the effects of vehicle speeds and dynamic systems on the acceleration-based pavement roughness metric. These methodologies are able to reduce the variety of the roughness measurements from the general vehicles.

- **The study results point to the feasibility of a connected vehicle-enabled pavement network screening system that can assess the pavement condition in a timely and cost-effective manner**

  The findings of this dissertation can serve as fundamental methodologies for a connected vehicle-enabled pavement network screening application. Once implemented, this system will continuously and remotely identify deficient sections of the whole pavement system at a relatively low cost. It is recommended that DOTs apply these findings to build a prototype system using state-owned vehicles, incorporate the prototype system into the pavement management applications, and then evaluate its limitations and benefits comprehensively.

- **This study expanded the possible connected vehicle applications beyond safety, mobility and environmental aspects**

  Currently, the connected vehicle research primarily focuses on safety, mobility and environmental improvements (*5*). As one of the first research efforts that utilize individual vehicular data to assess network-level infrastructure conditions, this research demonstrated a promising example of progressing transportation infrastructure management within a connected vehicle environment. It will bring incremental benefits to the overall connected vehicle program.

- **This is one of the first few studies that robustly quantify the safety effect of the general pavement condition**

  The role of pavement condition in highway safety is a longstanding research topic, but not much research has been done due to the lack of historical pavement condition data. Given pavement condition data that became available recently, this study applied the EB approach, the state-of-the-art method for highway safety analysis, to quantify the safety effect of the general pavement condition.

- **This study demonstrates a new way to use pavement condition data beyond current practice**

Originally, the pavement condition indexes calculated from the automated collected data are intended to help transportation agencies make decisions based on assets management targets. This study demonstrated that the pavement condition data can also be used to indicate the safety performance of the pavement. It is recommended that the pavement maintenance division of VDOT incorporate the developed CMFs in the pavement management applications, such as prioritizing sites for the agency's annual paving program or quantifying the benefits of preventative maintenance treatments

- **This study has shown the value in determining local SPFs and CMFs for use in estimating safety benefits of proposed safety improvement programs using the EB approach**

  This study developed Virginia-specific SPFs for rural two-lane primary roadways and CMFs for the general pavement conditions, which has the potential to be applied to the highway safety improvement program. The highway safety management division is recommended to add the CMFs for pavement conditions to the existing crash prediction models to provide more accurate safety estimations on rural two-lane primary roads in Virginia.

6.3 Limitations and Future Research

Although the findings from the two studies in Chapters 3 and 4 provide fundamental methodologies for a connected vehicle-enabled pavement network screening application, there are still great challenges for the implementation of this application. There are several opportunities to expand this research to further validate this approach. First of all, a prototype system can be developed using state-owned vehicles as probe vehicles to collect data. With the prototype system, a more comprehensive dataset can be generated by collecting data on more routes and in a wider area. It can be used to validate previous findings, address issues regarding implementation, assess the network benefit of this system, and explore the possibility of measuring other pavement condition data using a similar approach. Also, it is recommended to design filters to remove invalid data by identifying situations where the acceleration-based metric cannot work. For example, when a vehicle is stopping before a traffic light, the data do not contain useful information regarding pavement roughness. With the help of filters, only valid data points will remain.

For the study of pavement condition safety effect, this dissertation focuses specifically on rural two-lane undivided primary roads. It is plausible that the safety effect of pavement conditions varies between different functional classes of roadways. As a result, future research could expand this analysis to other facility types such as freeways or urban/rural multi-lane roads. This would give DOTs an idea about whether these findings are transferable to other locations and the need for developing individual CMFs according to facility class. Another direction could be to research the safety effect of pavement treatments other than resurfacing after which pavement condition could be improved from fair to good or from deficient to fair/good. With these information, DOTs could quantify the safety benefit of most pavement treatments across the entire network. However, it may be hard to find adequate before-after data to conduct the EB study, so a cross-sectional study design could be used to investigate these trends.

Last but not least, with more research efforts involved in highways safety research and connected vehicle/infrastructure research, it is possible to transfer the current pavement management program into a comprehensive, connected vehicle-enabled and multi-objective program. For instance, big data technology can be applied to analysis mass amount of connected vehicle data and provide actionable insights to help transportation agencies make better decisions by considering safety, operational, and economical objectives in pavement maintenance.

REFERENCES

1. Virginia Department of Transportation. *Fiscal Year 2015 VDOT Annual Budget*. http://www.virginiadot.org/VDOT/About_VDOT/asset_upload_file572_58764.pdf. Accessed September 20, 2014
2. Virginia Department of Transportation. *Pavement Management Program Overview*. http://www.virginiadot.org/business/resources/local_assistance/Microsoft_PowerPoint_-_Local_Assistance_TC.pdf. Accessed April 17, 2013.
3. Sauerwein, P.M., B.L. Smith. *Investigation of the Implementation of a Probe-Vehicle Based Pavement Roughness Estimation System*. Center for Transportation Studies at University of Virginia, 2011.
4. Michigan Department of Transportation (MDOT), *Connected Vehicle Technology Industry Delphi Study*, Lansing, Michigan, 2012.
5. U.S. Department of Transportation. *Connected Vehicle Research*. http://www.its.dot.gov/connected_vehicle/connected_vehicle.htm. Accessed July 2, 2013
6. SAE International, *DSRC Implementation Guide*, Warrendale, Pennsylvania, 2008
7. American Association of State Highway and Transportation Officials. *A Policy on Geometric Design of Highway/Street.* AASHTO, Washington, D.C., 2004.
8. Hauer, E., Terry, D., and Griffith, M.S. Effect of Resurfacing on Safety on Two-Lane Rural Roads in New York State. In *Transportation Research Record: Journal of the Transportation Research Board, No. 1467*, Transportation Research Board of the National Academies, Washington, D.C., 1994, pp. 30-37.
9. Cleveland, D. Relationship between Safety and Key Highway Features: A Synthesis of Prior Research. In State-of-the-Art Report 6, Transportation Research Board of the National Academies, Washington, D.C., 1987.
10. Flintsch, G., and K.K., McGhee. *Quality Management of Pavement Condition Data Collection*. NCHRP Synthesis 401. Transportation Research Board, Washington, D.C., 2009.
11. Robinson, R. *Slippery Road Detection and Evaluation*. Transportation Research Institute at the University of Michigan, 2012.
12. Dawkin, J., D. Bevly, B. Powell, and R. Bishop. *Investigation of Pavement Maintenance Applications of Intellidrive[SM]*, CTS PFS Report, 2010.
13. Flintsch, G.W., Valeri, S., Katicha, S.W., de Leon, E.D., Medina, A. Pilot Demonstration of the Use Probe Vehicle Dynamic Signatures to Measure Road Smoothness. *Journal of the Transportation Research Board*, No. 2304. Washington, D.C., 2012, pp. 158-165.
14. McGhee, K. H. *An Approach to Pavement Management in Virginia*. VTRC Report No. 82-R9, Transportation Research Council, Charlottesville, VA, 1981.
15. Virginia Department of Transportation (VDOT), *State of the Pavement 2012*, Richmond, Virginia, 2012.
16. Fugro Roadware. *Automatic Road Analyzer*. http://www.roadware.com/products/. Accessed October 4, 2013.
17. McGhee, K H. *Development and Implementation of Pavement Condition Indices for the Virginia Department of Transportation, Phase I: Flexible Pavement*. Virginia Department of Transportation, Maintenance Division, Sept. 2002.
18. Karamihas, S.M., and Sayers, M.W. Interpretation of Road Roughness Profile Data. *FHWA Report FHWA/RD-96/101*. 1996
19. Office of Highway Policy Information. *Highway Performance Monitoring System Field Manual.* http://www.fhwa.dot.gov/ohim/hpmsmanl/appe.cfm. Accessed July 2, 2013.

20. Stantec Consulting Service Inc. *Development of Decision Trees for Virginia Department of Transportation Pavement Management System*. Virginia Department of Transportation, Richmond, Virginia, 2007.
21. Virginia Transportation Research Council. *VDOT Special Provision for Rideability*. June 2006. http://www.virginiadot.org/vtrc/main/online_reports/pdf/06-r28.pdf. Accessed July 2, 2013
22. American Society of Testing and Materials. *ASTM E1170 – 97(2007): Standard Practices for Simulating Vehicular Response to Longitudinal Profiles of Traveled Surfaces.* http://www.astm.org/Standards/E1170.htm. Accessed July 2, 2013.
23. Sayers, M.W. On The Calculation of IRI from Longitudinal Road Profile. *Journal of the Transportation Research Board*, No. 1501. Washington, D.C., 1995.
24. American Society of Testing and Materials. *ASTM E950/E950M – 09: Standard Test Method for Measuring the Longitudinal Profile of Traveled Surfaces with an Accelerometer Established Inertial Profiling Reference.*
25. Ahlin, K., and Granlund, N.O.J.. Relating Road Roughness and Vehicle Speeds to Human Body Vibration and Exposure Limits. *The International Journal of Pavement Engineering*, Vol. 3, Issue 4, pp. 207-216, 2002.
26. Magnusson, G., Dahlstedt, S., and Sjogren, L. Measurements of the Road Surface Longitudinal Unevenness- Methods and Necessary Accuracy. *VTI Report No. 475*, Swedish National Road and Transport Institute, Sweden, 2002.
27. Prem, H., and Ayton, G. Improved Techniques for Assessing Ride Quality on Concrete Pavements. Proceeding of the 8th *International Conference on Concrete Pavements: Innovations for Concrete Pavement: Technology Transfer for the Next Generation*, Concrete Pavement Association, Washington, DC, 2005, Vol. 2, pp 733-754.
28. Cantisani, G., and Loprencipe, G. Road Roughness and Whole Body Vibration: Evaluation Tools and Comfort Limits. *Journal of Transportation Engineering*, Vol. 136, Issue 9, 2010, pp 818-826.
29. Bridgelall, R. A Connected Vehicle Approach for Pavement Roughness. *Journal of Infrastructure Systems*, Vol. 20, Issue 1, 2014.
30. Harwood, D.W., K. Bauer, I. Potts, D. Tobric, K. Richard, E. Kohlman Rabbani, E. Hauer, and L. Elefteriadou. Safety Effectiveness of Intersection Left- and Right- Turn Lanes. In *Transportation Research Record: Journal of the Transportation Research Board, No. 1840*, Transportation Research Board of the National Academies, Washington, D.C., 2003, pp. 131-139
31. American Association of State Highway and Transportation Officials. *Highway Safety Manual*. AASHTO, Washington, D.C., 2010.
32. Hauer, E. *Observational Before-After Studies in Road Safety*. Pergamon Press, Elsevier Science Ltd., Oxford, England, 1997.
33. Gross, F., B. Persaud, and C. Lyon. *A Guide to Developing Quality Crash Modification Factors*. Publication FHWA-SA-10-032. FHWA, U.S. Department of Transportation, 2010.
34. Cleveland, D. Relationship between Safety and Key Highway Features: A Synthesis of Prior Research. In State-of-the-Art Report 6, Transportation Research Board of the National Academies, Washington, D.C., 1987.
35. Hauer, E., Terry, D., and Griffith, M.S. Effect of Resurfacing on Safety on Two-Lane Rural Roads in New York State. In *Transportation Research Record: Journal of the Transportation*

Research Board, No. 1467, Transportation Research Board of the National Academies, Washington, D.C., 1994, pp. 30-37.

36. Hughes, W. E., L. M. Prothe, H. W. McGee, and E. Hauer. *Impacts of Resurfacing Projects With and Without Additional Safety Improvements*, NCHRP Research Results Digest 255, Transportation Research Board, May 2001.
37. Harwood, D.W., H.W. McGee, and G.L. Gittings. *Systemwide Impact of Safety and Traffic Operations Design Decisions for 3R Projects*, NCHRP Report 486, Transportation Research Board of the National Academies, Washington, D.C., 2003.
38. Labi, S. Efficacies of Roadway Safety Improvements across Functional Subclasses of Rural Two-Lane Highways. *Journal of Safety Research*, Vol. 42, 2011, pp. 231-239.
39. Sayers. M.W., T.D. Gillespie, and W. Paterson. *Guidelines for Conducting and Calibrating Road Roughness Measurements*. World Bank Technical Paper Number 46. The World Bank, Washington, DC, 1986.
40. Hastie, T., R., Tibshirani, and J., Friedman. *The Elements of Statistical Learning: Data Mining, Inference, and Prediction* (2nd Edition). Springer, 2009.
41. Wanshington, S., M., Karlaftis, and F., Mannering. *Statistical and Econometric Methods for Transportation Data Analysis* (2nd Edition). Taylor & Francis Group., Boca Raton, FL, 2011.
42. Agresti, A. *Categorical Data Analysis* (3rd Edition). Wiley, 2012.
43. Zeng, H., H. Park, M.D. Fontaine, B.L. Smith, K.K. McGhee. Identifying Deficient Pavement Sections using an Improved Acceleration-based Metric. A paper submit to *Journal of the Transportation Research Board*, Washington, D.C., 2014.
44. Jazar, R.N.. *Vehicle Dynamics: Theory and Application*, second edition, Springer, New York, 2013.
45. Hartman, P.. *Ordinary Differential Equations*, second edition, Society for Industry & Applied Math.
46. Abramowitz, M., and I.A. Stegun. *Handbook of Mathematical Functions with Formulas, Graphs, and Mathematical Tables*, Dover, New York, 1972.
47. Bridgelall, R. Precision Bounds of Pavement Deterioration Forecast from Connected Vehicles. *Journal of Infrastructure Systems*, 10.1061/(ASCE)IS.1943-555X.0000218, 2014.
48. Garber, N.J., P.R. Haas, and C. Gosse. *Development of Safety Performance Functions for Two-Lane Roads Maintained by the Virginia Department of Transportation*, FHWA/VTRC Report 10-R25, Virginia Transportation Research Council, Charlottesville, VA, 2010.
49. Zegeer, C.V., J. Hummer, D. Reinfurt, L. Herf, and W. Hunter. Safety Effects of Cross-Section Design for Two-Lane Roads. In *Transportation Research Record: Journal of the Transportation Research Board, No. 1195*, Transportation Research Board of the National Academies, Washington, D.C., 1988, pp. 20–32.
50. Gross, F., P.P. Jovanis, K. Eccles, and K. Chen. *Safety Evaluation of Lane and Shoulder Width Combinations on Rural, Two-Lane, Undivided Roads*. Publication FHWA-HRT-09-031. FHWA, U.S. Department of Transportation, 2009.
51. Zeng, H., and S.D. Schrock. Estimation of Safety Effectiveness of Composite Shoulders on Rural Two-Lane Highways. In *Transportation Research Record: Journal of the Transportation Research Board, No. 2279*, Transportation Research Board of the National Academies, Washington, D.C., 2012, pp. 99–107.
52. Miaou, S.P. *Measuring the Goodness-of-Fit of Accident Prediction Models*. Publication FHWA-RD-96-040. FHWA, U.S. Department of Transportation, 1996.

53. Fridstrom, L., J. Ifver, S. Ingebrigtsen, R. Kulmala, and L.K. Thomsen. Measuring the Contribution of Randomness, Exposure, Weather, and Daylight to the Variation in Road Accident Counts. *Accident Analysis and Prevention*, Vol. 27, No. 1, 1995, pp. 1-20.
54. Frankfort-Nachmias, C., and A. Leon-Guerrero. *Social Statistics for a Diverse Society (the 5th Edition)*. Pine Forge Press, SAGE Publications, Inc., California, USA, 2009.
55. Smadi, O., R.R. Souleyrette, D. Ormand, and N.R. Hawkins. Pavement Marking Retroreflectivity: Analysis of Safety Effectiveness. In *Transportation Research Record: Journal of the Transportation Research Board, No. 2056*, Transportation Research Board of the National Academies, Washington, D.C., 2008, pp. 17–24.
56. Carlson, P.J., E.S. Park, and C.K. Andersen. Benefits of Pavement Markings: A Renewed Perspective Based on Recent and Ongoing Research. In *Transportation Research Record: Journal of the Transportation Research Board, No. 2107*, Transportation Research Board of the National Academies, Washington, D.C., 2009, pp. 59–68.

APPENDIXES

Appendix 1 Samples of Raw Data

Appendix 1.1 Sample of Probe Vehicle Data

_id	latitude	longitude	time	speed	accuracy	x	y	z	stime
212631	37.94721	-78.2474	1.40E+12	4.127357	8	-0.6608	1.11091	9.768343	5.44E+13
212632	37.94721	-78.2474	1.40E+12	4.127357	8	-0.67995	1.206678	9.730036	5.44E+13
212633	37.94721	-78.2474	1.40E+12	4.127357	8	-0.67995	1.13964	9.77792	5.44E+13
212634	37.94721	-78.2474	1.40E+12	4.127357	8	-0.64165	1.034295	9.787497	5.44E+13
212635	37.94721	-78.2474	1.40E+12	4.127357	8	-0.69911	0.967258	9.844957	5.44E+13
212636	37.94721	-78.2474	1.40E+12	4.127357	8	-0.67995	1.091756	9.787497	5.44E+13
212637	37.94721	-78.2474	1.40E+12	4.127357	8	-0.76614	1.024718	9.864111	5.44E+13
212638	37.94721	-78.2474	1.40E+12	4.127357	8	-0.71826	1.120486	10.14184	5.44E+13
212639	37.94721	-78.2474	1.40E+12	4.127357	8	-0.7853	1.120486	10.03649	5.44E+13
212640	37.94721	-78.2474	1.40E+12	4.127357	8	-0.87149	1.225831	10.08438	5.44E+13
212641	37.94721	-78.2474	1.40E+12	4.127357	8	-0.7853	1.225831	10.05565	5.44E+13
212642	37.94721	-78.2474	1.40E+12	4.127357	8	-0.76614	1.043872	9.911995	5.44E+13
212643	37.94721	-78.2474	1.40E+12	4.127357	8	-0.79487	1.082179	10.0748	5.44E+13
212644	37.94721	-78.2474	1.40E+12	4.127357	8	-0.97683	1.312023	10.09395	5.44E+13
212645	37.94721	-78.2474	1.40E+12	4.127357	8	-0.91937	1.168371	10.14184	5.44E+13
212646	37.94721	-78.2474	1.40E+12	4.127357	8	-0.91937	1.091756	10.0748	5.44E+13
212647	37.94721	-78.2474	1.40E+12	4.127357	8	-0.92895	1.149217	9.854534	5.44E+13
212648	37.94721	-78.2474	1.40E+12	4.127357	8	-1.04387	1.206678	9.739613	5.44E+13
212649	37.94721	-78.2474	1.40E+12	4.127357	8	-1.08218	1.206678	9.662998	5.44E+13
212650	37.94721	-78.2474	1.40E+12	4.127357	8	-0.99599	1.187524	9.643845	5.44E+13
212651	37.94721	-78.2474	1.40E+12	4.127357	8	-1.04387	1.11091	9.768343	5.44E+13
212652	37.94721	-78.2474	1.40E+12	4.127357	8	-1.0343	1.187524	9.787497	5.44E+13
212653	37.94721	-78.2474	1.40E+12	4.127357	8	-0.90022	1.120486	9.768343	5.44E+13
212654	37.94721	-78.2474	1.40E+12	4.127357	8	-0.86191	0.948104	9.739613	5.44E+13
212655	37.94721	-78.2474	1.40E+12	4.127357	8	-0.96726	1.005565	9.77792	5.44E+13
212656	37.94721	-78.2474	1.40E+12	4.127357	8	-0.92895	1.024718	9.931149	5.44E+13
212657	37.94721	-78.2474	1.40E+12	4.127357	8	-0.95768	0.938527	10.00776	5.44E+13
212658	37.94721	-78.2474	1.40E+12	4.127357	8	-0.95768	0.852336	9.998186	5.44E+13
212659	37.94721	-78.2474	1.40E+12	4.127357	8	-0.9098	0.90022	10.29507	5.44E+13
212660	37.94721	-78.2474	1.40E+12	4.127357	8	-1.02472	0.890643	10.28549	5.44E+13
212661	37.94721	-78.2474	1.40E+12	4.127357	8	-1.01514	0.957681	10.3238	5.44E+13
212662	37.94721	-78.2474	1.40E+12	4.127357	8	-1.10133	0.986411	10.30465	5.44E+13
212663	37.94721	-78.2474	1.40E+12	4.127357	8	-1.00556	0.794875	10.1993	5.44E+13

Appendix 1.2 Data Sample for SPF Development

ID	year	route	number	Length	district	LW	SW	AADT	Total	FI
1	2007	SR	00003	0.1	6	10	6	7009	0	0
2	2007	US	00011	0.1	2	10	6	4779	0	0
3	2007	US	00011	0.1	8	10	3	3792	0	0
4	2007	US	00011	0.1	8	14	2	11921	0	0
5	2007	US	00011	0.1	8	14	6	4881	0	0
6	2007	US	00011	0.1	8	14	6	4881	0	0
7	2007	US	00011	0.1	8	14	6	4785	0	0
8	2007	US	00011	0.1	8	15	6	5321	0	0
9	2007	US	00015	0.1	A	10	3	18269	1	1
10	2007	SR	00040	0.1	4	11.5	6	903	0	0
11	2007	SR	00040	0.1	4	10	6	3707	0	0
12	2007	SR	00042	0.1	8	10	6	3187	0	0
13	2007	SR	00042	0.1	8	10	4	2514	0	0
14	2007	SR	00042	0.1	8	10	4	1388	1	1
15	2007	US	00058	0.1	1	10	4	616	0	0
16	2007	US	00058	0.1	1	10	4	2588	0	0
17	2007	US	00220	0.1	8	10	2	1417	0	0
19	2007	US	00360	0.1	6	11	6	5119	0	0
20	2007	SR	00005	0.1	4	10	6	2046	0	0
21	2007	SR	00010	0.1	4	10	3	5280	0	0
22	2007	SR	00013	0.1	4	10	3	1583	0	0
23	2007	SR	00018	0.1	8	9	3	1355	0	0
24	2007	SR	00018	0.1	8	10	4	2087	0	0
25	2007	SR	00024	0.1	2	11	8	1894	0	0
26	2007	SR	00030	0.1	6	11	6	4698	0	0
27	2007	US	00033	0.1	8	10.5	3	3365	0	0
28	2007	US	00033	0.1	8	10	3	7468	0	0
29	2007	SR	00040	0.1	2	10.5	6	4428	0	0
30	2007	SR	00045	0.1	3	9.5	3	1360	0	0
31	2007	SR	00049	0.1	4	10	4	1491	0	0
32	2007	US	00052	0.1	2	11	3	3658	0	0
33	2007	US	00052	0.1	2	10	5	3729	0	0
34	2007	SR	00056	0.1	3	10	6	882	0	0
35	2007	SR	00056	0.1	3	10	6	1199	0	0
36	2007	SR	00056	0.1	3	9.5	6	463	0	0
37	2007	SR	00056	0.1	3	10	6	1313	0	0
38	2007	SR	00057	0.1	2	11	4	8678	0	0
39	2007	SR	00063	0.1	1	12	8	1404	1	0

Appendix 2 RMS and Speed Results for GMC, Subaru and Volvo

ID	Distant	Route	IRI	RMS.GMC	Speed.GMC	RMS.Subaru	Speed.Subaru	RMS.Volvo	Speed.Volvo
1	0	I64W	267	0.713	28.750	0.645	31.860	0.785	32.692
2	0.1	I64W	144	0.498	29.060	0.413	30.406	0.533	33.110
3	0.2	I64W	56	0.219	29.215	0.196	31.582	0.275	33.863
4	0.3	I64W	47	0.217	29.213	0.184	33.070	0.314	34.556
5	0.4	I64W	62	0.248	29.121	0.231	34.057	0.354	35.376
6	0.5	I64W	61	0.252	28.892	0.228	33.919	0.329	35.995
7	0.6	I64W	55	0.233	28.900	0.241	33.261	0.303	34.821
8	0.7	I64W	50	0.217	28.797	0.201	33.672	0.302	34.363
9	0.8	I64W	53	0.233	28.792	0.197	33.310	0.320	34.744
10	0.9	I64W	88	0.390	28.832	0.367	32.384	0.463	34.766
11	1	I64W	68	0.254	28.842	0.263	33.170	0.323	35.254
12	1.1	I64W	51	0.213	28.938	0.217	32.684	0.352	34.625
13	1.2	I64W	100	0.304	29.018	0.284	31.789	0.339	35.139
14	1.3	I64W	70	0.242	29.344	0.251	31.499	0.372	35.580
15	1.4	I64W	74	0.292	29.110	0.261	30.831	0.319	35.763
16	1.5	I64W	83	0.299	29.160	0.288	31.258	0.372	35.809
17	1.6	I64W	90	0.317	29.147	0.317	31.326	0.368	36.149
18	1.7	I64W	89	0.319	28.965	0.298	32.164	0.325	34.660
19	1.8	I64W	55	0.250	28.755	0.228	32.084	0.351	34.845
20	1.9	I64W	58	0.215	28.790	0.228	32.045	0.344	35.025
21	2	I64W	57	0.248	28.827	0.246	31.977	0.338	34.909
22	2.1	I64W	54	0.231	28.898	0.226	31.433	0.320	34.516
23	2.2	I64W	79	0.253	29.078	0.280	31.815	0.327	35.153
24	2.3	I64W	71	0.248	29.263	0.239	32.506	0.348	35.287
25	2.4	I64W	68	0.243	29.245	0.255	32.622	0.325	35.506
26	2.5	I64W	79	0.284	29.111	0.302	31.688	0.337	35.158
27	2.6	I64W	65	0.227	28.900	0.241	31.192	0.385	34.431
28	2.7	I64W	59	0.223	28.929	0.230	31.209	0.356	33.908
29	2.8	I64W	52	0.227	29.056	0.226	31.407	0.349	33.789
30	2.9	I64W	67	0.249	29.104	0.241	31.919	0.334	34.042
31	3	I64W	81	0.244	29.165	0.279	32.473	0.351	34.613
32	3.1	I64W	66	0.231	29.094	0.240	32.360	0.364	34.457
33	3.2	I64W	66	0.227	29.043	0.257	32.361	0.330	34.454
34	3.3	I64W	76	0.265	28.984	0.277	31.886	0.370	34.399
35	3.4	I64W	78	0.266	29.038	0.294	31.370	0.366	33.739
36	3.5	I64W	52	0.268	28.848	0.289	31.698	0.420	33.616
37	3.6	I64W	70	0.265	28.812	0.255	31.827	0.355	33.566
38	3.7	I64W	56	0.227	28.881	0.226	32.400	0.315	34.241
39	3.8	I64W	108	0.332	28.910	0.315	31.999	0.354	34.233
40	3.9	I64W	234	0.733	28.859	0.610	31.176	0.800	33.732
41	4	I64W	153	0.651	28.722	0.599	30.538	0.832	33.023
42	4.1	I64W	63	0.230	28.837	0.253	30.715	0.301	31.563
43	4.2	I64W	55	0.239	28.874	0.264	31.488	0.376	32.060
44	4.3	I64W	46	0.182	28.933	0.221	31.949	0.346	33.476
45	4.4	I64W	43	0.197	28.867	0.215	32.308	0.309	34.432
46	4.5	I64W	37	0.183	28.946	0.183	32.838	0.319	34.801
47	4.6	I64W	43	0.167	28.945	0.205	32.436	0.293	34.495
48	4.7	I64W	55	0.216	29.111	0.246	31.916	0.348	34.436

49	4.8	I64W	75	0.260	29.145	0.299	31.907	0.395	34.720
50	4.9	I64W	66	0.206	29.210	0.306	32.125	0.346	34.841
51	5	I64W	200	0.572	29.276	0.416	31.874	0.618	35.062
52	5.1	I64W	68	0.396	28.861	0.466	32.528	0.559	34.720
53	5.2	I64W	57	0.210	28.804	0.307	34.309	0.363	34.619
54	5.3	I64W	53	0.202	28.719	0.241	35.078	0.349	34.691
55	5.4	I64W	60	0.201	28.661	0.242	35.210	0.332	34.944
56	5.5	I64W	45	0.187	28.912	0.224	34.978	0.334	34.972
57	5.6	I64W	56	0.182	28.949	0.230	34.698	0.289	33.968
58	5.7	I64W	70	0.268	29.037	0.245	34.077	0.334	33.474
59	5.8	I64W	63	0.240	29.052	0.226	32.722	0.307	32.918
60	5.9	I64W	110	0.408	28.959	0.413	32.204	0.475	32.611
61	6	I64W	63	0.264	29.177	0.274	32.237	0.378	32.121
62	6.1	I64W	72	0.241	29.300	0.282	34.092	0.327	33.562
63	6.2	I64W	74	0.271	28.981	0.248	35.058	0.346	34.351
64	6.3	I64W	71	0.261	28.870	0.255	34.172	0.324	34.499
65	6.4	I64W	83	0.305	28.826	0.359	34.071	0.430	35.151
66	6.5	I64W	72	0.282	28.893	0.303	34.281	0.356	34.232
67	6.6	I64W	65	0.224	28.957	0.270	34.043	0.344	34.343
68	6.7	I64W	67	0.226	28.973	0.270	34.468	0.327	34.673
69	6.8	I64W	65	0.227	28.954	0.251	34.150	0.333	34.834
70	6.9	I64W	70	0.249	29.022	0.274	33.316	0.430	35.617
71	7	I64W	62	0.248	29.014	0.278	33.359	0.358	35.070
72	7.1	I64W	62	0.208	29.035	0.246	33.501	0.344	34.612
73	7.2	I64W	67	0.225	28.987	0.261	33.889	0.343	34.349
74	7.3	I64W	67	0.273	29.145	0.274	33.241	0.347	34.174
75	7.4	I64W	61	0.313	31.011	0.266	32.298	0.395	34.090
76	7.5	I64W	60	0.275	32.483	0.245	33.749	0.347	34.215
77	7.6	I64W	56	0.264	32.138	0.265	33.715	0.341	34.961
78	7.7	I64W	68	0.270	32.714	0.252	33.495	0.359	35.234
79	7.8	I64W	73	0.325	32.613	0.295	33.038	0.381	34.606
80	7.9	I64W	72	0.283	32.519	0.272	33.710	0.388	34.292
81	8	I64W	51	0.213	32.510	0.220	34.194	0.328	34.933
82	8.1	I64W	55	0.218	32.572	0.224	34.357	0.323	35.154
83	8.2	I64W	56	0.202	33.090	0.206	34.144	0.307	34.779
84	8.3	I64W	64	0.291	33.233	0.260	33.955	0.374	34.663
85	8.4	I64W	76	0.255	32.307	0.291	33.626	0.366	34.592
86	8.5	I64W	77	0.263	31.671	0.247	34.147	0.352	34.673
87	8.6	I64W	60	0.333	31.918	0.303	34.185	0.371	35.039
88	8.7	I64W	66	0.239	31.776	0.265	34.576	0.345	34.911
89	8.8	I64W	69	0.259	30.508	0.249	34.625	0.383	35.482
90	8.9	I64W	59	0.263	30.801	0.289	35.097	0.394	35.461
91	9	I64W	56	0.234	31.069	0.234	35.287	0.321	35.020
92	9.1	I64W	132	0.372	31.103	0.307	35.275	0.384	34.674
93	9.2	I64W	146	0.718	31.021	0.559	34.959	0.635	33.787
94	9.3	I64W	85	0.278	31.087	0.374	34.900	0.449	33.296
95	9.4	I64W	105	0.348	29.306	0.287	34.689	0.448	34.802
96	9.5	I64W	103	0.282	29.036	0.288	34.267	0.402	34.686
97	9.6	I64W	89	0.265	28.998	0.265	33.615	0.376	34.248
98	9.7	I64W	211	0.804	29.071	0.585	33.313	0.840	33.480

99	9.8	I64W	87	0.309	28.981	0.236	33.683	0.360	33.180
100	9.9	I64W	87	0.281	28.811	0.279	34.536	0.354	33.286
101	10	I64W	82	0.297	28.669	0.314	34.592	0.398	33.737
102	10.1	I64W	95	0.297	28.805	0.316	34.689	0.402	34.031
103	10.2	I64W	85	0.281	28.979	0.284	34.454	0.386	34.286
104	10.3	I64W	93	0.293	28.891	0.295	34.091	0.374	34.167
105	10.4	I64W	77	0.260	29.012	0.252	33.854	0.326	32.331
106	10.5	I64W	80	0.253	28.968	0.284	32.464	0.339	31.830
107	10.6	I64W	91	0.313	28.997	0.236	32.008	0.295	31.802
108	10.7	I64W	90	0.296	28.818	0.259	31.372	0.342	31.079
109	10.8	I64W	76	0.262	28.806	0.292	31.262	0.361	31.189
110	10.9	I64W	94	0.280	29.062	0.265	32.301	0.331	32.094
111	11	I64W	87	0.263	29.022	0.282	32.218	0.324	33.105
112	11.1	I64W	99	0.329	28.945	0.293	32.179	0.364	33.759
113	11.2	I64W	92	0.296	29.080	0.290	31.799	0.366	32.628
114	11.3	I64W	124	0.402	28.820	0.377	31.785	0.481	32.507
115	11.4	I64W	196	0.735	28.868	0.612	32.191	0.762	32.261
116	11.5	I64W	113	0.385	28.849	0.333	32.856	0.403	31.079
117	11.6	I64W	88	0.273	28.985	0.309	32.897	0.389	31.225
118	11.7	I64W	95	0.324	28.982	0.373	33.081	0.391	31.355
119	11.8	I64W	97	0.355	28.949	0.350	32.993	0.372	31.050
120	11.9	I64W	86	0.305	29.205	0.347	33.245	0.384	30.953
121	12	I64W	79	0.236	29.094	0.298	34.121	0.370	31.931
122	12.1	I64W	94	0.278	29.216	0.307	33.765	0.371	32.155
123	12.2	I64W	89	0.298	29.072	0.327	33.573	0.365	31.115
124	12.3	I64W	136	0.432	28.860	0.350	32.683	0.405	29.502
125	12.4	I64W	114	0.336	28.763	0.310	32.358	0.365	28.958
126	12.5	I64W	127	0.391	28.914	0.428	32.082	0.493	29.763
127	12.6	I64W	117	0.534	28.900	0.473	31.284	0.555	30.235
128	12.7	I64W	79	0.269	28.936	0.269	31.429	0.333	30.688
129	12.8	I64W	75	0.238	29.017	0.325	32.173	0.409	31.311
130	12.9	I64W	92	0.275	28.924	0.358	32.251	0.447	32.832
131	13	I64W	65	0.249	28.949	0.346	32.199	0.446	33.321
132	13.1	I64W	83	0.306	29.110	0.339	32.201	0.408	32.954
133	13.2	I64W	83	0.251	29.270	0.349	33.004	0.441	32.575
134	13.3	I64W	78	0.244	29.265	0.326	32.135	0.418	32.223
135	13.4	I64W	86	0.240	29.029	0.326	31.317	0.402	31.987
136	13.5	I64W	106	0.334	29.046	0.347	31.939	0.439	32.116
137	13.6	I64W	89	0.294	28.759	0.339	31.781	0.398	31.682
138	13.7	I64W	93	0.283	28.644	0.294	31.371	0.353	31.139
139	13.8	I64W	78	0.257	28.784	0.360	31.565	0.420	30.392
140	13.9	I64W	144	0.431	28.739	0.367	31.533	0.465	28.976
141	14	I64W	230	0.837	29.124	0.537	31.682	0.558	28.072
142	14.1	I64W	82	0.353	28.983	0.397	31.435	0.408	27.153
143	14.2	I64W	77	0.239	28.814	0.255	31.535	0.275	26.702
144	14.3	I64W	85	0.284	28.768	0.287	30.958	0.285	26.529
145	14.4	I64W	76	0.260	28.601	0.247	30.731	0.280	26.896
146	14.5	I64W	89	0.281	28.716	0.262	30.277	0.295	28.057
147	14.6	I64W	75	0.257	29.078	0.253	30.413	0.333	28.546
148	14.7	I64W	74	0.258	28.989	0.242	30.634	0.304	28.984

149	14.8	I64W	72	0.234	28.967	0.248	31.103	0.326	30.028
150	14.9	I64W	83	0.285	29.087	0.295	31.727	0.361	30.379
151	15	I64W	79	0.261	29.001	0.274	33.293	0.323	31.272
152	15.1	I64W	82	0.257	29.191	0.280	32.098	0.357	31.664
153	15.2	I64W	97	0.313	29.041	0.318	32.027	0.395	31.420
154	15.3	I64W	93	0.329	28.838	0.327	32.255	0.385	31.277
155	15.4	I64W	88	0.267	28.863	0.300	31.686	0.372	31.565
156	15.5	I64W	153	0.335	28.829	0.421	33.113	0.570	31.434
157	15.6	I64W	164	0.820	28.855	0.687	34.949	0.794	32.161
158	15.7	I64W	77	0.315	28.717	0.451	35.159	0.377	31.984
159	15.8	I64W	83	0.290	28.790	0.304	33.616	0.349	31.871
160	15.9	I64W	68	0.284	28.809	0.308	33.681	0.354	31.517
161	16	I64W	77	0.231	28.769	0.265	32.993	0.348	31.360
162	16.1	I64W	69	0.256	28.788	0.265	32.484	0.331	31.358
163	16.2	I64W	91	0.271	28.807	0.264	31.403	0.353	31.336
164	16.3	I64W	153	0.409	28.896	0.424	31.380	0.522	32.317
165	16.4	I64W	150	0.869	28.650	0.665	31.591	0.702	32.416
166	16.5	I64W	75	0.250	28.835	0.277	31.210	0.338	31.909
167	16.6	I64W	75	0.279	29.470	0.261	29.897	0.343	30.976
168	16.7	I64W	69	0.224	28.913	0.211	28.201	0.302	30.627
169	16.8	I64W	193	0.522	28.856	0.353	26.866	0.500	30.279
170	16.9	I64W	113	0.549	29.109	0.524	26.333	0.493	29.297
171	17	I64W	98	0.383	29.078	0.244	26.243	0.315	29.752
172	17.1	I64W	87	0.333	28.947	0.296	27.426	0.416	30.806
173	17.2	I64W	93	0.353	29.099	0.265	27.058	0.379	30.982
174	17.3	I64W	136	0.307	29.084	0.341	26.422	0.526	28.972
175	17.4	I64W	179	0.616	28.843	0.518	25.204	0.547	25.820
176	17.5	I64W	135	0.556	28.743	0.336	22.530	0.435	22.327
177	17.6	I64W	159	0.651	28.742	0.315	20.808	NA	NA
178	17.7	I64W	77	0.440	28.735	NA	NA	NA	NA
179	17.8	I64W	70	0.252	28.942	NA	NA	NA	NA
180	0	I64E	257	0.972	29.593	NA	NA	NA	NA
181	0.1	I64E	128	0.523	29.426	0.398	23.643	0.433	19.679
182	0.2	I64E	216	0.859	29.490	0.535	24.235	0.634	25.601
183	0.3	I64E	99	0.508	29.423	0.314	24.009	0.581	30.525
184	0.4	I64E	55	0.250	29.314	0.188	24.775	0.286	32.516
185	0.5	I64E	51	0.191	29.267	0.204	25.681	0.275	33.106
186	0.6	I64E	49	0.188	29.371	0.204	25.162	0.256	32.651
187	0.7	I64E	63	0.246	29.234	0.207	24.463	0.279	31.829
188	0.8	I64E	196	0.730	29.296	0.546	23.910	0.724	32.600
189	0.9	I64E	83	0.303	29.515	0.284	24.709	0.381	32.713
190	1	I64E	87	0.246	29.779	0.269	25.791	0.342	33.423
191	1.1	I64E	84	0.236	29.948	0.242	25.969	0.335	33.367
192	1.2	I64E	171	0.540	29.724	0.319	26.571	0.500	33.120
193	1.3	I64E	98	0.455	29.556	0.579	26.925	0.574	32.892
194	1.4	I64E	95	0.300	29.394	0.224	25.853	0.376	33.441
195	1.5	I64E	77	0.265	29.437	0.233	24.981	0.328	32.570
196	1.6	I64E	84	0.301	29.451	0.243	24.419	0.378	33.117
197	1.7	I64E	60	0.200	29.345	0.218	24.861	0.285	33.325
198	1.8	I64E	104	0.342	29.525	0.215	25.430	0.386	32.656

199	1.9	I64E	92	0.381	29.496	0.316	27.153	0.423	32.061
200	2	I64E	167	0.618	29.447	0.508	28.525	0.623	30.989
201	2.1	I64E	153	0.626	29.280	0.626	30.179	0.711	31.854
202	2.2	I64E	82	0.324	29.012	0.300	31.185	0.331	32.739
203	2.3	I64E	68	0.244	29.045	0.261	30.298	0.340	32.371
204	2.4	I64E	62	0.207	28.927	0.219	29.187	0.287	32.226
205	2.5	I64E	69	0.249	29.055	0.250	28.613	0.330	32.289
206	2.6	I64E	77	0.262	29.009	0.250	28.515	0.307	32.067
207	2.7	I64E	90	0.351	29.288	0.350	29.989	0.374	32.425
208	2.8	I64E	67	0.241	29.525	0.272	30.621	0.332	32.582
209	2.9	I64E	73	0.228	29.790	0.251	30.563	0.308	32.871
210	3	I64E	72	0.226	29.731	0.277	31.687	0.317	32.136
211	3.1	I64E	85	0.267	29.672	0.286	31.736	0.328	31.720
212	3.2	I64E	97	0.288	29.828	0.303	31.329	0.339	31.566
213	3.3	I64E	106	0.332	30.049	0.349	31.625	0.362	32.478
214	3.4	I64E	73	0.288	30.183	0.322	32.744	0.334	32.596
215	3.5	I64E	86	0.265	30.071	0.322	33.427	0.319	32.662
216	3.6	I64E	195	0.559	29.895	0.535	32.700	0.574	32.311
217	3.7	I64E	143	0.594	29.760	0.555	32.342	0.535	32.587
218	3.8	I64E	98	0.293	29.664	0.323	31.941	0.354	33.332
219	3.9	I64E	97	0.306	29.884	0.326	32.845	0.382	33.137
220	4	I64E	81	0.248	29.610	0.271	32.977	0.330	32.961
221	4.1	I64E	79	0.247	29.308	0.277	32.834	0.340	32.889
222	4.2	I64E	76	0.277	29.134	0.321	32.510	0.392	33.088
223	4.3	I64E	88	0.261	29.139	0.313	32.710	0.314	32.880
224	4.4	I64E	93	0.241	29.040	0.263	32.913	0.302	32.136
225	4.5	I64E	90	0.306	29.216	0.302	31.528	0.327	31.884
226	4.6	I64E	114	0.336	29.340	0.344	31.893	0.363	32.440
227	4.7	I64E	136	0.443	29.529	0.401	32.548	0.482	33.267
228	4.8	I64E	107	0.352	29.629	0.327	31.880	0.426	32.888
229	4.9	I64E	92	0.220	29.719	0.302	31.724	0.327	32.958
230	5	I64E	101	0.371	29.689	0.286	31.596	0.488	33.366
231	5.1	I64E	134	0.361	29.592	0.419	31.623	0.422	32.630
232	5.2	I64E	92	0.317	29.355	0.349	32.809	0.392	32.706
233	5.3	I64E	132	0.510	29.349	0.326	32.795	0.573	32.731
234	5.4	I64E	103	0.327	29.337	0.499	32.663	0.362	32.988
235	5.5	I64E	94	0.311	28.876	0.297	32.653	0.392	34.146
236	5.6	I64E	87	0.254	28.579	0.315	32.893	0.355	34.113
237	5.7	I64E	99	0.327	28.724	0.289	32.553	0.461	33.936
238	5.8	I64E	90	0.282	29.253	0.321	31.120	0.394	33.818
239	5.9	I64E	87	0.267	29.215	0.255	29.507	0.339	33.394
240	6	I64E	94	0.344	29.538	0.269	30.035	0.405	33.542
241	6.1	I64E	108	0.387	29.430	0.323	29.916	0.463	33.657
242	6.2	I64E	179	0.543	29.449	0.362	30.530	0.582	33.457
243	6.3	I64E	116	0.288	29.258	0.466	30.391	0.326	32.945
244	6.4	I64E	81	0.255	29.216	0.272	30.371	0.338	32.928
245	6.5	I64E	87	0.301	29.232	0.250	30.793	0.339	33.253
246	6.6	I64E	79	0.255	29.003	0.277	30.897	0.316	33.088
247	6.7	I64E	78	0.248	29.282	0.259	30.396	0.341	32.519
248	6.8	I64E	76	0.249	29.232	0.249	30.045	0.356	33.512

249	6.9	I64E	92	0.319	29.450	0.295	31.550	0.419	34.188
250	7	I64E	78	0.225	29.755	0.337	32.212	0.350	34.374
251	7.1	I64E	80	0.249	29.766	0.276	32.817	0.330	33.710
252	7.2	I64E	76	0.250	29.702	0.272	31.773	0.321	32.597
253	7.3	I64E	104	0.312	29.635	0.288	32.157	0.399	33.561
254	7.4	I64E	86	0.273	29.806	0.360	33.838	0.383	33.782
255	7.5	I64E	72	0.279	29.781	0.286	33.593	0.368	34.002
256	7.6	I64E	72	0.264	29.719	0.307	33.549	0.350	34.548
257	7.7	I64E	70	0.282	29.843	0.269	33.700	0.355	35.234
258	7.8	I64E	74	0.391	29.644	0.262	33.816	0.506	34.116
259	7.9	I64E	181	0.563	29.327	0.381	33.349	0.546	33.203
260	8	I64E	87	0.329	29.242	0.416	32.449	0.304	33.146
261	8.1	I64E	86	0.329	29.210	0.269	32.594	0.328	32.780
262	8.2	I64E	79	0.302	29.310	0.286	34.157	0.319	32.199
263	8.3	I64E	91	0.346	29.295	0.286	34.025	0.371	31.983
264	8.4	I64E	173	0.706	29.566	0.330	33.315	0.654	32.474
265	8.5	I64E	147	0.552	29.905	0.604	32.538	0.435	33.126
266	8.6	I64E	75	0.309	29.806	0.236	33.750	0.314	34.479
267	8.7	I64E	82	0.357	29.614	0.331	33.936	0.404	34.857
268	8.8	I64E	81	0.336	29.360	0.303	34.101	0.359	34.931
269	8.9	I64E	87	0.376	29.090	0.338	34.665	0.398	35.022
270	9	I64E	76	0.359	28.971	0.294	33.961	0.328	34.411
271	9.1	I64E	64	0.301	29.372	0.260	33.410	0.325	34.497
272	9.2	I64E	65	0.322	29.352	0.293	33.610	0.340	33.764
273	9.3	I64E	62	0.290	29.270	0.252	33.794	0.266	33.322
274	9.4	I64E	69	0.285	29.176	0.260	33.051	0.291	33.382
275	9.5	I64E	79	0.325	29.527	0.306	32.363	0.363	34.196
276	9.6	I64E	70	0.314	29.689	0.273	33.923	0.324	33.485
277	9.7	I64E	84	0.313	29.631	0.279	35.017	0.312	32.249
278	9.8	I64E	73	0.298	29.687	0.289	34.486	0.317	31.067
279	9.9	I64E	65	0.266	29.605	0.291	34.021	0.296	31.859
280	10	I64E	76	0.312	29.570	0.278	33.983	0.312	31.738
281	10.1	I64E	65	0.332	29.595	0.288	34.116	0.309	31.704
282	10.2	I64E	73	0.328	29.388	0.304	33.793	0.322	32.748
283	10.3	I64E	62	0.301	29.476	0.255	33.119	0.307	33.044
284	10.4	I64E	64	0.303	29.362	0.255	32.503	0.313	34.014
285	10.5	I64E	65	0.323	29.273	0.251	31.908	0.336	34.388
286	10.6	I64E	69	0.336	29.252	0.285	32.074	0.402	34.917
287	10.7	I64E	67	0.293	29.551	0.257	30.969	0.329	35.209
288	10.8	I64E	70	0.302	29.553	0.266	30.614	0.303	34.135
289	10.9	I64E	66	0.298	29.516	0.273	30.981	0.289	32.747
290	11	I64E	78	0.326	29.352	0.283	31.100	0.334	33.042
291	11.1	I64E	73	0.295	29.681	0.268	31.115	0.313	33.055
292	11.2	I64E	56	0.287	29.770	0.252	31.801	0.284	33.213
293	11.3	I64E	64	0.313	29.554	0.259	32.581	0.296	33.767
294	11.4	I64E	65	0.303	29.367	0.254	33.155	0.321	33.670
295	11.5	I64E	73	0.369	29.225	0.236	33.404	0.323	34.496
296	11.6	I64E	54	0.275	29.010	0.254	33.435	0.331	34.441
297	11.7	I64E	59	0.284	29.185	0.304	33.604	0.338	33.785
298	11.8	I64E	75	0.306	29.491	0.301	33.989	0.375	33.950

299	11.9	I64E	61	0.249	29.678	0.354	33.590	0.396	34.753
300	12	I64E	61	0.237	29.739	0.300	33.208	0.342	35.338
301	12.1	I64E	60	0.254	29.821	0.286	33.603	0.338	34.809
302	12.2	I64E	67	0.285	29.817	0.266	33.587	0.415	35.179
303	12.3	I64E	66	0.290	29.821	0.319	33.105	0.347	35.195
304	12.4	I64E	69	0.251	29.822	0.279	33.912	0.336	34.963
305	12.5	I64E	86	0.365	29.792	0.336	34.246	0.401	35.344
306	12.6	I64E	187	0.665	29.491	0.659	34.726	0.752	35.278
307	12.7	I64E	85	0.529	29.383	0.334	34.955	0.333	34.751
308	12.8	I64E	77	0.265	29.059	0.295	35.254	0.383	35.017
309	12.9	I64E	62	0.326	29.196	0.314	34.041	0.373	34.831
310	13	I64E	63	0.235	29.190	0.233	32.618	0.306	34.506
311	13.1	I64E	54	0.249	29.417	0.256	34.192	0.333	34.476
312	13.2	I64E	52	0.201	29.798	0.319	35.222	0.360	33.988
313	13.3	I64E	61	0.220	29.795	0.295	35.036	0.314	32.910
314	13.4	I64E	50	0.229	29.701	0.241	34.134	0.303	32.946
315	13.5	I64E	57	0.251	29.596	0.279	34.228	0.323	34.097
316	13.6	I64E	148	0.457	29.434	0.338	34.313	0.449	33.222
317	13.7	I64E	171	0.577	29.367	0.513	33.895	0.553	33.442
318	13.8	I64E	76	0.474	29.358	0.465	33.796	0.483	34.717
319	13.9	I64E	57	0.281	29.483	0.291	34.899	0.369	34.757
320	14	I64E	60	0.264	29.459	0.267	34.048	0.319	33.776
321	14.1	I64E	65	0.242	29.431	0.244	33.265	0.289	33.519
322	14.2	I64E	50	0.269	29.457	0.283	33.311	0.342	33.222
323	14.3	I64E	57	0.245	29.253	0.271	32.137	0.309	32.614
324	14.4	I64E	54	0.249	29.033	0.238	31.673	0.291	32.900
325	14.5	I64E	67	0.291	29.043	0.265	32.437	0.354	33.651
326	14.6	I64E	57	0.233	29.158	0.253	32.019	0.312	33.776
327	14.7	I64E	59	0.275	29.038	0.247	31.765	0.296	34.097
328	14.8	I64E	54	0.234	29.081	0.244	32.318	0.295	33.889
329	14.9	I64E	80	0.281	29.052	0.253	33.216	0.319	33.497
330	15	I64E	60	0.328	29.205	0.301	33.073	0.351	33.738
331	15.1	I64E	55	0.221	29.736	0.266	33.513	0.319	34.021
332	15.2	I64E	62	0.207	29.613	0.267	33.739	0.310	34.249
333	15.3	I64E	69	0.293	29.467	0.260	33.500	0.325	33.862
334	15.4	I64E	58	0.302	28.986	0.227	33.908	0.307	34.069
335	15.5	I64E	62	0.230	28.746	0.292	34.111	0.328	34.101
336	15.6	I64E	65	0.254	28.693	0.263	33.928	0.316	33.772
337	15.7	I64E	60	0.281	29.329	0.266	33.808	0.293	33.632
338	15.8	I64E	65	0.238	29.732	0.353	34.362	0.379	33.255
339	15.9	I64E	74	0.266	29.776	0.266	34.786	0.313	33.853
340	16	I64E	67	0.287	29.718	0.280	34.355	0.364	33.988
341	16.1	I64E	60	0.230	29.532	0.279	33.624	0.357	34.028
342	16.2	I64E	68	0.264	29.196	0.261	32.716	0.340	33.763
343	16.3	I64E	64	0.238	29.140	0.264	32.978	0.313	34.464
344	16.4	I64E	59	0.225	29.012	0.262	33.923	0.329	34.562
345	16.5	I64E	49	0.206	29.339	0.268	33.717	0.324	34.326
346	16.6	I64E	74	0.244	29.540	0.282	33.902	0.326	34.322
347	16.7	I64E	68	0.288	29.511	0.333	34.834	0.405	34.564
348	16.8	I64E	62	0.257	29.569	0.397	35.533	0.467	34.545

349	16.9	I64E	49	0.232	29.547	0.278	34.944	0.336	34.253
350	17	I64E	53	0.232	29.543	0.291	34.871	0.358	34.546
351	17.1	I64E	70	0.230	29.434	0.328	34.928	0.400	35.048
352	17.2	I64E	45	0.287	29.414	0.317	34.908	0.384	35.174
353	17.3	I64E	57	0.230	29.119	0.265	33.912	0.382	35.162
354	17.4	I64E	55	0.244	29.201	0.250	33.109	0.315	34.857
355	17.5	I64E	117	0.290	29.165	0.238	31.240	0.344	34.126
356	17.6	I64E	159	0.588	29.266	0.463	31.095	0.523	34.133
357	17.7	I64E	114	0.500	29.514	0.483	31.282	0.505	34.855
358	0.4	US15	85	0.239	20.961	0.176	16.768	0.218	16.698
359	0.5	US15	95	0.290	23.727	0.171	19.297	0.307	22.303
360	0.6	US15	114	0.313	23.255	0.238	19.919	0.335	23.189
361	0.7	US15	84	0.247	23.353	0.231	20.349	0.310	23.276
362	0.8	US15	66	0.194	23.067	0.222	20.864	0.280	23.148
363	0.9	US15	64	0.199	23.857	0.250	21.136	0.297	22.629
364	1	US15	101	0.279	23.897	0.284	22.550	0.358	24.371
365	1.1	US15	93	0.233	22.933	0.285	23.762	0.381	25.433
366	1.2	US15	82	0.237	23.177	0.278	23.526	0.321	24.160
367	1.3	US15	86	0.245	23.113	0.292	24.026	0.338	24.564
368	1.4	US15	88	0.249	23.532	0.280	23.248	0.311	22.721
369	1.5	US15	80	0.228	23.287	0.266	23.110	0.325	23.647
370	1.6	US15	83	0.249	23.243	0.275	23.191	0.330	24.231
371	1.7	US15	66	0.196	23.769	0.261	23.272	0.304	24.171
372	1.8	US15	63	0.202	23.486	0.255	24.254	0.290	24.962
373	1.9	US15	73	0.209	23.752	0.258	24.642	0.315	25.655
374	2	US15	81	0.239	23.640	0.297	25.276	0.378	25.333
375	2.1	US15	101	0.272	23.282	0.309	24.404	0.372	25.348
376	2.2	US15	76	0.247	24.028	0.292	23.813	0.343	25.758
377	2.3	US15	87	0.274	24.175	0.291	24.268	0.416	26.527
378	2.4	US15	106	0.324	24.020	0.327	23.693	0.421	26.585
379	2.5	US15	101	0.297	23.411	0.275	22.234	0.341	24.034
380	2.6	US15	91	0.283	22.454	0.294	21.872	0.344	23.046
381	2.7	US15	102	0.299	22.853	0.252	17.894	0.283	16.081
382	2.8	US15	92	0.248	23.739	0.247	18.471	0.282	20.600
383	2.9	US15	79	0.211	23.345	0.245	20.503	0.319	24.008
384	3	US15	81	0.222	23.499	0.258	21.928	0.303	25.027
385	3.1	US15	80	0.230	23.326	0.278	23.319	0.321	25.540
386	3.2	US15	79	0.228	23.881	0.276	24.104	0.341	25.635
387	3.3	US15	79	0.224	23.257	0.268	24.201	0.314	26.473
388	3.4	US15	82	0.256	23.415	0.299	24.915	0.364	26.536
389	3.5	US15	81	0.251	23.383	0.288	25.692	0.331	26.478
390	3.6	US15	83	0.253	23.503	0.276	26.029	0.328	26.510
391	3.7	US15	126	0.372	23.636	0.354	25.592	0.422	26.650
392	3.8	US15	72	0.232	23.049	0.263	25.325	0.342	26.695
393	3.9	US15	100	0.239	23.469	0.275	22.669	0.319	25.945
394	4	US15	271	0.354	17.670	0.301	17.730	0.363	19.343
395	0.22	SR616	97	0.214	18.404	0.216	17.373	0.220	19.312
396	0.32	SR616	148	0.293	19.982	0.258	19.171	0.277	18.521
397	0.42	SR616	129	0.270	18.466	0.278	20.070	0.295	20.426
398	0.52	SR616	101	0.194	18.823	0.217	19.645	0.277	20.847

399	0.62	SR616	98	0.228	19.639	0.227	20.742	0.281	21.670
400	0.72	SR616	86	0.210	20.985	0.222	22.163	0.248	21.737
401	0.82	SR616	120	0.257	20.761	0.253	21.361	0.348	21.624
402	0.92	SR616	102	0.252	21.125	0.213	21.382	0.271	20.541
403	1.02	SR616	148	0.387	21.391	0.325	21.129	0.452	22.077
404	1.12	SR616	172	0.381	20.342	0.294	20.700	0.360	22.220
405	1.22	SR616	122	0.235	20.968	0.225	20.928	0.311	21.997
406	1.32	SR616	88	0.231	21.221	0.222	20.732	0.241	21.465
407	1.42	SR616	142	0.314	21.086	0.268	21.366	0.348	21.820
408	1.52	SR616	125	0.256	21.182	0.258	21.962	0.315	21.616
409	1.62	SR616	135	0.303	20.068	0.317	21.932	0.317	21.842
410	1.72	SR616	102	0.229	20.305	0.260	22.429	0.287	22.013
411	1.82	SR616	158	0.361	19.380	0.286	21.170	0.303	21.440
412	1.92	SR616	131	0.324	18.877	0.284	19.671	0.290	18.789
413	2.02	SR616	140	0.320	20.332	0.283	21.230	0.379	21.457
414	2.12	SR616	116	0.235	19.932	0.222	20.523	0.249	19.937
415	2.22	SR616	125	0.295	19.450	0.246	18.199	0.237	17.804
416	2.32	SR616	650	0.160	14.467	0.158	10.717	0.214	10.898
417	0.11	SR600	182	0.355	17.340	0.340	15.336	0.307	15.352
418	0.21	SR600	144	0.351	19.214	0.286	16.689	0.336	17.687
419	0.31	SR600	149	0.365	19.593	0.312	18.319	0.392	19.083
420	0.41	SR600	118	0.275	19.613	0.277	18.232	0.303	19.961
421	0.51	SR600	175	0.363	19.095	0.366	19.352	0.425	20.225
422	0.61	SR600	165	0.350	18.711	0.318	19.312	0.349	19.457
423	0.71	SR600	134	0.287	19.645	0.306	19.052	0.362	20.886
424	0.81	SR600	114	0.231	18.533	0.229	18.031	0.299	21.313
425	0.91	SR600	219	0.452	16.248	0.373	15.667	0.441	19.226
426	0.23	SR600	121	0.196	15.194	0.221	16.831	0.285	17.439
427	0.33	SR600	134	0.264	16.112	0.331	16.974	0.363	17.689
428	0.43	SR600	97	0.205	18.688	0.225	16.853	0.238	18.600
429	0.53	SR600	122	0.290	21.464	0.242	19.296	0.344	21.121
430	0.63	SR600	177	0.404	22.555	0.373	20.854	0.477	23.166
431	0.73	SR600	214	0.439	18.879	0.418	18.850	0.437	17.275
432	0.83	SR600	114	0.217	18.175	0.252	18.024	0.272	16.281
433	0.93	SR600	147	0.224	17.818	0.196	16.713	0.270	17.621
434	1.03	SR600	139	0.246	15.295	0.237	15.124	0.276	15.793
435	1.13	SR600	104	0.176	15.784	0.203	15.649	0.234	17.374
436	1.23	SR600	96	0.184	16.489	0.204	14.227	0.217	16.349
437	1.33	SR600	87	0.169	16.026	0.173	16.492	0.199	16.181
438	1.43	SR600	93	0.206	18.029	0.196	17.187	0.251	19.222
439	1.53	SR600	117	0.198	17.111	0.236	17.535	0.282	18.333
440	1.63	SR600	123	0.214	15.378	0.248	16.649	0.238	17.363
441	1.73	SR600	111	0.200	16.362	0.205	17.408	0.287	17.872
442	1.83	SR600	115	0.226	17.935	0.236	16.627	0.281	18.166
443	1.93	SR600	126	0.232	18.333	0.238	18.552	0.283	18.530
444	2.03	SR600	122	0.241	18.189	0.266	19.126	0.304	19.300
445	2.13	SR600	125	0.232	17.025	0.298	18.446	0.316	18.134
446	2.23	SR600	112	0.224	18.330	0.246	19.772	0.274	18.817
447	2.33	SR600	89	0.194	19.080	0.229	20.598	0.242	19.751
448	2.43	SR600	86	0.191	19.505	0.221	19.940	0.247	20.624

449	2.53	SR600	99	0.242	19.946	0.232	18.828	0.293	20.643
450	2.63	SR600	104	0.232	20.138	0.186	16.004	0.253	20.642
451	2.73	SR600	1128	0.241	12.260	0.171	7.500	0.294	14.571
452	0.25	SR799	101	0.227	17.996	NA	15.941	0.248	16.669
453	0.35	SR799	109	0.258	21.617	0.241	20.097	0.300	23.367
454	0.45	SR799	142	0.269	20.753	0.253	20.414	0.366	23.924
455	0.55	SR799	145	0.217	17.730	0.244	20.058	0.310	22.506
456	0.65	SR799	161	0.306	18.801	0.316	21.249	0.430	24.456
457	0.75	SR799	123	0.225	19.255	0.238	20.495	0.269	22.123
458	0.85	SR799	147	0.293	18.112	0.287	17.949	0.333	18.879
459	0.95	SR799	161	0.373	21.573	0.302	18.372	0.390	21.563
460	1.05	SR799	186	0.426	22.057	0.376	19.568	0.453	21.623
461	1.15	SR799	147	0.274	18.234	0.273	17.971	0.271	16.935
462	1.25	SR799	229	0.394	17.430	0.372	17.637	0.400	16.600
463	1.35	SR799	123	0.250	18.278	0.240	18.473	0.274	19.308
464	1.45	SR799	125	0.261	18.263	0.283	18.490	0.313	19.093
465	1.55	SR799	113	0.241	18.387	0.224	20.550	0.286	20.844
466	1.65	SR799	139	0.240	17.154	0.277	19.456	0.323	19.790
467	1.75	SR799	131	0.208	16.528	0.251	18.780	0.257	19.088
468	1.85	SR799	126	0.189	14.302	0.240	17.283	0.261	17.916
469	1.95	SR799	125	0.201	14.308	0.238	16.451	0.249	16.954
470	2.05	SR799	115	0.196	16.331	0.222	17.641	0.246	18.866
471	2.15	SR799	115	0.212	16.580	0.270	18.481	0.294	19.876
472	2.25	SR799	112	0.188	15.968	0.247	19.161	0.285	20.627
473	2.35	SR799	121	0.234	17.018	0.268	18.907	0.347	21.883
474	2.45	SR799	108	0.226	17.089	0.233	19.636	0.271	20.869
475	2.55	SR799	130	0.224	16.644	0.258	19.413	0.288	20.164
476	2.65	SR799	113	0.215	17.725	0.250	19.721	0.272	19.500
477	2.75	SR799	120	0.208	16.712	0.251	19.336	0.271	19.216
478	2.85	SR799	106	0.223	17.728	0.235	18.554	0.285	19.850
479	2.95	SR799	87	0.189	16.466	0.219	17.998	0.220	18.620
480	3.05	SR799	104	0.206	16.549	0.240	17.516	0.254	17.673
481	3.15	SR799	214	0.274	9.524	0.377	10.546	0.313	12.691
482	0.09	SR676	173	0.320	16.990	0.280	15.431	NA	15.162
483	0.19	SR676	174	0.345	18.404	0.304	17.515	0.286	13.805
484	0.29	SR676	233	0.400	17.308	0.357	15.903	0.374	15.775
485	0.39	SR676	206	0.316	17.055	0.338	16.384	0.380	17.654
486	0.49	SR676	171	0.337	17.527	0.355	17.245	0.375	17.885
487	0.59	SR676	248	0.462	18.488	0.422	18.720	0.481	19.949
488	0.69	SR676	205	0.386	18.235	0.354	18.779	0.424	20.408
489	0.79	SR676	171	0.285	18.356	0.353	19.739	0.389	21.062
490	0.89	SR676	178	0.351	19.054	0.388	19.822	0.436	21.565
491	0.99	SR676	215	0.391	18.158	0.410	19.262	0.451	20.743
492	1.09	SR676	190	0.390	18.102	0.382	18.667	0.472	19.180
493	1.19	SR676	193	0.411	17.467	0.379	17.923	0.437	18.368
494	1.29	SR676	183	0.379	18.739	0.374	18.576	0.423	20.004
495	1.39	SR676	216	0.446	19.020	0.396	19.137	0.450	21.730
496	1.49	SR676	191	0.382	20.433	0.375	20.050	0.455	22.804
497	1.59	SR676	152	0.311	20.458	0.320	19.654	0.395	21.487
498	1.69	SR676	208	0.359	17.004	0.308	14.932	0.410	15.348

499	1.79	SR676	174	0.329	16.181	0.284	13.782	0.352	15.172
500	1.89	SR676	178	0.334	16.735	0.317	17.305	0.338	17.506
501	1.99	SR676	181	0.288	14.968	0.301	16.188	0.329	17.514
502	2.09	SR676	172	0.285	15.903	0.336	16.586	0.319	17.448
503	2.19	SR676	223	0.338	15.307	0.355	15.120	0.387	15.704
504	2.29	SR676	221	0.364	15.199	0.341	14.776	0.404	15.689
505	2.39	SR676	190	0.353	15.870	0.341	14.058	0.330	14.598
506	2.49	SR676	186	0.365	18.365	0.365	15.323	0.383	17.362
507	2.59	SR676	200	0.510	18.407	0.378	15.341	0.442	17.251
508	2.69	SR676	195	0.300	12.937	0.305	10.721	0.349	12.261

Appendix 3 Quarter Car Simulation Results

ID	Route	Distant	Sim1	Sim2	Sim3	Sim4	Sim5	Sim6	Sim7	Sim8	Sim9
1	SR799	0.1	0.765	0.774	0.749	0.902	0.677	0.775	0.759	0.769	0.760
2	SR799	0.2	0.403	0.427	0.394	0.457	0.351	0.399	0.411	0.402	0.404
3	SR799	0.3	0.570	0.574	0.575	0.620	0.515	0.562	0.582	0.571	0.569
4	SR799	0.4	0.619	0.624	0.621	0.686	0.554	0.612	0.631	0.621	0.616
5	SR799	0.5	0.765	0.773	0.770	0.915	0.589	0.748	0.792	0.766	0.762
6	SR799	0.6	0.669	0.697	0.629	0.817	0.561	0.666	0.677	0.672	0.663
7	SR799	0.7	0.487	0.495	0.483	0.617	0.362	0.486	0.496	0.490	0.484
8	SR799	0.8	0.718	0.744	0.697	0.826	0.593	0.714	0.729	0.720	0.714
9	SR799	0.9	0.650	0.670	0.649	0.756	0.503	0.638	0.672	0.651	0.649
10	SR799	1	0.982	1.007	0.964	1.093	0.902	0.980	0.988	0.983	0.980
11	SR799	1.1	0.625	0.628	0.637	0.800	0.474	0.602	0.660	0.627	0.622
12	SR799	1.2	0.798	0.819	0.777	0.841	0.703	0.787	0.815	0.800	0.793
13	SR799	1.3	1.213	1.223	1.228	1.477	0.962	1.188	1.254	1.215	1.210
14	SR799	1.4	0.483	0.491	0.478	0.511	0.389	0.472	0.503	0.486	0.479
15	SR799	1.5	0.549	0.564	0.541	0.642	0.467	0.547	0.559	0.551	0.547
16	SR799	1.6	0.520	0.534	0.503	0.645	0.418	0.522	0.522	0.523	0.516
17	SR799	1.7	0.678	0.693	0.670	0.718	0.572	0.669	0.695	0.682	0.674
18	SR799	1.8	0.691	0.694	0.700	0.795	0.534	0.672	0.719	0.693	0.688
19	SR799	1.9	0.679	0.693	0.679	0.721	0.589	0.667	0.698	0.681	0.677
20	SR799	2	0.653	0.667	0.652	0.678	0.596	0.643	0.671	0.654	0.651
21	SR799	2.1	0.478	0.483	0.490	0.510	0.388	0.465	0.499	0.479	0.478
22	SR799	2.2	0.453	0.463	0.452	0.578	0.339	0.446	0.467	0.455	0.452
23	SR799	2.3	0.462	0.470	0.463	0.591	0.340	0.455	0.476	0.464	0.461
24	SR799	2.4	0.492	0.512	0.481	0.588	0.421	0.494	0.494	0.493	0.491
25	SR799	2.5	0.456	0.488	0.419	0.552	0.406	0.466	0.448	0.458	0.454
26	SR799	2.6	0.484	0.496	0.479	0.563	0.388	0.477	0.496	0.485	0.482
27	SR799	2.7	0.552	0.557	0.551	0.617	0.474	0.546	0.564	0.555	0.548
28	SR799	2.8	0.629	0.631	0.634	0.685	0.581	0.621	0.642	0.631	0.627
29	SR799	2.9	0.543	0.551	0.539	0.653	0.428	0.539	0.554	0.546	0.539
30	SR799	3	0.273	0.300	0.245	0.300	0.247	0.278	0.270	0.274	0.272
31	SR799	3.1	0.331	0.355	0.301	0.378	0.293	0.341	0.322	0.332	0.329
32	SR799	3.2	0.539	0.555	0.526	0.677	0.421	0.535	0.550	0.541	0.536
33	SR799	3.3	0.953	1.006	0.888	0.971	0.913	0.975	0.935	0.961	0.944
34	SR799	3.4	0.676	0.760	0.568	0.726	0.620	0.686	0.669	0.672	0.673
35	SR600	0	1.066	1.135	0.985	1.313	0.887	1.080	1.062	1.069	1.060
36	SR600	0.1	0.952	0.993	0.924	1.183	0.733	0.947	0.971	0.956	0.948
37	SR600	0.2	0.764	0.784	0.750	0.853	0.673	0.760	0.776	0.766	0.761
38	SR600	0.3	0.814	0.825	0.778	0.977	0.686	0.824	0.813	0.823	0.804
39	SR600	0.4	0.767	0.800	0.728	0.919	0.627	0.773	0.767	0.768	0.766

40	SR600	0.5	1.147	1.171	1.126	1.487	0.849	1.136	1.172	1.156	1.137
41	SR600	0.6	0.748	0.764	0.734	0.942	0.613	0.751	0.751	0.752	0.744
42	SR600	0.7	0.670	0.672	0.671	0.840	0.504	0.664	0.686	0.674	0.666
43	SR600	0.8	0.742	0.803	0.678	0.847	0.627	0.744	0.748	0.740	0.740
44	SR600	0.9	0.640	0.668	0.601	0.816	0.579	0.657	0.630	0.645	0.634
45	SR600	1	0.597	0.616	0.590	0.703	0.471	0.591	0.611	0.599	0.595
46	SR600	1.1	0.577	0.621	0.524	0.619	0.524	0.592	0.567	0.580	0.572
47	SR600	1.2	0.454	0.470	0.430	0.520	0.367	0.450	0.462	0.455	0.451
48	SR600	1.3	0.529	0.544	0.529	0.602	0.453	0.520	0.547	0.529	0.528
49	SR600	1.4	0.851	0.877	0.821	0.982	0.761	0.851	0.855	0.855	0.846
50	SR600	1.5	0.991	1.145	0.806	1.113	0.892	1.009	0.979	0.983	0.991
51	SR600	1.6	0.423	0.434	0.425	0.448	0.348	0.416	0.436	0.423	0.422
52	SR600	1.7	0.687	0.687	0.708	0.781	0.518	0.664	0.722	0.688	0.685
53	SR600	1.8	0.578	0.614	0.547	0.675	0.489	0.578	0.585	0.580	0.576
54	SR600	1.9	0.515	0.526	0.511	0.581	0.444	0.509	0.526	0.516	0.513
55	SR600	2	0.343	0.363	0.323	0.379	0.312	0.347	0.341	0.344	0.341
56	SR600	2.1	0.368	0.379	0.368	0.400	0.317	0.363	0.378	0.369	0.368
57	SR600	2.2	0.551	0.561	0.552	0.558	0.523	0.544	0.561	0.551	0.550
58	SR600	2.3	0.614	0.620	0.622	0.653	0.540	0.607	0.626	0.616	0.612
59	SR600	2.4	0.633	0.644	0.622	0.754	0.532	0.639	0.634	0.638	0.629
60	SR600	2.5	0.373	0.385	0.363	0.432	0.333	0.377	0.373	0.375	0.372
61	SR600	2.6	0.428	0.459	0.397	0.456	0.390	0.433	0.425	0.428	0.426
62	SR600	2.7	0.504	0.518	0.502	0.610	0.396	0.498	0.518	0.505	0.503
63	SR600	2.8	0.641	0.662	0.645	0.720	0.499	0.624	0.668	0.642	0.641
64	SR600	2.9	0.750	0.767	0.755	0.816	0.622	0.736	0.776	0.750	0.749
65	SR600	3	0.472	0.489	0.466	0.498	0.428	0.469	0.480	0.473	0.471
66	SR600	3.1	0.375	0.386	0.366	0.456	0.308	0.375	0.380	0.377	0.373
67	SR600	3.2	0.377	0.391	0.368	0.423	0.325	0.374	0.385	0.378	0.376
68	SR600	3.3	0.446	0.459	0.437	0.539	0.361	0.445	0.452	0.448	0.444
69	SR600	3.4	0.525	0.536	0.518	0.588	0.449	0.519	0.536	0.527	0.523
70	SR616	0.1	0.549	0.560	0.551	0.580	0.478	0.542	0.562	0.551	0.547
71	SR616	0.2	0.636	0.642	0.649	0.685	0.513	0.620	0.658	0.637	0.635
72	SR616	0.3	0.667	0.696	0.632	0.753	0.604	0.669	0.671	0.672	0.662
73	SR616	0.4	0.513	0.550	0.480	0.548	0.456	0.514	0.517	0.513	0.512
74	SR616	0.5	0.439	0.447	0.439	0.506	0.364	0.433	0.451	0.440	0.438
75	SR616	0.6	0.431	0.439	0.429	0.485	0.362	0.426	0.440	0.432	0.429
76	SR616	0.7	0.382	0.398	0.373	0.421	0.344	0.383	0.384	0.383	0.381
77	SR616	0.8	0.559	0.571	0.558	0.661	0.452	0.548	0.578	0.560	0.558
78	SR616	0.9	0.445	0.479	0.419	0.476	0.386	0.444	0.450	0.444	0.445
79	SR616	1	0.793	0.828	0.775	0.910	0.655	0.791	0.803	0.793	0.792
80	SR616	1.1	0.638	0.691	0.594	0.680	0.556	0.637	0.645	0.637	0.637

81	SR616	1.2	0.506	0.509	0.515	0.579	0.390	0.488	0.534	0.508	0.503
82	SR616	1.3	0.335	0.355	0.319	0.377	0.302	0.337	0.334	0.335	0.334
83	SR616	1.4	0.454	0.492	0.394	0.531	0.399	0.462	0.450	0.458	0.449
84	SR616	1.5	0.588	0.593	0.593	0.668	0.478	0.576	0.607	0.590	0.586
85	SR616	1.6	0.535	0.550	0.506	0.636	0.466	0.549	0.525	0.540	0.530
86	SR616	1.7	0.605	0.613	0.610	0.622	0.521	0.594	0.623	0.607	0.603
87	SR616	1.8	0.590	0.646	0.553	0.646	0.483	0.590	0.599	0.589	0.591
88	SR616	1.9	0.404	0.436	0.386	0.435	0.355	0.405	0.406	0.403	0.405
89	SR616	2	0.600	0.613	0.594	0.698	0.522	0.593	0.612	0.602	0.598
90	SR616	2.1	0.601	0.618	0.574	0.652	0.511	0.599	0.610	0.606	0.595
91	SR616	2.2	0.550	0.577	0.539	0.611	0.459	0.540	0.569	0.550	0.549
92	SR676	0	0.885	0.957	0.810	0.966	0.832	0.920	0.852	0.889	0.881
93	SR676	0.1	0.657	0.711	0.581	0.771	0.591	0.679	0.639	0.661	0.651
94	SR676	0.2	0.730	0.786	0.671	0.799	0.656	0.736	0.729	0.733	0.726
95	SR676	0.3	0.852	0.883	0.815	0.906	0.702	0.849	0.870	0.860	0.842
96	SR676	0.4	0.601	0.636	0.539	0.665	0.538	0.617	0.589	0.606	0.593
97	SR676	0.5	0.648	0.680	0.553	0.711	0.598	0.673	0.625	0.660	0.632
98	SR676	0.6	1.187	1.392	0.919	1.256	1.131	1.234	1.141	1.192	1.180
99	SR676	0.7	0.730	0.810	0.630	0.782	0.666	0.750	0.714	0.731	0.724
100	SR676	0.8	0.696	0.721	0.673	0.744	0.589	0.690	0.712	0.699	0.691
101	SR676	0.9	0.951	0.969	0.932	1.157	0.744	0.946	0.967	0.956	0.944
102	SR676	1	0.910	0.968	0.834	1.048	0.771	0.932	0.900	0.917	0.900
103	SR676	1.1	0.861	0.884	0.797	1.093	0.725	0.887	0.840	0.875	0.847
104	SR676	1.2	0.920	0.986	0.814	1.014	0.826	0.949	0.898	0.926	0.909
105	SR676	1.3	0.775	0.819	0.739	0.839	0.671	0.782	0.777	0.778	0.771
106	SR676	1.4	0.950	1.041	0.815	1.058	0.860	0.973	0.932	0.954	0.940
107	SR676	1.5	0.832	0.891	0.741	0.916	0.757	0.854	0.815	0.839	0.822
108	SR676	1.6	0.652	0.680	0.607	0.732	0.569	0.662	0.650	0.659	0.645
109	SR676	1.7	1.089	1.110	1.081	1.201	0.905	1.075	1.119	1.095	1.082
110	SR676	1.8	0.863	0.893	0.848	1.001	0.697	0.850	0.888	0.865	0.860
111	SR676	1.9	1.022	1.077	0.904	1.250	0.905	1.046	1.001	1.032	1.007
112	SR676	2	0.671	0.714	0.632	0.779	0.583	0.679	0.669	0.673	0.667
113	SR676	2.1	0.675	0.708	0.652	0.764	0.577	0.673	0.686	0.677	0.673
114	SR676	2.2	0.821	0.909	0.726	0.842	0.762	0.822	0.825	0.815	0.821
115	SR676	2.3	1.189	1.252	1.118	1.237	1.104	1.185	1.203	1.192	1.183
116	SR676	2.4	1.004	1.053	0.914	1.119	0.930	1.010	1.002	1.010	0.993
117	SR676	2.5	0.778	0.830	0.732	0.953	0.640	0.779	0.784	0.777	0.776
118	SR676	2.6	0.919	0.980	0.848	1.002	0.847	0.931	0.911	0.920	0.914

Appendix 4 Matlab Code for Quarter-car Simulation

Appendix 4.1 Quarter-car Model Function

```
function [Y, Y1, tstep, X, dX] = qcar(x,p,v,f,f1,f2,c,mu)
if nargin<5
    f1 = 1;
    f2 = 1;
    c = 6;
    mu = 0.15;
end
N = 1;
% calculates the quarter car response
[x, ia] = unique(x);
p = p(ia);
X = linspace(min(x),max(x),length(x));
P = interp1(x,p,X);
t = (X-min(X))/v;
% Dt = (t(2)-t(1))*ones(4);
Dt = (t(2)-t(1));
tstep = Dt(1);
dX = X(2)-X(1);
SR = f/dX;
k = max(1,round(SR));
SP = (P(1+(2*floor(k/2)+1):end)-P(1:end-(2*floor(k/2)+1)))/((2*floor(k/2)+1)*dX);
Y = zeros(4,length(SP)+1);
XLEAD = 11;
[~, ind] = min(abs(t-XLEAD/v));
ind = min(2,ind);
XIN = [(P(ind)-P(1))/XLEAD,0,(P(ind)-P(1))/XLEAD,0]';
Y(:,1) = XIN;
k1 = 653*f1;
k2 = 63.3*f2;
A = [ 0        1        0        0;...
     -k2      -c        k2       c;...
      0        0        0        1;...
    k2/mu     c/mu -(k1+k2)/mu -c/mu];
iA = inv(A);
B = [0 0 0 k1/mu]';
EXPA = expm(Dt*A);
P = iA*(EXPA-eye(4))*B;
for i=1:length(SP)
    Y(:,i+1) = EXPA*Y(:,i)+P*SP(i);
end
Y1 = zeros(size(Y));
for i=1:4
    Y1(i,:) = cumsum(Y(i,:))*dX;
end
```

Appendix 4.2 Simulation Code

```
D = csvread('C:\Users\hz3xm\Documents\Dropbox\2014 Summer-
Fall\Dissertation\Sensitivity\sr600-3.csv',1,1);
xp = D(:,1)'*0.3048; % distant in meter
zp = D(:,2)'*0.0254; % elevuation in meter
zp = mvaveragec(zp,5); % need to change to number of averaging points
F=0.270; % window size of moving average 10*0.984252
interval=(xp(2)-xp(1)); % sampling interval
n=round(160.934/interval); % number of recores every 0.1 mile
m=1609.934/interval; % ratio of mile/interval
V=22.2222; % simulating speeds
noseg=floor(length(xp)/n); % number of segments in the profile data
IRI=zeros(noseg+1,10); % initalize IRI matrix
ABS=zeros(noseg+1,10); % initalize ABS
RMS=zeros(noseg+1,10); % initalize RMS
for i=1:noseg
   IRI(i,1)=(i-1)*0.1; % distant
end
IRI(noseg+1,1)=noseg*0.1;
ABS(:,1)=IRI(:,1);
RMS(:,1)=IRI(:,1);
f1=[1;1.44;0.56;1;1;1;1;1;1];
f2=[1;1;1;1.54;0.46;1;1;1;1];
%c=[6;6;6;6;6;6.9;5.1;6;6];
c=[3;3;3;3;3;3.45;2.55;3;3];
mu=[0.15;0.15;0.15;0.15;0.15;0.15;0.15;0.17;0.13];
for j=1:9
   [Y, Y1, dt, ~, dX] = qcar(xp,zp,V,F,f1(j),f2(j),c(j),mu(j));
   %[Y, Y1, dt, ~, dX] = qcar(xp,zp,V(j),F,1.34,1,6,0.08);
   %[Y, Y1, dt, ~, dX] = qcar(xp,zp,V(j),F,1.34,1.25,8,0.08);
   iri=abs(Y(3,:)-Y(1,:));
   ab=abs(Y(2,:));
   ACC=Y(2,:)*dX/dt;
   for k=1:noseg
      IRI(k,j+1)=m*mean(iri(((k-1)*n+1):((k-1)*n+n)));
      ABS(k,j+1)=mean(ab(((k-1)*n+1):((k-1)*n+n)));
      %RMS(k,j+1)=sqrt((1/n)*Y(2,((k-1)*n+1):((k-1)*n+n))*transpose(Y(2,((k-1)*n+1):((k-
1)*n+n))));
      RMS(k,j+1)=sqrt((1/n)*ACC(((k-1)*n+1):((k-1)*n+n))*transpose(ACC(((k-1)*n+1):((k-
1)*n+n))));
   end
   IRI(noseg+1,j+1)=m*mean(iri((noseg*n+1):length(iri)));
   ABS(noseg+1,j+1)=mean(ab((noseg*n+1):length(iri)));
end
%plot(IRI(:,1),IRI(:,2),IRI(:,1),IRI(:,3),IRI(:,1),IRI(:,4),IRI(:,1),IRI(:,5),IRI(:,1),IRI(:,6),IRI(:,1),
IRI(:,7),IRI(:,1),IRI(:,8),IRI(:,1),IRI(:,9));
```

```
%xlabel('Distant(mile)');
%ylabel('IRI(in/mile)');
%legend('20 mph','30 mph','40 mph','50 mph','60 mph','70 mph','80 mph','90 mph');
dlmwrite('IRIsimL.txt', IRI, 'delimiter', '\t', 'precision',6);
dlmwrite('ABSsimL.txt', ABS, 'delimiter', '\t', 'precision',6);
dlmwrite('RMSsimL.txt', RMS, 'delimiter', '\t', 'precision',6);
```